INTENS

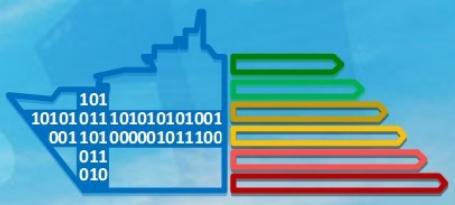

VTT

beyond
the obvious

Integrated Energy Solutions to Smart and Green Shipping

2021 Edition

Zou Guangrong | Saara Hänninen (Editors)

VTT TECHNOLOGY 394

VTT TECHNOLOGY 394

Integrated Energy Solutions to Smart and Green Shipping

2021 Edition

Zou Guangrong | Saara Hänninen (Editors)

VTT Technical Research Centre of Finland Ltd

ISBN 978-951-38-8755-1

VTT Technology 394

ISSN-L 2242-1211
ISSN 2242-122X (Online)
DOI: 10.32040/2242-122X.2021.T394

JULKAISIJA – PUBLISHER

VTT
PL 1000
02044 VTT
Puh. 020 722 111
https://www.vtt.fi

VTT
P.O. Box 1000
FI-02044 VTT, Finland
Tel. +358 20 722 111
https://www.vttresearch.com


Smart & Green
Shipping Together!
Innovation
Business
Platform

INTENS

co-funded by

BUSINESS FINLAND

Arctic Seas

Industrial partners

3D Studio BLOMBERG

DELTAMARIN®

dinex

Jeppo Biogas Ab
Jepuan Biokaasu Oy

JTK Power

MEYER TURKU
SHIPYARD 1737

NAPA

Parker

PINJA

TALLINK

SILJA LINE

VAHTERUS

VISORC

wasaline

WÄRTSILÄ

Research partners

Aalto University

LUT University

University of Vaasa

Åbo Akademi

VTT

Preface

Finland has a long tradition of maritime technological innovation. Back to 2017 when shipping industry was on the verge of digital transformation and decarbonization, a number of Finnish companies and research institutions had foreseen the strong urge for and the potential of maritime digitalization and decarbonization in the future shipping, and committed themselves to proactively advance, digitalize and promote the consortium expertise specifically in ship energy efficiency improvement and emissions reduction, which consequently gave birth to the INTENS project[1].

From its inception, INTENS has been a blessing to the consortium partners and wider Finnish maritime cluster. It has given the INTENS partners a unique opportunity to dedicate enormous efforts to jointly research and develop industry-leading novel solutions and innovations to address the major challenges faced by the global shipping industry. The special focuses have been put on seven trendy and highly potential research topics, i.e. emissions reduction, maritime data analytics, waste heat recovery, ship operation, hybridization and electrification, Arctic-specific solutions, and maritime information exchange and enrichment. Thanks to the great commitment, collaboration and hard work, the INTENS project has been a notable success. Specifically, over 60 novel software and hardware products have been developed and over 150 scientific publications and theses have been generated during the last three and a half years. Many of the results have led to significant research and business impacts, resulting in 26 new business and R&D projects with total volume of over 22 M€. Another 15 projects, with total volume of 12 M€, are currently in the pipeline.

Interactive research-industry co-innovation has been the other crucial factor in the INTENS' success. Shipping is of a collaborative nature. Innovative collaboration is essential for maritime digitalization, decarbonization and automation. The INTENS consortium consists of 19 partners, covering the large part of the maritime technical value chain, which has been an advantage to larger extent than a challenge. The complementary consortium has provided us an ideal network for collaborative innovation, not only on paper but also in practice. It has been a great honour to lead such a highly committed and cooperative consortium. Besides actual research and development, considerable efforts have been put into knowledge sharing and technology transfer. A number of project internal meetings and

[1] INTENS - Integrated energy solutions to smart and green shipping (2018 - 2021), co-funded by Business Finland's (formerly Tekes) Arctic Seas program (2014 - 2017) and the INTENS consortium. http://intens.vtt.fi

workshops have been held regularly for knowledge sharing, co-learning and co-innovation.

The INTENS consortium has not been doing things alone and, instead, has been actively networked with other 20 national and international project consortia. Besides, the partners have been very active in participating in over 100 scientific and business events, which could have been doubled if there were not COVID-19 pandemic. Especially, as a tradition, we have hosted three annual public seminars / webinars to disseminate the achieved results, and their extended abstracts have been collected as proceedings available for the wider maritime community. This book is the third and last edition of the proceedings. Together with the 2019 edition[2] and 2020 edition[3], they also act as the INTENS project final report to showcase part of the R&D results achieved during the project period.

INTENS intensifies smart and green shipping by maritime digitalization and collaboration. Although the project itself has come to an end, the actual collaboration and co-innovation among the INTENS partners is continuing in many ways. The direct and indirect research and business impacts will be surely visible, not only generating scientific and technological innovations but also creating sustainable and globally competitive businesses, and hence strengthen Finland's green and innovative global image in years to come.

Acknowledgement

We gratefully acknowledge the great support of Business Finland, 19 INTENS consortium partners, including 14 industrial partners (3D Studio Blomberg Ltd, Deltamarin Ltd, Dinex Finland Oy, Jeppo Biogas Ab, JTK Power Oy, Meyer Turku Oy, NAPA Oy, Parker Hannifin Manufacturing Finland Oy, Pinja Oy (Protacon Technologies Oy), Tallink Silja Oy, Vahterus Oy, Visorc Oy, NLC Ferry Ab Oy and Wärtsilä Oyj Abp) and 5 research institutions (Aalto University, LUT University, University of Vaasa, Åbo Akademi University, and VTT Technical Research Centre of Finland), and other INTENS supporting partners.

Special thanks are due to the INTENS steering group, international advisory group and project group, especially to all the main contributors to the INTENS project during the last three and a half years. Without your great commitment, support, collaboration and hard work, it would not have been possible to make INTENS another great success.

Zou Guangrong
INTENS coordinator, Senior Scientist
VTT Technical Research Centre of Finland

[2] (2019 Edition) VTT Technology No. 354. https://doi.org/10.32040/2242-122X.2019.T354
[3] (2020 Edition) VTT Technology No. 380. https://doi.org/10.32040/2242-122X.2020.T380

Financier's perspective

"INTENS – Integrated energy solutions to smart and green shipping" is a joint action that was created to produce novel knowledge and technologies having a significant effect on the development of sustainable sea traffic and on the renewal of Finnish maritime industry. This is done by developing new technologies increasing the energy efficiency and decreasing the emissions caused by the vessels and their operations. INTENS combined two strong Finnish technology and competence area, namely digitalization and maritime industries in one action, which was an excellent base to create globally new technologies, competitiveness and export opportunities for Finnish companies. This was the main motivation for Business Finland (Tekes at the time when INTENS started) to make a financing decision for the joint action.

INTENS brought together about 20 Finnish organizations in the same research and innovation action and supported also in this way the aim of Tekes / Business Finland to create and develop internationally competitive innovation and business ecosystems in Finland. Big number of participating organizations and large variation of studied technologies were seen as a great strength and possibility for INTENS but at the same time it also formed potential challenges, difficulties and risks for the joint action.

Now three and half years later, we can see that main part of the aims and expectations that Tekes / Business Finland had for INTENS have been achieved. This can clearly be seen in the generated results, such as the three proceedings of the INTENS yearly public dissemination events, and heard from the feedback and experiences of the participants. A number of new products and product concepts based on the results of INTENS have been developed and launched by companies and a lot of new research results and new knowledge have been created. The co-operation between partners have been active and fruitful for new achievements. None of the participants could have achieved the aims of the action alone; an active and real co-operation was needed. Thus, co-operation will go on to achieve new innovation and business results.

Matti Säynätjoki
Chief Advisor
Business Finland

Industrial partners' perspective

Taking part in the INTENS project was a valuable chance for NAPA to explore how we use voyage optimization to solve an existing issue for our customers – how to rapidly decarbonize in the face of a climate emergency and strict rules from the IMO. In the past years, we have seen huge investments in clean technology from various stakeholders across shipping, intense debate about the best way to reduce emissions, and strong incentives from banks and cargo owners to prioritize clean shipping. We are now more aware than ever of the scale of the challenge, but the industry is more committed than ever to solving it.

As experts in ship modelling and maritime data analysis, NAPA has devoted to create a completely new approach to collaborative and holistic voyage planning and monitoring, specifically for large merchant fleets, aiming to increase transparency and reduce conflicts of interest by connecting ship operators, charterers and crew to work on a single voyage plan. INTENS helped us make this a reality. As part of the usability and user experience research, NAPA utilized external experts to speed up the process and accumulate know-how in-house, resulting in a significant impact on our product development approach. Almost all the lessons learned during the project are taken into use in our product development activities today. Besides, we worked on a new generation of our routing algorithm. It now considers navigational restrictions, wind, sea and tidal currents, waves and swell, and water depth, giving users a highly detailed, real-time picture of the factors that will affect the voyage and how to manage them. Furthermore, we were able to collaborate with many partners within and outside the INTENS, both industrial and academic, and to develop a number of new commercial partnership opportunities.

Overall, INTENS has moved us much further towards our goal. Through INTENS, our concept refinement and research progressed successfully, and our product, NAPA Voyage Optimization, has now been launched. Being part of INTENS has helped us create a platform that will allow more of the shipping industry than ever before to benefit from advanced voyage optimization and routing and, in turn, helping to mitigate one of the 21st century's most difficult climate challenges.

Pekka Pakkanen
Executive Vice President
NAPA Shipping Solutions

Research partners' perspective

The timing for the INTENS project has been excellent! When we started the project, the International Maritime Organization (IMO) had just set goals to reduce shipping's total emissions by 50% by 2050 compared to 2008. Finding means to mitigate the global climate change has become an ever-increasing part of R&D for the shipping cluster to respond to the current and future requirements. Significant business can also be seen at the end of the path.

During the past three and a half years, significant research and development resources have been allocated for finding new innovative solutions for smart and green shipping. It has been challenging but also extremely rewarding for such a committed industry-wide consortium consisting of a good number of research and industrial partners! The project provides excellent opportunities for the research partners and researchers to work closely with industrial partners to address the need and challenges faced by the consortium partners and the wider shipping industry in the everyday operations, and to develop innovative solutions to maritime digitalization and decarbonization. A large number of tangible R&D results and products have been achieved, which will further strengthen Finland's global position as a technology-innovation leader in ship design, system integration, building and operation. The consortium has also been able to expand the community and strengthen the research project portfolio both nationally and internationally through a large number of new interesting initiatives.

The visionary INTENS project has provided a great ecosystem networking between people and organizations, and also a unique platform for creating and advancing high-level expertise and new competences for the Finnish maritime cluster, which would not have been possible without the firm commitment and close collaboration within the consortium. The great co-operation has been successful and extremely inspiring! Although the INTENS project is now coming to the end but mutual activities will be surely continued for the benefit of all current and coming partners on an arduous journey towards smart and green shipping!

Johannes Hyrynen
Vice President
VTT Technical Research Centre of Finland, Mobility and Transport

INTENS in numbers

FACTS	
Duration	01.01.2018 – 30-06-2021
Consortium partners	19
Industrial partners	14
Research partners	5
Number of projects	10
Industrial projects	9
Public research project	1
Budget	~13.3 M€
Industrial projects	~10.1 M€
Public research project	~3.2 M€
People involved	~200

Achievements	(realized)	(progressing)	(total)
Product development (software & hardware)	59	8	67
Scientific activities and outputs			
Scientific papers	63	22	85
Scientific abstracts	26	8	34
Theses (MSc & PhD)	13	10	23
Books, chapters, reports, etc.	19	3	22
Patents, invention disclosures, etc.	6	2	8
Public seminars (No. / Presentations)	3/60		3/60
Project workshops (No. / Presentations)	7/45		7/45
Business activities (event, exhibition, etc.)	90	8	98
Projects in collaboration (outside INTENS)	20	4	24
New business and R&D projects			
Number	26	15	41
Volume	~22 M€	~12 M€	~34 M€

List of significant contributors to the INTENS

(in the order of surnames)

Aalto University: Olof Calonius, Janne Huotari, Anton Jokinen, Ossi Kaario, Shervin Karimkashi, Hoang Nguyen Khac, Armin Narimanzadeh, Matti Pietola, Antti Ritari, Kari Tammi, Bulut Tekgül, Ville Vuorinen, Kai Zenger

Deltamarin Ltd: Jyri-Pekka Arjava, Mia Elg, Esa Jokioinen, Arun Krishnan, Ossi Mettälä, Bogdan Molchanov, Matti Tammero, Lien Tran

Dinex Finland Oy: Kauko Kallinen, Teuvo Maunula

LUT University: Jani Alho, Jurii Demidov, Radheesh Dhanasegaran, Andrey Lana, Tuomo Lindh, Henri Montonen, Pasi Peltoniemi, Antti Pinomaa, Olli Pyrhönen, Teemu Turunen-Saaresti, Antti Uusitalo

Meyer Turku Oy: Wilhelm Gustafsson, Tero Mäki-Jouppila, Farbod Raubetean, Kari Sillanpää

NAPA Oy: Risto Kariranta, Kimmo Laaksonen, Pekka Pakkanen

Parker Hannifin Manufacturing Finland Oy: Jagan Gorle

Pinja Oy (Protacon Technologies Oy): Jukka Halme, Esa Tikkanen

Vahterus Oy: Valtteri Haavisto, Kerttu Kupiainen

University of Vaasa: Saana Hautala, Seppo Niemi, Kirsi Spoof-Tuomi, Emmi Söderäng, Xiaoguo Storm

Wärtsilä Oyj Abp: Jari Hyvönen, Heikki Kahila, Heikki Korpi, Juha Kortelainen, Ville Kumlander, Eric Lendormy, Juho Könnö, Jonatan Rösgren

Åbo Akademi University: Jerker Björkqvist, Jari Böling, Salman Gill, Joachim Hammarström, Wictor Lund, Mikael Manngård

VTT Technical Research Centre of Finland: Päivi Aakko-Saksa, Marko Antila, Antti Hynninen, Johannes Hyrynen, Jari Kataja, Päivi Koponen, Juha Kortelainen, Timo Korvola, Jari Lappalainen, Kati Lehtoranta, Jukka K Nurminen, Hannu Rummukainen, Mikko Tahkola, Hannu Vesala, Zou Guangrong

Contents

1. Prediction of on-board energy usage combining physics-based modelling and machine learning

Mikael Manngård[1a], Joachim Hammarström[1a], Wilhelm Gustafsson[2b], Jari Böling[1a], Jerker Björkqvist[1a]
[a] Faculty of Science and Engineering, Åbo Akademi University
[b] Meyer Turku Oy

1.1 Introduction

Global sustainability goals drive the maritime industries to improve the overall energy efficiency of ships. To use energy more efficiently, we first need to understand how energy is being utilized. In this work, a framework for predicting the distribution of energy onboard cruise ship is presented. Predictions are based on available route plans and weather forecasts. A physics-based model of the engine cooling and waste-heat recovery systems is used together with machine learning regression models to predict energy consumption and demand for the next 24 hours. The proposed method is meant to give officers onboard cruise ships a tool for visualizing how their actions affect the onboard energy distribution ahead in time. The proposed method is meant as an aid for making informed decisions related to scheduling and operations which can improve the overall energy efficiency of the vessel.

1.2 Process description

The main components of the cruise ship considered in this case-study are four 4-stroke medium-speed diesel gensets (DG), with a total shaft power of 48 MW, engine cooling systems, propulsion, and other on-board energy consumers. Excess heat from the engine cooling system is extracted by a waste-heat recovery (WHR)

[1] Contact: firstname.lastname@abo.fi
[2] Contact: firstname.lastname@meyerturku.fi

system and used for fresh-water production. Waste heat in exhaust gasses is used for steam conversion which is, for the most part, used for heating.

The engine cooling system in the ship is divided into a high-temperature (HT) and a low temperature (LT) cooling circuit. The HT cooling circuit is used for engine-jacket cooling, high-temperature charge-air cooling (HT-CAC) and for waste-heat recovery (WHR). The LT cooling circuit is used for cooling of the lubrication oil (LO) and for low-temperature charge-air cooling (LT-CAC). Excess heat that cannot be recovered via the WHR-system is transferred to the sea via a seawater heat exchanger (SW-HE). Thus, the engine cooling system, for the most part, can be considered a network of heat exchangers.

1.3 Modeling framework

Cruise ships act as small floating cities and have thus a more varying load compared to cargo vessels of a similar size [1]. It is reasonable to assume that the hotel load on cruise ships experiences a periodic behavior, with 24h periods and with periods corresponding to the port-to-port duration. Such patterns can be learnt from history data. Machine learning models are used to forecast the engine and hotel loads based on available route plans and weather forecasts. The distribution of energy onboard is modeled based on physics.

1.3.1 Physics-based modeling

The dynamic behavior of unit processes onboard a ship is modeled based on mass and heat balances. A model of an engine cooling system has previously been presented in [2] and has been validated against history data. The model was implemented in MATLAB & Simulink. A screen-capture of the cooling-system model for a single diesel engine is presented in Figure 1. The cooling system consists of a series of heat exchangers, heat sources, heat sinks and control valves. Heat exchangers are modeled based on a so-called ‘multi cell’ principle where the heat exchanger is discretized over its length and perfect mixing as assumed within a cell [2,3,4,5]. Ideal control valves are used in the model and PI-based control strategies are used to control the engine jacket, lubrication oil, CAC and LT water temperatures to the desired setpoints.

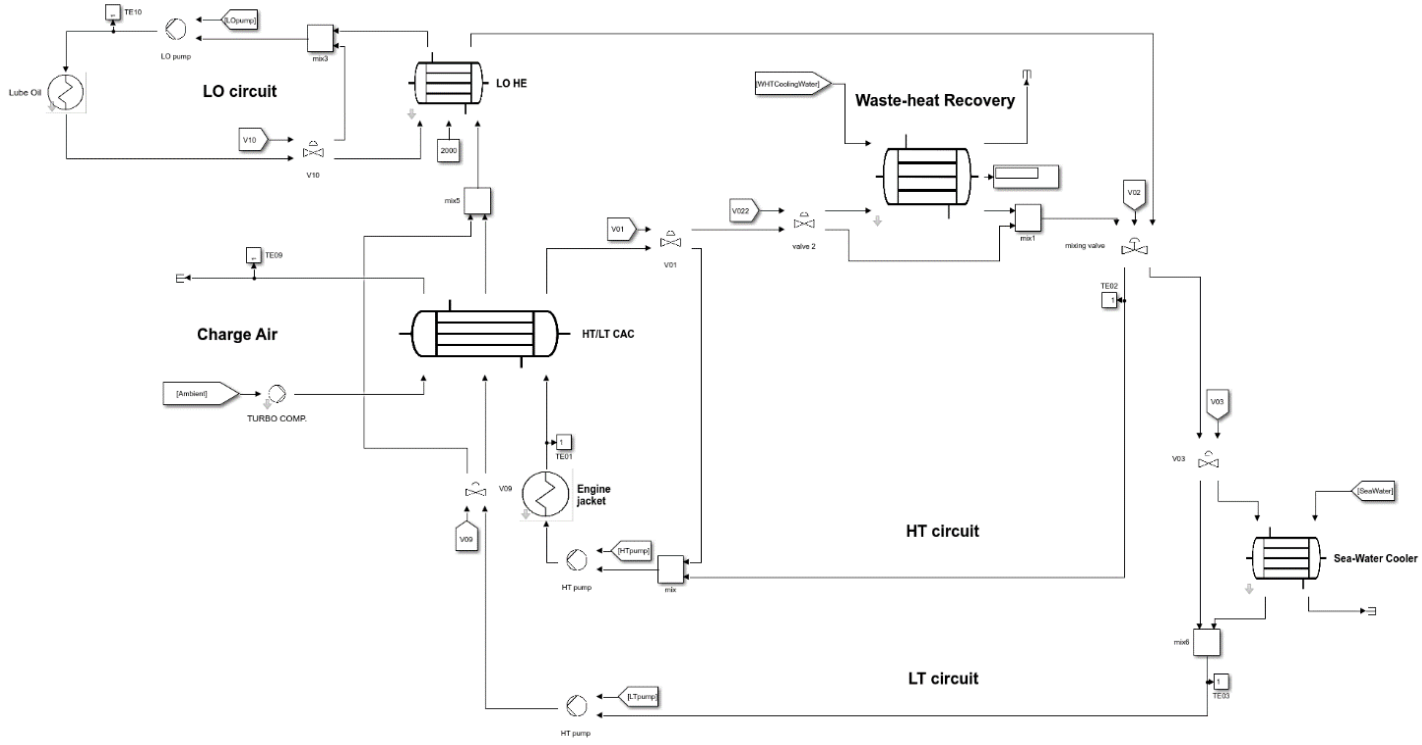

Figure 1. Physics-based model of the engine cooling system implemented in MATLAB & Simulink.

1.3.2 Machine learning models

The machine learning is done with MATLAB's Regression Learner app which supports linear regression models, regression trees, support vector machines (SVM), gaussian process regression (GPR) models and ensembles of trees, see e.g. [6]. Regression models were trained to

(i) Predict the WHR temperature based on the planned cruising speed through water and seawater temperature.
(ii) Predict the engine intake air temperature based on the ambient air temperature and the engine power.
(iii) Predict the total engine power and propulsion power based on the planned ship speed through water.
(iv) Predict the seawater temperature based on coordinates and date.
(v) Calculate the WHR mass-flow rates based on the estimated number of running engines.

The available data is split into training and validation data sets, where 21 days of data is used for training and ten days of data is used for validation. Various machine learning regression models were trained and compared based on the root-mean-square error (RMSE) criteria. Overall, in this case study, the GPR, Bagged Trees and polynomial regression models resulted the lowest prediction errors. A selection of the trained regression models for the estimation of WHR temperature are presented in Table 1.

Table 1. Root mean square error for various machine learning regression models for predicting the waste-heat recovery temperature (°C).

Method	Training RMSE	Validation RMSE
Bagged trees	1.05	2.62
Ensamble models	0.97	2.66
GPR	0.78	2.80
SVM	2.49	2.90

1.4 Results

The power distribution on a 24-hour period where the ship enters and leaves a harbor is presented in Figure 2 (a). During the first 4.5 hours the ship is traveling at 13 knots before entering the harbor. After 11 hours, the ship leaves the harbor after which it travels at full load at approximately 20.5 knots. The 24-hours-ahead predictions of onboard power distribution are presented in Figure 2 (b). Snapshots of the power distribution at various time points are presented in Figure 3. The predicted power distribution at the various time instances matches the measured power within a few percentage points. However, note that the total power at full load (16-24h) is overestimated by approximately 12%. Note also that 13-20% of the total

power is transferred to the sea at any given time. This suggests that it might be possible to achieve a significant improvement in overall energy efficiency by improve waste-heat utilization. Waste-heat utilization can either be improved by scheduling energy consuming tasks (if there are such) at times where there are excess heat available. Alternatively, designs that allow waste-heat to be converted into more usable forms could be considered for future vessels. For example, organic rankine cycle technologies [7,8] can be used to convert waste-heat into electrical power.

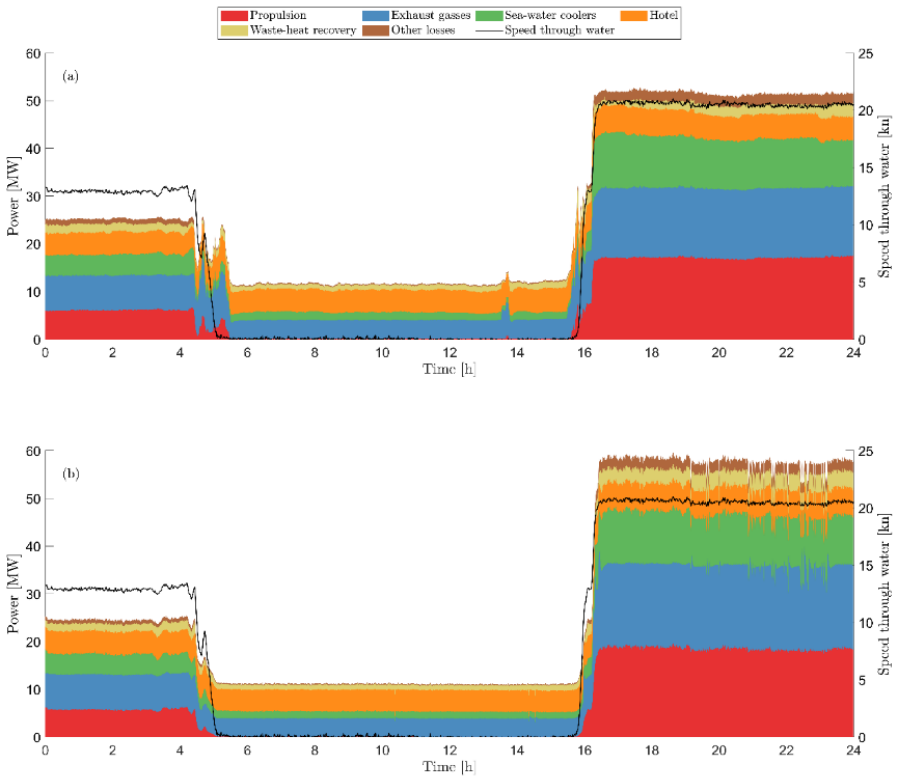

Figure 2. (a) Power distribution based on data, (b) forecasted power used based on the actual route plan.

Figure 3. Measured (left) and predicted (right) power distributions at (a) 4h, (b) 8h, (c) 20h.

1.5 Conclusions

A machine learning and physics-based method for predicting the onboard energy use has been proposed. The proposed method can predict the onboard power distribution 24-hours ahead in time with a prediction error of <3 %-units. Having access to accurate predictions of the onboard energy distribution allows crew and officers onboard to make informed decisions of how their actions affect the overall energy distribution on the ship. For example, optimized scheduling of energy consuming tasks based on the available predictions will result in an increased energy efficiency.

References

[1] Baldi, F., Ahlgren, F., Nguyen, T. V., Thern, M., & Andersson, K. Energy and exergy analysis of a cruise ship. *Energies*, 11(10), 2508, 2018.

[2] Hammarström, J. (2020). Validation of a Digital Twin for a Ship Engine Cooling System. M.Sc. (Tech.) Thesis. Åbo Akademi University.

[3] Varbanov, P. S., Klemeš, J. J. and Friedler, F. Cell-based dynamic heat exchanger models—direct determination of the cell number and size. *Computers & chemical engineering*, 2011;35(5), 943-948.

[4] Mathisen, K. W., Morari, M. and Skogestad, S. Dynamic models for heat exchangers and heat exchanger networks. *Computers & chemical engineering*, 1994;18,459-463.

[5] Manngård, M., Lund, W. and Björkqvist, J. Using Digital Twin Technology to Ensure Data Quality in Transport Systems. Proceedings of the *8th TRA Transport Research Arena*, 2020.

[6] Bishop, C. M. Pattern recognition and machine learning. Springer, 2006.

[7] Sprouse III C, Depcik C. Review of organic Rankine cycles for internal combustion engine exhaust waste heat recovery. *Applied thermal engineering*, 2013;51(1-2), 711-722.

[8] Baldasso E, Gilormini TJ A, Mondejar M. E, Andreasen JG, Larsen LK, Fan J, Haglind F. Organic Rankine cycle-based waste heat recovery system combined with thermal energy storage for emission-free power generation on ships during harbor stays. *Journal of Cleaner Production*, 2020; 271, 122394.

2. New design methods for low-carbon shipping

Bogdan Molchanov[1], Tran Lien[1], Mia Elg[1]
Deltamarin Ltd

2.1 Introduction

2.1.1 Nomenclature

AE	Auxiliary engines
BF	Brute force search method
CST	Condensing type steam turbine
EGB	Exhaust gas boiler
ESD	Energy-saving device
HT ORC	High-temperature organic Rankine cycle unit
IMO	International Maritime Organisation
KPI	Key performance indicators
LT / HT water	Low/High-temperature cooling water
ME	Main engines
NSGA	Non-dominated sorting genetic algorithm
SMCR	Specified maximum continuous rating

2.1.2 The complexity of the Ship Design Process

The ship design process is inherently a complex problem, where several domain experts work as a team with a broad range of regulatory and client requirements to develop a vessel design that is safe and meets all desired design targets. The complexity is especially apparent in the early phases of the ship design when most of the trade-off decisions are made with little design knowledge available. Those decisions are needed to set constraints and narrow down the set of possible solutions.

[1] Contact: firstname.lastname@deltamarin.com

The early ship design phases are typically time-limited, meaning there is rarely enough time to develop a fully new concept from scratch – often the design team utilises reference vessel designs that are close enough to the set targets as a starting point, and then iterative design process is started until all requirements are met. This process is typically referred to as the ship design spiral due to its tendency to converge over several iterations into a satisfactory or superior design, depending on time invested in the process (dashed lines on Figure 1). Figure 1 suggests that, by shifting the design effort to the early stages of projects, more design knowledge is available at the time when decisions are locked, leading to a more efficient design process with fewer changes in the latter design phases and fewer associated costs (continuous lines on Figure 1).

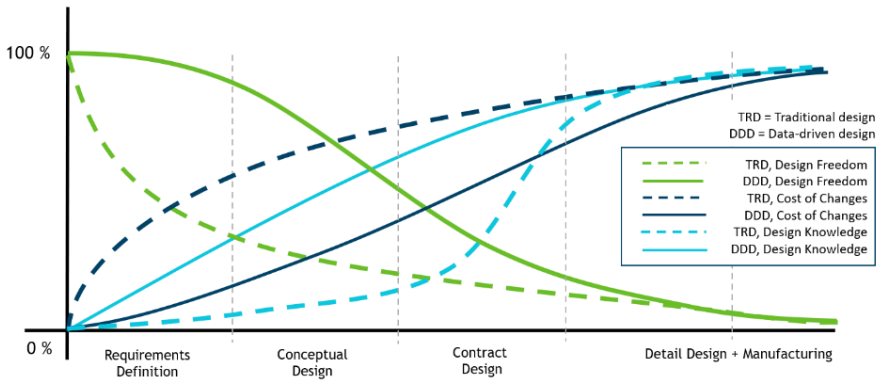

Figure 1. Design Knowledge vs Cost to make changes in early design phases.

Modern design workflows make use of data analysis, parametric models and rapid prototyping, toolboxes, and databases to gain more design knowledge – some of these methods have been covered in [1], such as the DeltaWay method for ship initial concept design. Nevertheless, in addition to ship main parameter sizing, there is also a need to identify various processes that could increase ship sustainability. These processes, such as energy-saving devices (ESDs), are normally studied in a ship project in form of cost-benefit analysis, where energy simulations indicate the fuel-saving or emission reduction potential. During the early ship design phases, the time for these analyses is even more limited than for the ship's main system design and dimensioning.

Together with VTT, we have studied frameworks of simulation-based optimisation [2]. The article at hand focuses on model-based multi-objective optimisation for increasing design knowledge at the early stages of the project. This area of study is limited to finding a set of optimum solutions by maximising the ship's energy efficiency and minimising capital and operational expenditures (CAPEX and OPEX) within a typical concept development project for a newbuild.

2.1.3 Multi-objective optimisation vs manual simulation approach

The standard or manual design approach in the context of energy-efficiency modelling at Deltamarin consists of the steps listed below. Such a process is time-consuming because it requires the designer to manually configure the model and parameters suitable for simulation and analyse all the results so as to find the most promising solutions. This process is typically limited to 10–20 simulations due to time constraints.

1. Collect ship design requirements and targets
2. Collect design documentation and operational data
3. Configure energy flow model to represent the concept ship on an intended operational profile
4. Set up a baseline against which alternative designs are compared (IMO targets, reference ship's KPIs, "default design")
5. Configure tunable parameters for the model such as machinery capacities and combinations of ESDs or operational decisions – anything that can positively influence the energy efficiency of the newbuild
6. Run simulations with alternative technology combinations that seem feasible based on the analyses of the base case and reference designs.
7. Analyse and select cases with the best KPIs or study additional cases until enough feasible design alternatives are found
8. Select the best case together with the client and the design team, and continue to the next phase

Since ship design is a multi-domain problem with varying and sometimes conflicting targets, there exists a set of optimum solutions that represent the best trade-offs between the conflicting targets. Multi-objective optimisation can help find the best trade-off solutions for a given problem that is well formulated. Mathematically the multi-objective optimisation is defined by a set of functions to be minimised or maximised and a set of constraints imposed by physical, safety and design limitations.

If the simulation model were connected to the optimisation routine, the simulation model would become a black box that takes tunable parameters as inputs, and outputs the required results for objective functions back into the optimisation algorithm. Figure 2 illustrates the schematic of the closed-loop cycle interaction of the simulation model and optimisation algorithm. In this way, several hundred to several thousand simulations can be performed and non-optimal solutions will be automatically filtered off. The designer gains both more time for analysis and richer and more accurate results to select from. The drawback of the optimisation is that configuration of the model might be time-consuming if new design targets and design alternatives are introduced.

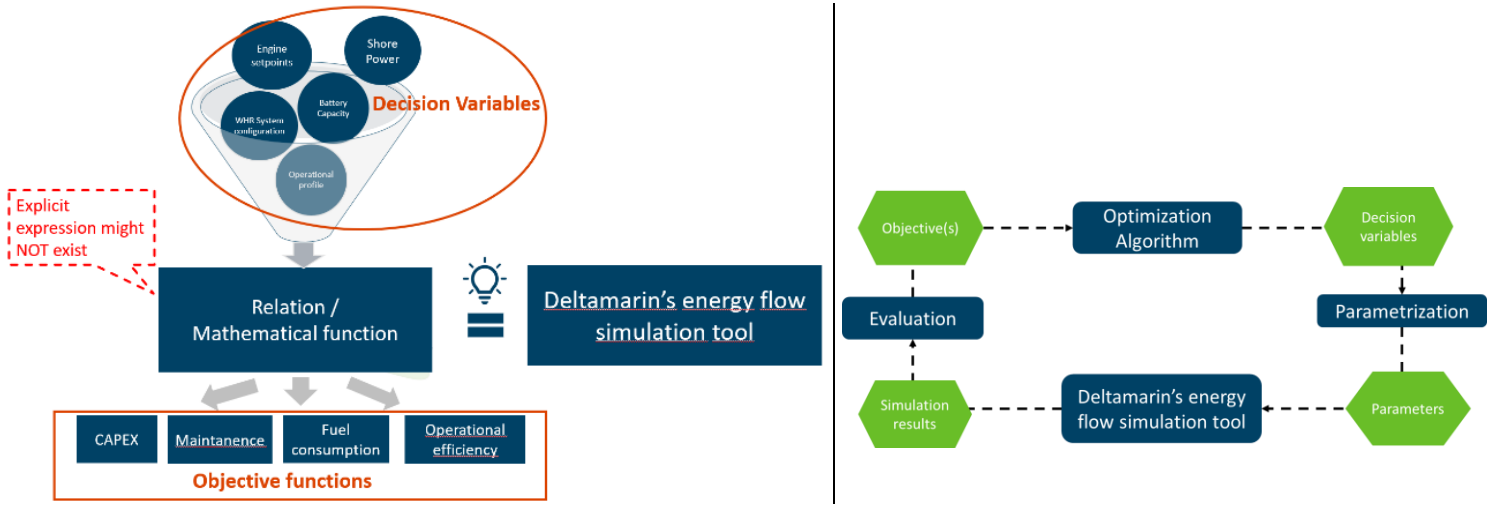

Figure 2. The schematic process of using the parameterised simulation model as a part of the optimisation routine

With the optimisation-driven simulations, the design process changes as described below.

1. – 5. Same as for “Manual Simulations”
6. Translate project goals, constraints and design alternatives into optimisation problems (Table 1)
7. Select optimisation type and configure optimisation settings; run optimisation until a satisfactory coverage of the Pareto frontier is obtained
8. Select best configurations with the team based on further analyses, experiences and client wishes; continue to the next phase

Table 1. Project description translation into an optimisation problem

In Project context:	Examples:	In Optimisation context:
Design Targets	Obtain high energy efficiency with the lowest possible CAPEX	Objective functions
Design alternatives	Types of ESDs, their capacities, setpoints and number of units installed	Decision variables
Design requirements and constraints	Limited deck space, maximum/minimum available machinery capacities	Limits and constraint functions

In this study, the non-dominated sorting genetic algorithm (NSGA-II) was selected for optimisation and the brute force search method (BF) was used for validation of the results. The non-dominated sorting genetic algorithm II, or NSGA-II algorithm, developed by Srinivas and Deb in 2002 is the improved version of NSGA, which was first introduced by Deb in 2001.

Schematically, the NSGA-II algorithm first initialises the population based on the problem range and constraint. Once the initial population has been generated and evaluated, the sorting process starts. The algorithm will carry over the best-performing solutions from previous generations to the next generation. The algorithm will preserve the diversity of the population by selecting not only the best solutions but also considering the density of solutions around each solution – preferring less dense options. The worse-performing solutions are replaced by offspring population from the better performing solution. In addition to crossover, the algorithm includes a mutation, which adds a small degree of randomness to offspring generation, thus increasing diversity and the chances of finding new solutions that would otherwise be impossible by crossover only. The full process is shown in Figure 3.

Brute force search or exhaustive search is a very general problem-solving technique that works by systematically enumerating all possible candidates for the solution and checking whether each candidate satisfies the problem’s statement.

BF always guarantees to find a solution if it exists and is known for its simplicity in implementation. However, the implementation costs are proportional to the number of candidate solutions, which tends to grow very rapidly as the size of the problem increases. In Figure 3 at the bottom, the BF schematic shows all possible combinations of moving from point 1 through points 2, 3, and 4.

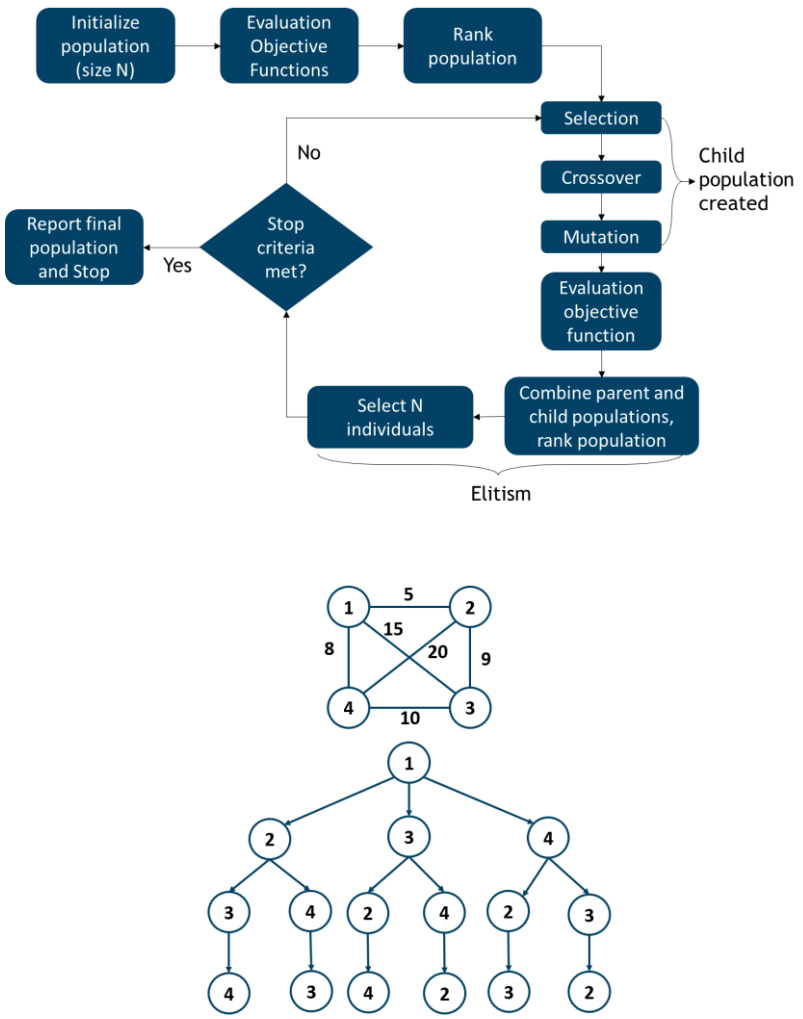

Figure 3. Top: Schematic of the NSGA-II algorithm. Bottom: the brute force search method describing all possible solutions when moving from vertex 1 to other vertices 2, 3, and 4 with their corresponding costs.

2.2 Case description

2.2.1 Case ship

The case ship is a generic RoPax ship that is expected to run on LSHFO fuel on a typical route in the Baltic Sea. The ship particulars are shown in Table 2. It operates on the same operational profile all year round and spends 62% of its time in transit, 3% in manoeuvring, and 35% in port. The machinery configuration with several optional ESDs for waste heat recovery is shown in Figure 4. In addition, battery capacity and shore charging (cold ironing) were also introduced into the study for the case ship. Each main engine is equipped with an exhaust gas boiler (EGB) and HT water heat is recovered after both main and auxiliary engines into a waste heat recovery circuit. The recovered steam and HT heat are prioritised for onboard consumers, and excess heat is available for waste heat recovery equipment.

Table 2. Main particulars of the case ship

Scantling, DWT	23,000
Gross tonnage, GT	65,000
Propulsion configuration	Twin Skeg mechanical propulsion
Main engine arrangement	2 x 4-stroke engines per shaft
Main engine, SMCR	4 x 7,200 kW
Auxiliary engines, SMCR	3 x 2,900 kW
Shaft generators, SMCR	2 x 2,500 kW

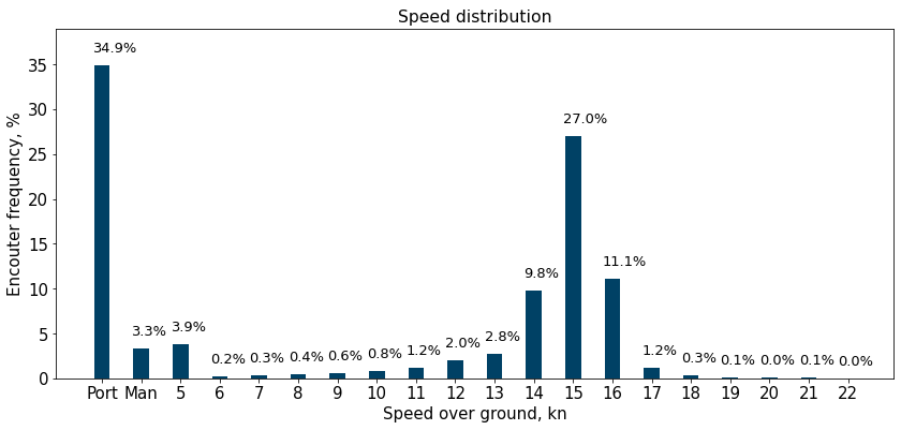

Figure 4. Ship route and annual speed distribution

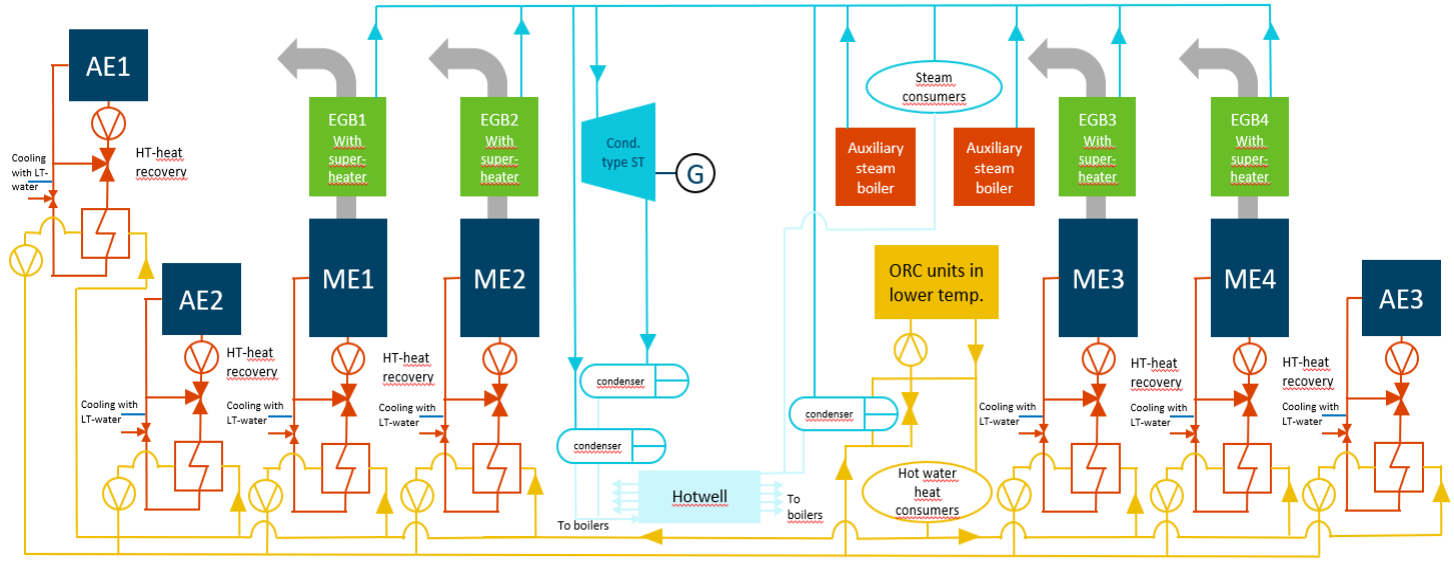

Figure 5. Case ship waste heat recovery principal figure with four main engines (ME) and three auxiliary engines (AE), including various alternatives for waste heat recovery that were design variables in the optimisation task.

2.2.2 Optimisation Problem

The design goal is the same as reported in [2] to find the best trade-off solutions between ESDs' Capex, fuel expenditures and engine running hours. In this case, the propulsion configuration is mechanical, so hours in operation for main and auxiliary engines were considered separately. The decision variables are shown in Table 3.

The objective functions were formulated as shown below:

1. Minimise the total Capex of ESDs, based on prices per kW or per unit as shown in Table 3. Cold ironing was assumed to be already installed, and only available capacity on the shore side could be varied.
2. Minimise average annual fuel consumption by the main, auxiliary engines and boilers combined
3. Minimise the total number of running hours for the main engines
4. Minimise the total number of running hours for the auxiliary engines

Table 3. Decision variables and limits for the optimisation problem

Technology parameter	Unit	Limits	Type	Cost (Capex)
Battery capacity	*kWh*	*0 – 10,000*	*real*	*USD 1,000/kWh*
Battery c-rate	-	*1 – 3*	*integer*	-
Main engine setpoint	*% of M/E SMCR*	*80 – 90%*	*real*	-
Zero emission setpoint	*% of M/E SMCR*	*20 – 40%*	*real*	-
Condensing steam turbine power	*kW*	*300 – 800*	*real*	*USD 700 – 1,000/kW*
Number of hot water-driven organic Rankine cycle units, 150 kW each	*#*	*1 – 6*	*integer*	*USD 310,000unit*
Cold ironing capacity	*kW*	*0 – 10,000*	*real*	-

2.3 Results and discussion

Figure 6 shows the Pareto frontier of the optimisation objectives. The lower left part is a pairwise scatter against each other and the upper right part illustrates where the highest concentration of the pairwise plotted objectives. It shows the trade-off line between conflicting objectives. It can be seen that the benefit of investment in ESDs vs fuel consumption and the number of main engines online is highest up until

5 MUSD, while minimal investment is needed to bring utilisation of AEs down. To confirm how well the Pareto front was covered, the problem was discretised, and the brute force search method was applied, covering about 18,000 possible ESD equipment combinations. The comparison of Pareto front coverage by brute force and NSGA-II is shown in Figure 6 and 7.

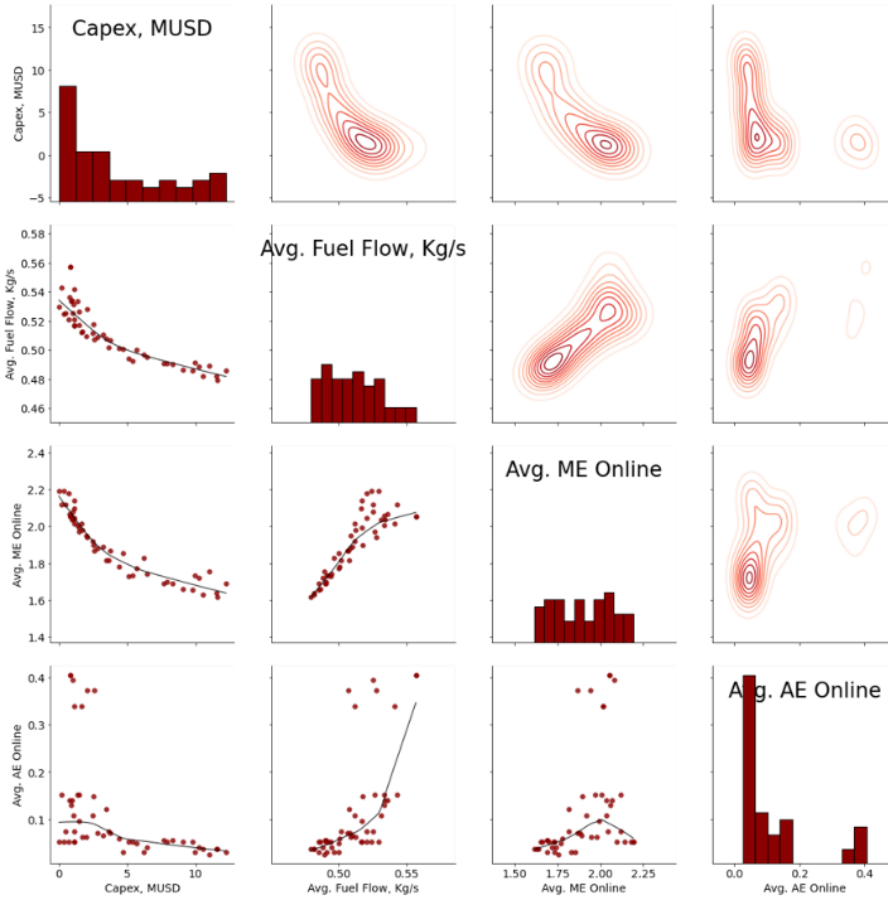

Figure 6. NSGA - II optimisation, optimum solution set only. Population size = 50, generation size = 100

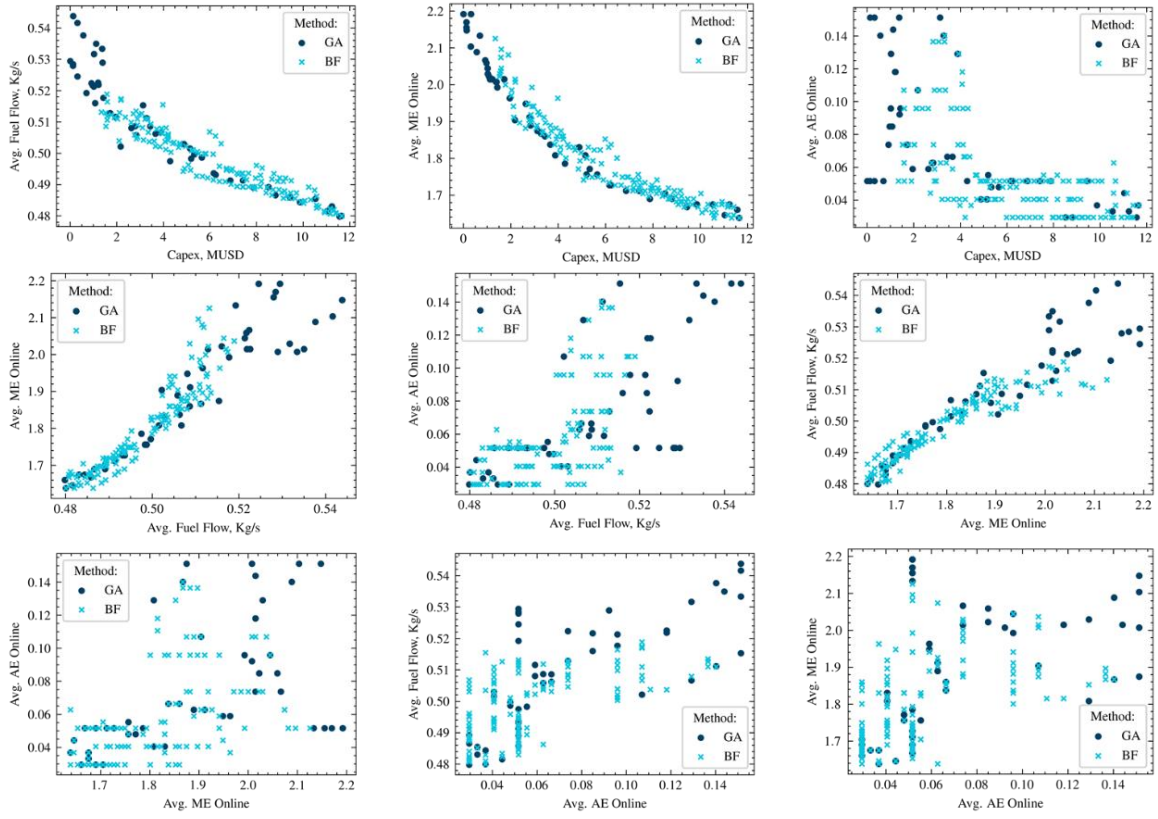

Figure 7. NSGA-II vs brute force Pareto frontier coverage

Table 4. Comparison of brute force, NSGA-II and the traditional approach to energy-efficiency study

	Brute Force search	NSGA-II	Manual
Alternatives studied	18 000	2040	20
Simulation time*	80 hours	15 hours	5 hours
Hypervolume**	1.96	1.65	0.5
Designer's involvement	10 %	25 %	80 %

**Includes model preparation and simulation time*

***A measure of Pareto frontier coverage. Higher value is better*

As part of further analysis, three points representing low (~1 MUSD), medium (~6 MUSD), and high (~12 MUSD) Capex were compared against bare hull design and against the designer's selection from manual simulations. The results of the simulations are shown in Table 5.

Large operational improvements are already possible with minimal investment (Low Capex scenario) by tweaking operational choices and installing minimal ESD capacity on board. The Mid Capex scenario is very close to the selected alternative, at a slightly higher cost but with better performance in other objectives. The maximum investment leads to the best results. It can be seen that, with 10 MWh battery capacity, the number of main engines on-line drops significantly compared to other cases. This means that the battery was preventing 4 main engines from running simultaneously and switching the ship machinery into zero-emission mode at low engine speeds. For hotel load, the main saving was from enabling sufficient shore power capacity, which in this case came at no cost. The second largest improvement came from extending the operational limits of the auxiliary engines due to the presence of a battery in the system, allowing fewer engines to run at a time (Low Capex NSGA-II case). The final savings came from the battery taking over the hotel load at sea when MEs were running at peak capacity to supply propulsion load, and PTO mode was not possible.

Table 5. Comparison of base case and selection from manual simulations vs three solutions from the Pareto-frontier of NSGA-II

		Base Case, 0 Capex	Designer's choice, Manual simulations	Low Capex, NSGA-II	Mid Capex, NSGA-II	High Capex, NSGA-II
Decision variables	Battery capacity, kWh	0	5000	820	4966	9994
	Battery c-rating	1	3	3	3	2
	Cold ironing, max kW	0	5000	7628	6764	9377
	ME cut-off load %	22 %	22 %	33 %	27 %	22 %
	ME set load %	85 %	90 %	85 %	89 %	85 %
	CST SMCR, kW	-	-	377	373	378
	# ORC units, 150 kW eac	0	3	1	4	3
Objective functions	Capex, MUSD	0	5.9 (ref %)	1.1 (-81%)	6.2 (5%)	11.6 (96%)
	Avg Fuel flow, kg/s	0.57 (ref %)	0.51 (-11%)	0.52 (-9%)	0.5 (-13%)	0.48 (-16%)
	Avg # MEs online	2.19 (ref %)	2.16 (-1%)	2.04 (-7%)	1.83 (-16%)	1.62 (-26%)	
	Avg # AEs online	0.61 (ref %)	0.03 (-95%)	0.07 (-88%)	0.03 (-95%)	0.04 (-94%)
Opeartional Performance	AER, *gCO2/(GT * Distance)*	10.27 (ref %)	9.17 (-11%)	9.37 (-9%)	8.94 (-13%)	8.63 (-16%)

2.4 Conclusions

This work focused on streamlining the optimisation process for the early design phases of the shipbuilding process, building on accumulated knowledge from INTENS activities. The goal was to apply optimisation to the selection of the ESD equipment for a RoPax ship where a balance between Capex and the vessel's performance was sought.

One finding of the study is that we already have all the pieces needed to implement optimisation in ship building projects, such as parametric models, design targets, domain expertise, optimisation algorithms and problems suitable for optimisation. The challenge is to connect all these pieces together into a workflow that can fit into the timeline of normal project work.

The optimisation algorithms helped generate thousands of concepts that would be too time-consuming to define and analyse using the manual simulation approach, while Pareto-frontier visualisations have helped filter out less optimal solutions. In addition, the Pareto frontier makes it easier to understand how different targets correlate with each other. In the studied case, there is a clear trade-off between investment cost and energy savings while energy savings correlate almost linearly with the average number of main engines on-line. The brute force method was implemented to verify solutions found by the NSGA-II algorithm. It was found that while generating the largest set of optimal solutions, BF in normal project work must be limited to a small number of decision variables. BF could be done to create a more refined search around the optimum points found using the NSGA-II algorithm.

The results indicate that in the current ship design projects where the number of design variables starts to be large, optimisation brings more confidence and quality to the results. The amount of time spent by the designer in a typical round of manual energy simulations would equal the optimisation method but, in the case example, the optimisation led to better results in terms of the optimisation targets. The expertise of ship energy efficiency engineers is always required in setting up the optimisation problem and further developing the models, including a growing number of variables. Nevertheless, the optimisation method is a powerful addition to covering the entire design space, and we predict that this method will be required in the majority of new ship projects from the start.

Acknowledgments

We thank our INTENS partners from VTT, Timo Korvola and Hannu Rummukainen, for fruitful cooperation and support in preparing our tools for the optimisation framework. We also would like to thank MathWorks for its continuous support in converting our energy model into a format compatible with optimisation routines.

References

[1] M. Elg, J-P. Arjava, M. Tammero, E. Jokioinen, B. Molchanov, and L. Tran, Data driven ship design for digitalizingmaritime industry, in Integrated Energy Solutions to Smart And Green Shipping: 2020 Edition, no. 380, G. Zou and S. Hänninen (Eds.). Finland: VTT Technical Research Centre of Finland, 2020, pp. 9–16.

[2] T. Korvola, M. Elg, O. Mettälä, J. Lappalainen, B. Molchanov, and L. Tran, Taking ship energy efficiency to a new level with cloud-based optimization, in Integrated Energy Solutions to Smart And Green Shipping: 2020 Edition, no. 380, G. Zou and S. Hänninen (Eds.). Finland: VTT Technical Research Centre of Finland, 2020, pp. 24–33.

3. Bayesian optimisation of a ship energy system model

Hannu Rummukainen[1a], Timo Korvola[1a]
Mia Elg[2b], Bogdan Molchanov[2b], Lien Tran[2b]
[a] VTT Technical Research Centre of Finland Ltd
[b] Deltamarin Ltd

3.1 Introduction

Simulation experiments can be used by marine engineers to study the effects of design parameters on ship performance indicators. Despite the growth of computational capacity, an exhaustive simulation of parameter value combinations is only possible in limited cases. Simulation efforts can be effectively focused to the most promising parameter combinations by methods of simulation-based optimisation. The faster and easier it is to perform simulation optimisation studies, the more effective tool they can make for the ship engineering process.

Earlier in the INTENS project we have reported [1,2,3] optimisation experiments using a multiobjective genetic algorithm and a cloud-based simulation framework. As genetic algorithms can be relatively inefficient in the required number of evaluations, i.e. simulation runs, we have experimented with Bayesian optimisation as an alternative multiobjective optimisation method. The goal was to compare the efficiency of Bayesian optimisation with genetic algorithms in ship energy system optimisation, using an updated version of the same optimisation case.

3.2 Multiobjective black-box optimisation methods

In engineering design, there are trade-offs between different objectives, such as cost, emissions, and ship performance. Since there is no single solution that is best on all objectives, alternative solutions have to be carefully considered by the stakeholders to select the most suitable one. The purpose of multiobjective

[1] Contact: firstname.lastname@vtt.fi
[2] Contact: firstname.lastname@deltamarin.com

optimisation methods is to construct a wide variety of alternative efficient solutions that demonstrate different trade-offs between the objectives, for example designs ranging from low-cost low-performance designs to high-cost high-performance designs, with different emission profiles. Specifically, we focused on methods of multiobjective simulation-based optimisation, in which the optimisation algorithm needs to carefully choose the inputs of each simulation run, in order to be effective. In multiobjective optimization, a solution is considered better than another (*dominates* the other solution), if it is better or at least equal in terms of *all* objectives; otherwise the two solutions are non-comparable. A solution is called *Pareto-optimal* or *efficient*, if there is no better solution, i.e. the solution is not dominated by any other solution. Instead of a single optimal solution, there is typically a very large set of Pareto-optimal solutions, which is called the *Pareto front*; see Figure 1.

In challenging optimisation problems, it is usually not practically possible to determine the exact Pareto front, but instead the goal is to find a set of solutions that provides a good approximation of the exact Pareto front. There are many ways to measure how good a proposed solution set is in multiobjective optimisation, with different advantages and weaknesses [4]. In this study, multiobjective optimisation methods were compared in terms of two well-known measures of solution set quality: hypervolume indicator and distance to reference Pareto front. Although only minimisation objectives are discussed in this abstract, the same techniques apply if some objectives are to be maximised instead (such objectives can be simply negated).

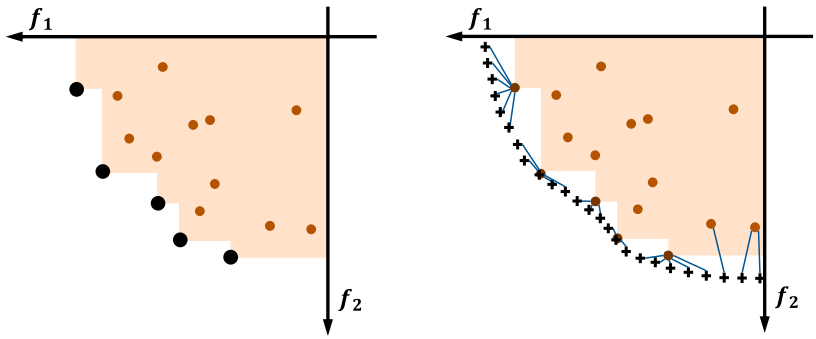

Figure 1. Comparing solution sets in a multiobjective optimisation problem with two minimisation objectives f_1 and f_2. Each round dot represents a single solution produced by some algorithm of interest. On the left, the Pareto-optimal solutions are marked with larger dots. Every other solution is worse on both objectives than some Pareto-optimal solution.
a) The hypervolume of dominated objective space (shaded) extends from the reference point (at the crossing of the f_1 and f_2 axes in the figure) to the Pareto-optimal solutions. A two-dimensional hypervolume is equivalent to area, i.e. the shaded area.
b) Distance to reference Pareto set. The crosses indicate a reference Pareto set, which dominates all algorithm solutions. Blue lines indicate point-to-point distances from each reference Pareto point to the closest algorithm solution. The distance measure is defined as the mean distance from a reference Pareto point to an algorithm solution, equal to the mean length of the blue line segments.

Suppose that the optimisation problem is to find points in a multi-dimensional configuration space X minimising the objectives $f_1, \ldots, f_m$, which are functions from X to the reals $\mathbb{R}$. An optimisation algorithm must produce a solution set $S = \{x_1, \ldots, x_n\}$ in the configuration space X. Each solution $x_i \in X$ has a vector of objective values $F(x_i) = (f_1(x_i), \ldots, f_m(x_i)) \in \mathbb{R}^m$. Both quality measures in this study are defined using the set of objective vectors $F(S) = \{F(x_1), \ldots, F(x_n)\}$.

The **hypervolume indicator** measures how much of the objective space $\mathbb{R}^m$ is dominated by the set of objective vectors. The hypervolume is defined in terms of a *reference point* r that provides an upper bound for the region of interest in objective space. The reference point can be specified directly by the decision maker, or set dynamically based on the objective vectors of the solution set, for example at $(\max_{x \in S} f_1(x), \ldots, \max_{x \in S} f_m(x))$. The indicator is the hypervolume of the region

$$\{y \in \mathbb{R}^m \text{ such that } F(x) \leq y \leq r \text{ for some } x \in S\},$$

which is illustrated by shading in Figure 1a.

Computing the **distance to reference Pareto front** requires a Pareto front of solutions R that is close to the ideal Pareto front (the measure is also known as IGD, "inverse generational distance"). When comparing multiple algorithms, such a Pareto front is easily constructed by joining the results of all the algorithm test runs, and then selecting the Pareto-optimal subset of the joined solution set, i.e. the best known solutions. Even if the objectives are in incomparable units, a distance between objective vectors y and y' can be defined as

$$d(y, y') = \max_{k=1,\ldots,m} \mathrm{w_k} |y_k - y'_k|,$$

where the objective weights can be set e.g. by normalizing the ranges of the objectives with

$$w_k = 1/(\max_{x \in R} f_k(x) - \min_{x \in R} f_k(x)).$$

The distance from solution set S to reference Pareto front R is then defined as

$$\frac{1}{|R|} \sum_{\mathrm{v} \in \mathrm{R}} \min_{\mathrm{x} \in \mathrm{S}} d(F(v), F(x)).$$

In other words, the indicator value is the mean distance from points of the reference Pareto front to the closest solution objective vector. The measure is illustrated in Figure 1b.

Both measures depend on arbitrary parameter choices; the choices noted above work reasonably in practice. Both measures are well behaved in the sense that whenever an algorithm updates the solution set with a new Pareto-optimal solution, the hypervolume indicator either increases or stays the same, and the distance to reference Pareto front either decreases or stays the same.

3.2.1 Multiobjective Bayesian optimisation

In simulation-based optimisation, the objective function values are known only for the configurations that have already been simulated. In Bayesian optimisation, the behaviour of the objective functions at other points of the configuration space is modelled probabilistically, typically by Gaussian process models. For any potential configuration, the probabilistic model provides an estimate of the objective values as a *probability distribution*, in such a way that the values at near-by points in configuration space (similar simulation inputs) are strongly correlated.

In Bayesian optimisation the most promising evaluation points (i.e. the input parameters of the next simulation runs) are chosen by maximising a so-called *acquisition function*, for example the expectation of the improvement over the best currently known solution(s): this is illustrated in Figure 2. The basic mathematics of Bayesian optimisation is well explained in [5], and recent research reviews can be found in [6,7]. To date, multiobjective Bayesian optimisation has received relatively little attention, and few Bayesian optimisation software packages support it.

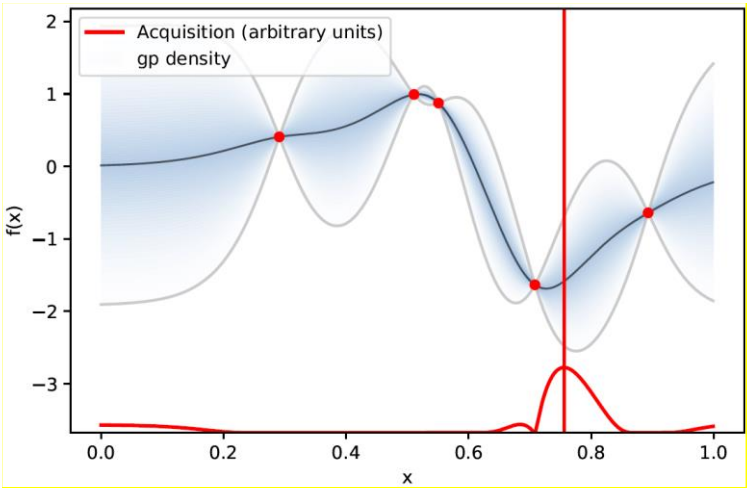

Figure 2. Example of one-dimensional Bayesian optimisation in a minimisation problem. The decision variable is on the x-axis and the function value on the y-axis. Red dots indicate points at which the value of the objective function has been determined. The black line is the estimated mean value, and the grey lines indicate the lower and upper confidence bound (95 % confidence interval) of possible function values. The red curve at the bottom indicates the expected improvement acquisition function: the next function evaluation is performed at the x-value indicated by the vertical line, at which the expected improvement is the largest.

The easy way to apply single-objective optimisation methods to multiobjective problems is to combine the multiple objectives into a single objective, for example as a weighted linear scalarisation $\sum_{k=1}^{m} \mathrm{w_k} y_k$, or a weighted maximum (Chebyshev) scalarisation $\max_{k=1,\ldots,m} \mathrm{w_k} y_k$. Different points on the Pareto front can be then found by varying the weights. Random weighted scalarisations were already

applied in the earliest multiobjective Bayesian optimisation algorithm, the ParEGO algorithm of Knowles [8]. It must be noted that with varying weights, the Chebyshev scalarisation can find the entire Pareto front, whereas the linear scalarisation is limited to a subset of Pareto-optimal points unless the Pareto front is convex.

As an alternative to weighted scalarisation, the hypervolume indicator described above provides a natural objective for multiobjective optimisation. Using a Bayesian model of the objective function, it is possible to estimate the expected hypervolume improvement (EHVI) from evaluating a given configuration, so that EHVI can be used as an acquisition function in multiobjective Bayesian optimisation [9].

3.2.2 Optimisation methods compared

Seven different multiobjective optimisation methods were tested in the case study on two optimisation problem variants. All algorithms were provided the same capability of 25 parallel simulations, i.e. the objectives of 25 solutions could be evaluated in parallel. A baseline for the comparison was provided by running a random search algorithm.

Random The decision variables were selected from a uniform random distribution.

Two different multiobjective genetic algorithms from the Opt4J library [10] were run. Both were configured with a population of 50 solutions (in experiments, populations of 30 or 40 performed significantly worse, and a population of 100 about the same as 50). The initial population of 50 was generated from a uniform random distribution. On each generation 25 new solutions were created using, as in [11], binary tournament selection and a cross-over probability of 90 %. The algorithms differed in how a population of 50 solutions was then selected for the next iteration.

NSGA2 NSGA-II of Deb et al. [11] selects solutions using a so-called *crowding distance* metric, aiming to find solutions that are evenly distributed around the Pareto front.

SMS SMS-EMOA of Beume et al. [12] selects solutions using the so-called S-Metric, maximising improvement in hypervolume with a penalty term for solutions inside the dominated hypervolume of the best current Pareto front.

Four different multiobjective Bayesian optimisation algorithms were run. All were initialised with 30 solutions selected from a uniform random distribution, to get sufficient accuracy from the first Gaussian process estimation step. The hyperparameters of the Gaussian processes were estimated automatically from data by all the algorithms (*automatic relevancy determination*). Some algorithms performed better when the objectives were manually scaled to similar ranges: these are noted specifically below.

qParEGO A variant of the ParEGO algorithm of Knowles [8], in which the evaluations that are currently running in parallel are explicitly considered in the expected improvement acquisition function. The implementation of the algorithm in the BoTorch library was used through its Ax front-end [13]. The objectives were scaled manually.

EHVI Expected hypervolume improvement over a Gaussian process model, formulated in a differentiable form by Daulton et al. [9] The implementation in the BoTorch library was used through its Ax front-end [13]. Due to performance reasons, the explicit consideration of parallel evaluations was disabled. The reference point for hypervolume computation was provided manually.

Dragonfly Another variant of the ParEGO algorithm [8], in which alternative acquisition functions are used in an adaptive manner. The implementation is from the Dragonfly library [14,15]. The explicit consideration of parallel evaluations was disabled to improve performance. The objectives were scaled manually.

GRAMBO An experimental gradient-based multiobjective Bayesian optimisation algorithm. The algorithm was based on a differentiable formulation of the S-Metric [12], which combines hypervolume improvement with penalty terms for solutions within the dominated hypervolume, using the differentiable function sampling approach of Wilson et al. [17] and the hypervolume scalarisation approach of Zhang and Golovin [18]. Parallel evaluations were explicitly considered. The reference point for hypervolume computation and the scaling of the objectives were set dynamically by the algorithm. Other hyperparameters were adjusted manually during algorithm development, using variant B of the optimisation problem described in Section 3.3.

3.3 Case description

The engineering case concerns the retrofit of energy-saving and emission-reducing technologies on a generic 4000-passenger cruise ship with a diesel-electrical propulsion plant. The retrofit options included battery capacity for reducing fuel usage and emissions, and several alternative technologies for waste heat recovery: organic Rankine cycle (ORC) units connected to either steam or high-temperature water circuits, condensing steam turbines, and back-pressure steam turbines. The problem is to decide how many units of each technology to install at what capacity. Alternative designs were evaluated on three objectives: capital investment cost, fuel usage and main engine running hours. The fuel usage objective is linked to CO_2 emissions. Engine running hours are relevant to maintenance requirements, and together with fuel usage can be linked to the operational cost of the design.

An energy system simulation model was implemented by Deltamarin in the Matlab Simulink environment. The simulation followed a representative one-year profile of vessel propulsion and hotel power usage. For optimisation purposes, we ran a compiled version of the model in a cloud computing environment, so as to enable parallel simulations.

The case is an extended version of the one reported last year [3]. At that point, the simulation could fail on unexpected combinations of input parameter values, which caused difficulties for the optimisation process. The model has now been updated to properly simulate all energy system configurations within the optimisation case study.

3.3.1 Optimisation problem variants

Two variants of the optimisation problem were defined, as condensing steam turbines and back-pressure steam turbines could not be simultaneously installed in the simulation model. Here the variants are referred to as problem B and problem C. The energy system retrofit options were specified in the optimisation by the following decision variables. The "Problem" column indicates which variables were included in which problem.

Variable	Range	Unit	Description	Problem
batt_cap	0 – 10 000	kWh	Total battery capacity installed	B, C
sorc_n	0 – 8	-	Number of steam ORC units	B, C
htorc_n	0 – 8	-	Number of high-temperature-water ORC units	B, C
bpst_n	0 – 4	-	Number of back-pressure steam turbines	B
bpst_P	100 – 1000	kW	Size of back-pressure steam turbines	B
cst_n	0 – 4	-	Number of condensing steam turbines	C
cst_P	400 – 1000	kW	Size of condensing steam turbines	C

The solutions were evaluated in terms of the following objectives. All three objectives were to be minimized. The "Reference point" column indicates the reference values used in the reported hypervolume computations.

Objective	Unit	Description	Reference point
capex	k€	Capital expenditure	17 500
fuel	kg/s	Average fuel consumption over the entire operation profile	1.21
n_me	-	Average number of main engines in operation	2.75

The capital expenditure was computed as

$$\text{capex} = 1\ \text{k€/kWh} \cdot \text{batt\_cap} + 300\ \text{k€} \cdot \text{n\_sorc} + 300\ \text{k€} \cdot \text{n\_htorc} + 1\ \text{k€/kW} \cdot \text{n\_bpst} \cdot \text{bpst\_P} + 1\ \text{k€/kW} \cdot \text{n\_cst} \cdot \text{cst\_P}$$

3.4 Results

The progress of the algorithms is compared by hypervolume in Figures 9 and 10, and by distance to reference Pareto front in Figures 11 and 12. The algorithms were stopped after 6 h or 1500 evaluations, whichever came first. Figure 13 illustrates Pareto fronts after 2 hours of optimisation.

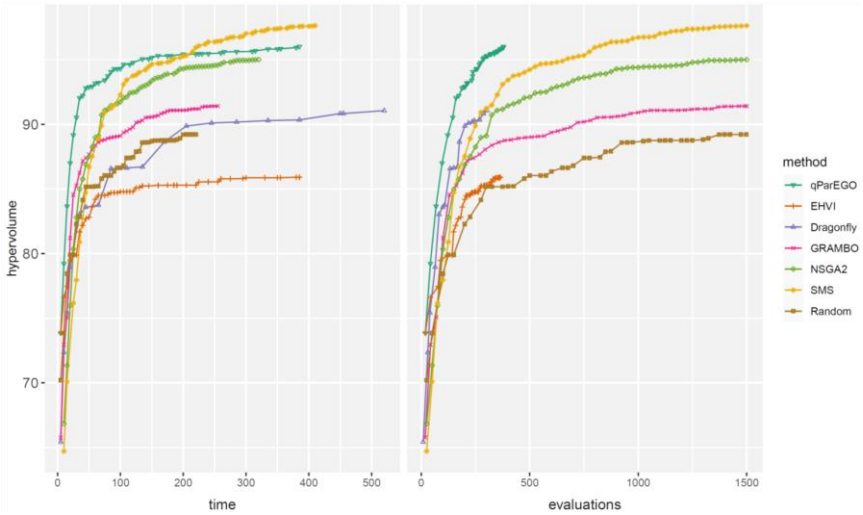

Figure 3. Hypervolume growth on problem B as a function of time in minutes (left) and number of simulation runs (right).

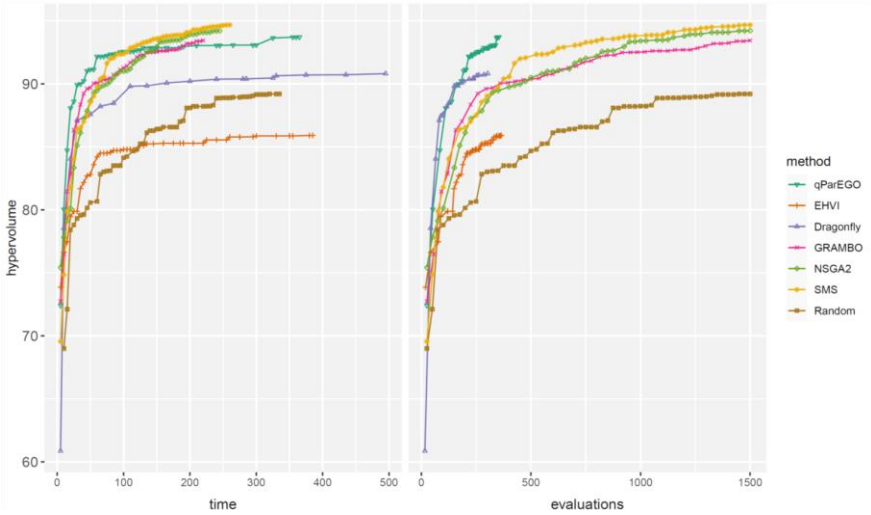

Figure 4. Hypervolume growth on problem C as a function of time in minutes (left) and number of simulation runs (right).

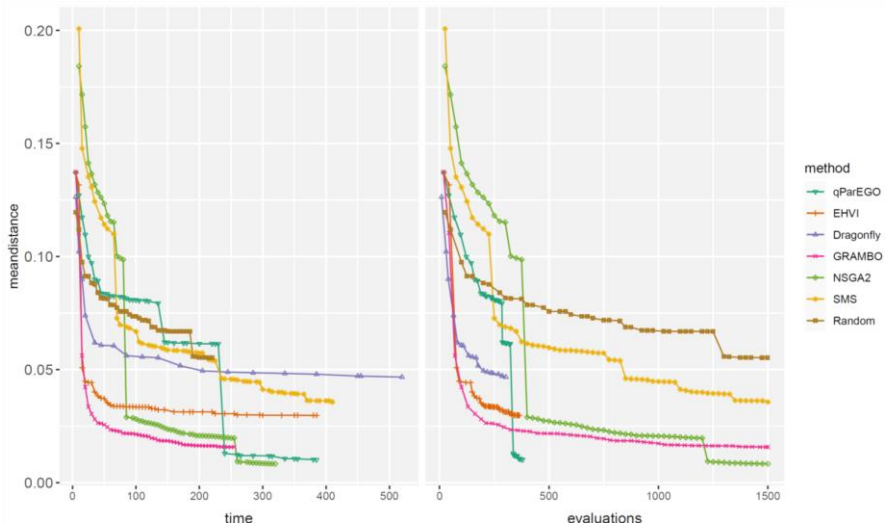

Figure 5. Distance to reference Pareto set on problem B as a function of time in minutes (left) and number of simulation runs (right).

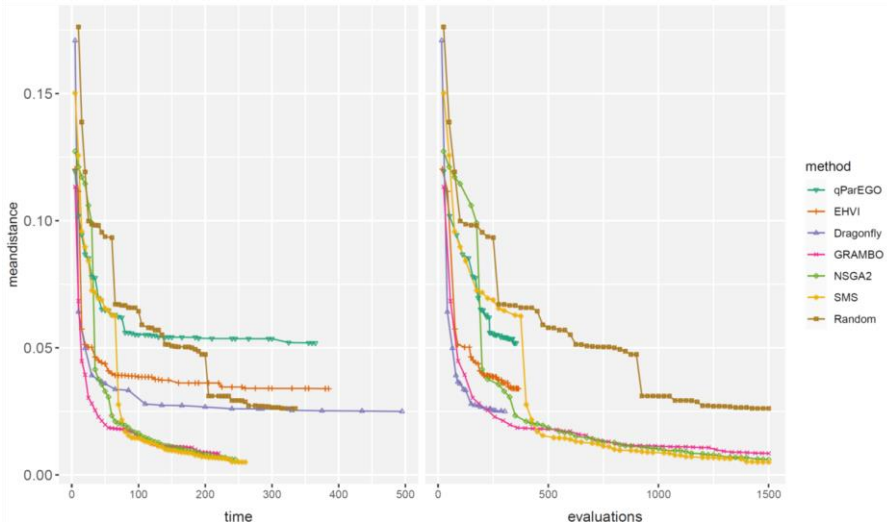

Figure 6. Distance to reference Pareto set on problem C as a function of time in minutes (left) and number of simulation runs (right).

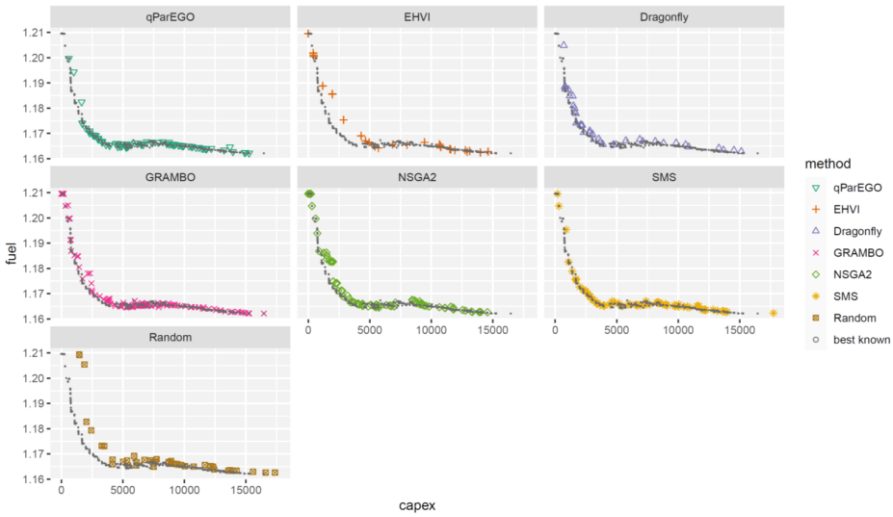

Figure 7. Comparison of Pareto fronts in terms of capex and fuel objectives after 2 hours of optimization on problem C. The Pareto front of each algorithm is shown in a separate subplot. For comparison, every subplot includes black dots that indicate the best known Pareto-optimal solutions, as produced by any algorithm over 6 hours of optimization time.

3.5 Conclusions from the algorithm comparison

Overall, there were substantial differences in speed, accuracy and sample efficiency between the algorithms. There were also clear differences in algorithm behaviour on the two variant optimisation problems, even though the problem variants were very similar. Based on visual inspection of Pareto front plots such as Figure 13, the general shape of the objective function trade-offs was nevertheless found by all algorithms in 1–4 h. The indicators in Figures 9–12 show that the best algorithms continue steadily improving even after 4 h, although these improvements were not very visible in plots such as Figure 13.

As a simple example of a ship design issue, consider how to cost-effectively decrease fuel usage with minimal capital expenditure. As can be seen in the leftmost parts of the capex-fuel plots of Figure 13, the region was not well explored by all algorithms. The region was best covered in 2 h by GRAMBO, NSGA-II, and SMS, less well by Dragonfly and qParEGO, and there were significant gaps in the results of EHVI and Random.

The Bayesian optimisation algorithms Dragonfly, qParEGO and GRAMBO started very strongly on some of the metrics, and less well on others. EHVI was particularly problematic and may have needed more parameter tuning to perform well in this case study. Compared to genetic algorithms, Bayesian optimisation algorithms generally needed fewer simulations for similar results, but except for GRAMBO they spent so much computation time to determine the next simulation inputs that they could not effectively use the available simulation capacity.

Moreover, Bayesian optimisation algorithms slowed down over time. As the simulation time of the case model was on the order of 3–5 minutes, and 25 parallel simulations were in use, an optimisation algorithm should be able to pick the next evaluation point in approximately 10 seconds to be effective. Of the Bayesian optimisation algorithms, only GRAMBO was able to reach this level of performance, due to the use of fast function approximations, but in the latter stages of optimisation runs GRAMBO lost efficiency due to the inaccuracy of the approximations.

The Bayesian optimisation algorithms also needed more case-specific parameter settings and tuning effort compared to genetic algorithms. For example, Dragonfly and qParEGO, which applied random weighted scalarisation, needed manual objective function scaling to perform well – and they still left some extremes of the objective function ranges sparsely explored.

The NSGA-II algorithm, and to a lesser extent the SMS algorithm, are well established robust tools with many available software implementations. Importantly they were able to provide competitive results with their default parameter values, and only minimal speed tuning was performed. Overall NSGA-II and SMS performed similarly, but NSGA-II appeared to obtain better Pareto front coverage on problem B.

Multiobjective Bayesian optimisation tools are still maturing, and the algorithms in the case study required several parameter adjustments to compete with NSGA-II and SMS. Nevertheless, it can be concluded that the best Bayesian optimisation tools can compete with genetic algorithms and beat them on specific metrics, especially if the simulation model is particularly slow, or computation time is strictly limited.

Acknowledgement

We gratefully acknowledge CSC for providing their cloud computing services.

References

[1] J. Lappalainen, T. Korvola, and J. K. Nurminen, Cloud-based framework for optimising complex systems including dynamic simulation, in Integrated Energy Solutions to Smart And Green Shipping: 2019 Edition, no. 354, G. Zou, Ed. Finland: VTT Technical Research Centre of Finland, 2019, pp. 36–40.

[2] J. Lappalainen, T. Korvola, J. K. Nurminen, V. Lepistö, and T. Mäki-Jouppila, Cloud-based framework for simulation-based optimization of ship energy systems, in Proceedings of the 2nd International Conference on Modelling and Optimisation of Ship Energy Systems, 2019, pp. 65–71.

[3] T. Korvola, M. Elg, O. Mettälä, J. Lappalainen, B. Molchanov, and L. Tran, Taking ship energy efficiency to a new level with cloud-based optimization, in Integrated Energy Solutions to Smart And Green Shipping: 2020 Edition, no. 380, G. Zou and S. Hänninen (Eds.). Finland: VTT Technical Research Centre of Finland, 2020, pp. 24–33.

[4] E. Zitzler, L. Thiele, M. Laumanns, C. M. Fonseca, and V. Grunert da Fonseca, Performance Assessment of Multiobjective Optimizers: An Analysis and Review, IEEE Transactions on Evolutionary Computation 7(2), 2003, pp. 117–132.

[5] D. R. Jones, M. Schonlau, and W. J. Welch, Efficient Global Optimization of Expensive Black-Box Functions, Journal of Global Optimization 13, 1998, pp. 455–492.

[6] B. Shahriari, K. Swersky, Z. Wang, R. P. Adams, and N. de Freitas, Taking the Human out of the Loop: A Review of Bayesian Optimization, Proceedings of the IEEE 104(1), 2016, pp. 148–175.

[7] S. Greenhill, S. Rana, S. Gupta, P. Vellanki, and S. Venkatesh, Bayesian Optimization for Adaptive Experimental Design: A Review, IEEE Access, 8, 2020, pp. 13937–13948.

[8] J. Knowles, ParEGO: A Hybrid Algoriithm With On-Line Landscape Approximation for Expensive Multiobjective Optimization Problems, IEEE Transactions on Evolutionary Computation 10(1), 2005, pp. 50–66.

[9] S. Daulton, M. Balandat, and E. Bakshy, Differentiable Expected Hypervolume Improvement for Parallel Multi-Objective Bayesian Optimization, Advances in Neural Information Processing Systems 33 (NeurIPS 2020), 2020.

[10] M. Lukasiewycz, M. Glaß, F. Reimann, and J. Teich, Opt4J – A Modular Framework for Meta-heuristic Optimization, Proceedings of the Genetic and Evolutionary Computing Conference (GECCO 2011), Dublin, Ireland, 2011, pp. 1723—1730.

[11] K. Deb, S. Agrawal, A. Pratap, and T. Meyarivan, A Fast Elitist Non-Dominated Sorting Genetic Algorithm for Multi-Objective Optimization: NSGA-II, Proceedings of the 6th International Conference on Parallel Problem Solving from Nature (PPSN 2000), 2000, pp. 849–858.

[12] N. Beume, B. Naujoks, and M. Emmerich, SMS-EMOA: Multiobjective selection based on dominated hypervolume, European Journal of Operational Research 181, 2007, pp. 1653–1669.

[13] M. Balandat, B. Karrer, D. R. Jiang, S. Daulton, B. Letham, A. G. Wilson, and E. Bakshy, BoTorch: A Framework for Efficient Monte-Carlo Bayesian Optimization, Advances in Neural Information Processing Systems 33 (NeurIPS 2020), 2020.

[14] B. Paria, K. Kandasamy, B. Póczos, A Flexible Framework for Multi-Objective Bayesian Optimization using Random Scalarizations, arXiv preprint arXiv:1805.12168, 2018.

[15] K. Kandasamy, K. R. Vysyaraju, W. Neiswanger, B. Paria, C. R. Collins, J. Schneider, B. Póczos, and E. P. Xing, Tuning Hyperparameters without Grad Students: Scalable and Robust Bayesian Optimisation with Dragonfly, arXiv preprint arXiv:1903.06694, 2019.

[16] J. T. Wilson, V. Borovitskiy, A. Terenin, P. Mostowsky, and M. P. Deisenroth, Efficiently Sampling Functions from Gaussian Process Posteriors,

Proceedings of the 37th International Conference on Machine Learning (PMLR 119), 2020, pp. 10292–10302.

[17] R. Zhang and D. Golovin, Random Hypervolume Scalarizations for Provable Multi-Objective Black Box Optimization, Proceedings of the 37th International Conference on Machine Learning (PMLR 119), 2020, pp. 11096–11105.

4. Physical system classification from measurement data – case exhaust gas economizer

Mikko Tahkola[1]
VTT Technical Research Centre of Finland Ltd

4.1 Introduction

Signal classification has been utilized, for example, in clinical diagnosis and digital communication applications. Neural network-based approaches have been proposed for electroencephalography [1] and electrocardiogram signal classification to detect a cardiac arrhythmia, i.e., too fast, too slow or irregular heart rhythm [2]. [3] proposed a deep learning-based approach for signal classifier development to identify used modulation type and wireless technology. Authors in [4] proposed a support vector machine-based signal classification model development method for wireless signal identification. A new method for distinguishing radio frequency devices using signal classification was proposed in [5]. Marine domain applications of signal classification include, for example, fault diagnosis applications. In [6], a model is developed to classify healthy conditions, engine gain faults, shaft speed sensor and propeller pitch sensor faults.

Here, a classification model is developed to classify exhaust gas economizers using measurement data. Random convolutional kernel transform method is utilized to convert the measurement data for the classifier training. Cross-validation (CV) is used to estimate model's generalization performance. Hyperopt Python-library is used to evaluate different classifier types and hyperparameters within CV. The effect of input segment length, i.e., the length of time-series that the classification is based on, is evaluated by repeating the experiment with four different lengths from 2h to 8h.

[1] Contact: firstname.lastname@vtt.fi

4.2 Exhaust gas economizer

Maximum thermal efficiency of large maritime engines is practically around 50%, i.e., that amount of the energy contained in the fuel can be converted into usable form while the rest is dissipated as heat mainly via engine water cooling systems and exhaust gases. Typically, the heat of the exhaust gases is utilized in steam production using exhaust gas economizers (as shown in Figure 1) to increase the efficiency of the energy conversion on a ship. Consequently, the higher efficiency leads to lower fuel consumption as well as decreased GHG emissions.

Figure 1. Water tube exhaust gas economizer from Alfa Laval. (https://www.alfalaval.com/products/heat-transfer/boilers/exhaust-gas-economizer/aalborg-xw/, 25.3.2021)

4.3 Case study – classification of exhaust gas economizers

The case study dataset contains measurement data from exhaust gas economizers with different capacities. There are eight exhaust gas economizers in total, including four economizers with 2500 kg/h mass flow capacity in the water side, two economizers with 920 kg/h and another two economizers with 680 kg/h capacities respectively. The exhaust gas economizers are group into two WHR subsystems with the same total capacity. In each subsystem, there are two economizers with 2500 kg/h capacity, one with capacity of 920 kg/h and similarly one with 680 kg/h capacity. The largest economizers are used to recover heat from main engines of the ship, whereas the smaller ones make use of auxiliary engine exhaust gases to produce steam.

Due to the unavailability of measurement data from the water side of the economizers, the water side mass flows were derived from other measurements using energy balance equation. For this purpose, a few assumptions were made. Specifically, the water was assumed to enter the exhaust gas economizer as saturated water and to exit it as saturated steam. Thus, the enthalpies of saturated water and steam at each time instance can be obtained using enthalpy tables and

pressure information of two boilers that the two subsystems mentioned above are connected to. Next, the heat flow from exhaust gas side to the water side, $\dot{Q}_{eg}$, in each economizer is estimated using Equation 1.

$$\dot{Q}_{eg} = \dot{m}_{eg} \times c_{p\_eg} \times \left(T_{eg\_2} - T_{eg\_1}\right) \qquad \text{Equation 1}$$

where $\dot{m}_{eg}$ is the exhaust gas mass flow [kg/h], c_{p_eg} is the specific heat capacity of exhaust gas (1 kJ/kg°C, assumed to be constant), and T_{eg_1} and T_{eg_2} are the exhaust gas temperatures before and after the economizer, respectively.

The estimated heat flows and water side enthalpies are then used to compute the water side mass flows, $\dot{m}_{ws}$, using Equation 2.

$$\dot{m}_{ws} = \frac{\dot{Q}_{eg}}{h_{ws\_2} - h_{ws\_2}} \qquad \text{Equation 2}$$

where h_{ws_1} and h_{ws_2} are the enthalpies of water and steam, respectively.

The computed water side mass flows are visualized in Figure 2.

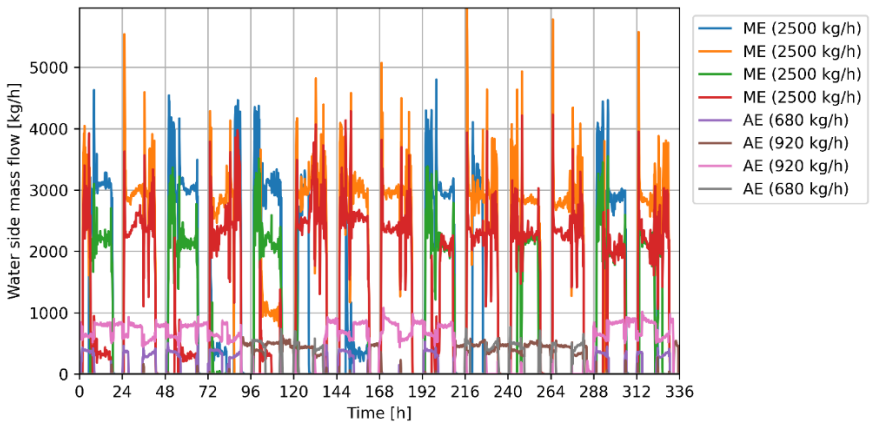

Figure 2. Computational water side mass flows in the exhaust gas economizers. ME and AE stands for economizers of main engine and auxiliary engine, respectively.

The exhaust gas economizer identification was formulated as a classification problem by giving each economizer a unique class identifier and by labelling the measurement data with these identifiers. The labelled data was next split into development and independent testing datasets. 80% of the samples starting from the beginning of the time-series forms the development dataset, and the rest 20% forms the testing dataset. Both datasets were then split into overlapping segments (i.e., windows). To compare how the segment length affects the model performance, four separate versions of the datasets were created with segment lengths of 20, 40, 60, and 80 time-steps respectively. In each case, the overlapping of successive segments was fixed to 50%. Next, the segments where the exhaust gas

economizers were practically not in use were removed by setting a minimum mass flow limit of 5 kg/h for the mean of values in the segments.

Classifier development was done in Python environment. Five classifiers of different type were included in the model search. These included AdaBoost, k-nearest neighbors, logistic regression, and random forest classifiers implemented in Scikit-learn library [7], and open-source CatBoost library [8] that is based on gradient boosting. The model's generalization performance was estimated with 8-fold cross-validation procedure. Sequential model-based optimization algorithm Tree of Parzen Estimators (TPE) implemented Hyperopt [9] was used within CV to find the best performing model. The TPE algorithm was initialized first with 50 randomly chosen models and hyperparameter, followed by 50 guided iterations.

Random convolutional kernel transformation (ROCKET) method [10] was used to convert the windowed measurement data into features to be used as input for the classifiers. In hyperparameter optimization, possible values for the number of kernels in ROCKET were 250, 500, …, 2500. Logistic loss function implemented in Scikit-learn library was used to rank the 100 models trained within CV, balanced accuracy scores (BACs) were computed for the models, and the one achieving the best logistic loss was reported. Here, Scikit-learn's implementation of BAC computation was used. Finally, a model with the best found hyperparameters was trained on the whole training dataset and tested using independent test dataset.

4.3.1 Results

AdaBoost classifier from Scikit-learn library obtained the highest CV score with all four input segment lengths. Therefore, the results shown in Table 1 represent accuracies of AdaBoost classifiers. As expected, the longer segment length resulted in higher score than short ones. This holds for BACs obtained from CV and on independent testing dataset. The CV score increases from 61.2% up to 80.4% when increasing the segment length from 2 hours to 8 hours. The BACs on independent testing dataset are slightly lower than the corresponding CV scores with the same segment length. This might be due to relatively small amount of training data, more difficult samples in the testing data or slight overfitting despite the CV. To confirm this, one could repeat the experiment multiple times, using different samples for development and testing each time. Naturally, suitable segment length depends on the application and the available data.

Table 1. Balanced accuracy of AdaBoost classifiers computed in CV and on independent testing dataset.

	Balanced accuracy	
Segment length	**CV**	**Independent testing data**
20 (2 hours)	61.2%	53.6% (-7.6%)
40 (4 hours)	64.7%	60.0% (-4.6%)
60 (6 hours)	68.5%	66.0% (-2.4%)
80 (8 hours)	80.4%	70.3% (-10.1%)

Economizer-specific recall and precision scores of the final AdaBoost classifiers trained with different input segment lengths are shown in Figure 3 and 4, respectively. Recall quantifies the fraction of true positive predictions among the number of true positive and false negative predictions, i.e., the fraction of correctly classified cases among the total number of examples in the dataset corresponding to that class. Precision quantifies the fraction of true positive predictions among the number of true and false positives, i.e., how often the prediction is correct when a specific class is predicted.

There are clear differences between the recall and precision scores for different economizers. For example, recalls for EGEs 1, 4, and 6 are low with each segment length but recalls for EGEs 5 and 7 are above 80% and 90%, respectively. Recall for EGE 6 even decreases by increasing the segment length but on the other hand, the precision for EGE 6 increases. The average of economizer-specific recall scores shows that, in general, the recall increases by increasing the segment length. The same trend is seen in precision scores, although the average precision is 0.7% lower with 6-hour segments than with 4-hour segments.

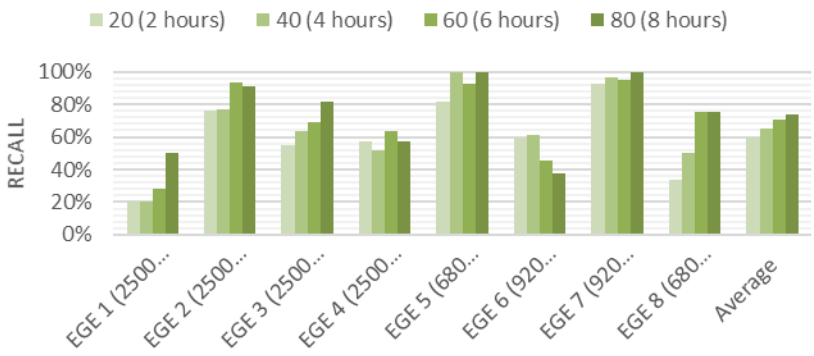

Figure 3. Economizer specific recall score of AdaBoost classifiers trained with different input segment lengths.

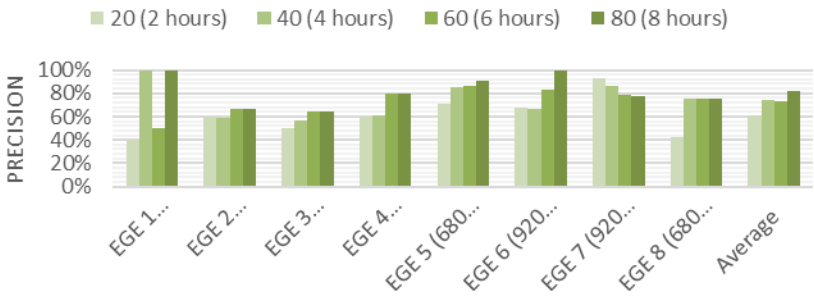

Figure 4. Economizer specific precision score of AdaBoost classifiers trained with different input segment lengths.

4.4 Conclusions

The generalization performance of models developed with four different input segment lengths was evaluated using CV procedure. With each segment length, AdaBoost classifier was found to be the most accurate in identifying the correct exhaust gas economizer. With segment length corresponding to 2 hours of real time, the generalization performance measured as balanced accuracy was 61.2%, whereas with the longest segment length that corresponds to 8 hours of real time, the BAC was 80.4%.The BACs on independent testing data were 7.6% and 10.1% lower compared those of CV. The results show that a classifier with acceptable accuracy can be developed for identifying exhaust gas economizers from measurement data, although there was relatively small amount of data available.

References

[1] G. Zhang *et al.*, "A Dynamic Multi-Scale Network for EEG Signal Classification," *Front. Neurosci.*, vol. 14, no. January, pp. 1–10, 2021, doi: 10.3389/fnins.2020.578255.

[2] Z. Xiong, M. P. Nash, E. Cheng, V. V. Fedorov, M. K. Stiles, and J. Zhao, "ECG signal classification for the detection of cardiac arrhythmias using a convolutional recurrent neural network," *Physiol. Meas.*, vol. 39, no. 9, 2018, doi: 10.1088/1361-6579/aad9ed.

[3] M. Kulin, T. Kazaz, I. Moerman, and E. De Poorter, "End-to-End Learning from Spectrum Data: A Deep Learning Approach for Wireless Signal Identification in Spectrum Monitoring Applications," *IEEE Access*, vol. 6, pp. 18484–18501, 2018, doi: 10.1109/ACCESS.2018.2818794.

[4] K. Tekbiyik, O. Akbunar, A. R. Ekti, A. Gorcin, and G. Karabulut Kurt, "Multi-dimensional wireless signal identification based on support vector machines," *IEEE Access*, vol. 7, pp. 138890–138903, 2019, doi: 10.1109/ACCESS.2019.2942368.

[5] X. Wang, Y. Zhang, H. Zhang, Y. Li, and X. Wei, "Radio Frequency Signal Identification Using Transfer Learning Based on LSTM," *Circuits, Syst. Signal Process.*, vol. 39, no. 11, pp. 5514–5528, 2020, doi: 10.1007/s00034-020-01417-7.

[6] J. Zhou, Y. Yang, and R. Liu, "Fault diagnosis system design for ship propulsion system via classification," *Chinese Control Conf. CCC*, pp. 7285–7289, 2017, doi: 10.23919/ChiCC.2017.8028507.

[7] F. Pedregosa *et al.*, "Scikit-learn: Machine Learning in Python," *J. Mach. Learn. Res.*, vol. 12, pp. 2825–2830, 2011.

[8] A. V. Dorogush, V. Ershov, and A. Gulin, "CatBoost: Gradient boosting with categorical features support," *arXiv*, pp. 1–7, 2018.

[9] J. Bergstra, D. Yamins, and D. D. Cox, "Making a Science of Model Search:

Hyperparameter Optimization in Hundreds of Dimensions for Vision Architectures," in *ICML 2013*, 2013, no. 28, pp. 115–123.

[10] A. Dempster, F. Petitjean, and G. I. Webb, "ROCKET: exceptionally fast and accurate time series classification using random convolutional kernels," *Data Min. Knowl. Discov.*, vol. 34, no. 5, pp. 1454–1495, 2020, doi: 10.1007/s10618-020-00701-z.

5. Towards optimal design and management of future ship energy systems

Janne Huotari[1], Antti Ritari[1], Kari Tammi[1]
Aalto University

5.1 Introduction

We present a summary of our research on ship energy system design and control optimization. The primary goal of the developed models was to produce solutions that alleviate the ongoing energy transition in the marine sector. The shipping sector is undergoing an energy transition that will last for multiple decades to come. This energy transition aims at reducing total greenhouse gas emissions from shipping by 50 % by 2050, compared to values in 2008 (IMO, Strategy on the reduction of GHG emissions from ships, 2018). Growing environmental awareness of stakeholders and regulatory pressure are the driving forces behind this transition.

Carbon dioxide, sulfur oxide, nitrogen oxide and particulate matter emissions of ships are regulated in MARPOL Annex VI (IMO, Index of MEPC resolutions and guidelines related to MARPOL Annex VI, 2020a). The emission of carbon dioxide is currently regulated by the so-called energy efficiency design index, which mandates that a certain energy efficiency level is reached by newbuilds. However, planned amendments to MARPOL Annex VI will consider the environmental impact of existing ships as well, incentivising retrofits that increase energy efficiency and carbon intensity reduction through operational measures (IMO, Draft amendments to the marpol convention would require ships to combine a technical and an operational approach to reduce their carbon intensity, 2020). Effective methods for energy efficient ship system design and their operation must be envisioned now because the ships built today will operate through the foreseen energy transition.

Our research focuses on novel ship energy systems and their management. For the last century, ship energy systems have relied on internal combustion engines (ICE) to produce power required for propulsion and hotel loads. Introducing alternative power sources into the energy system, such as energy storages or fuel

[1] Contact: firstname.lastname@aalto.fi

cells (Baldi;Moret;Tammi;& Maréchal, 2020), or energy saving devices like waste heat recovery systems can be an effective way to increase the overall efficiency of the ship. Assessing the benefit of these systems requires the development of advanced tools. Our research demonstrates methods to assess the impact of these new systems and establishes novel control methods for future ship energy systems.

5.2 System level design optimization

Optimization-based approach to the assessment of ship energy system alternatives involves formulating the design problem as a mathematical optimization problem. A number of decision variables, which can be either discrete or continuous, define the design. The quality of the design is a function of the decision variables according to an objective function, which is typically a measure of cost. The decision variables, which influence the objective, are varied in order to attain the minimum of the objective function.

The decision variables are categorized as either concerning the plant design (e.g. power rating of an electrical machine) or control design (e.g. motor torque). The plant design can be further divided to three interconnected layers: (i) connections between components (topology), (ii) component technology and (iii) sizing. Since all the four design levels are typically coupled and influence each other, a simultaneous analysis of these levels ensures that the optimal design is not excluded.

Installation decisions of components in plant design optimization give rise to binary (yes/no) decision variables. The resulting problem is then inherently combinatorial and scales exponentially in the worst case as the problem size increases. Mathematical programming offers remarkable advantages for solving combinatorial problems. The solver codes allow exploitation of convexity structure in problems and the elimination of large part of the search space. This removes the need to exhaustively enumerate all the combinations of discrete choices.

The authors have contributed to system level design optimization by formulating mixed integer linear programming (MILP) problems for simultaneous design and heat integration optimization (Ritari;Huotari;Tammi;& Narimanzadeh) and scheduling of low emission technology investments and vessel dockings (Ritari;Spoof-Tuomi;Huotari;Tammi;& Niemi). Both of these models take as an input measured operation profiles from case vessels. This ensures that the resulting problems are relevant for industry, but also lead to incorporation of hundreds of binary variables and large-scale combinatorial problems. However, despite the resulting complexity, convergence to a good solution is typically attained in a few seconds, which demonstrates the power of state-of-the-art solver codes for mixed-integer programming problems.

5.3 Ship energy system unit commitment optimization

Energy system control can be divided into unit commitment and lower level control. The goal of unit commitment is to come up with a high-level strategy for the energy

system, answering questions such as: “Should generating set nr. 3 start in 5 minutes?”. On the contrary, lower level control ensures that the plan laid out by unit commitment is carried out efficiently, usually with traditional control engineering approaches. The research discussed here is focused on the unit commitment problem of complex energy systems.

Ship energy systems with ICEs as the sole energy providers are typically controlled via rule-based control systems, which encode actions to measured values. An example could be to start a new generating set when a certain power demand threshold is reached. Such methods are robust and simple to create but suffer from scaling issues when the underlying system becomes more complicated. For example, introducing an energy storage into the energy system decouples energy production from demand in the time domain, making control of such a system infeasibly complex for rule-based approaches.

Novel solutions to the unit commitment problem in complex energy systems tend to rely on mathematical optimization (Kanellos, 2013), (Anvari-Moghaddam;Dragicevic;Meng;Sun;& Guerrero, 2016), (Paran;Vu;El Mezyani;& Edrington, 2015), (Van Vu;Gonsoulin;Diaz;Edrington;& El-Mezyani, 2017), (Haseltalab;Negenborn;& Lodewijks, 2016). An off-line control approach was taken in (Kanellos, 2013) and (Anvari-Moghaddam;Dragicevic;Meng;Sun;& Guerrero, 2016), where a linear optimization model is solved assuming that the future demand profile is known. On-line approaches based on mathematical optimization were studied in (Paran;Vu;El Mezyani;& Edrington, 2015), (Van Vu;Gonsoulin;Diaz;Edrington;& El-Mezyani, 2017) and (Haseltalab;Negenborn;& Lodewijks, 2016) by formulating a model predictive control (MPC) model of the energy system. In MPC models, a prediction of power demand for example is used to optimise the instantaneous response of the energy system. This procedure is repeated continuously to increase the accuracy of the model. However, previous research into this topic usually assumed some a priori knowledge of the future power demand profile or then used a short prediction horizon. Optimal and automatic creation of a rule-based expert system for the unit commitment of a ship’s energy system was studied in (Radan, 2008).

Our research on the topic of ship energy system unit commitment focused on developing online control methodologies that did not depend on a known future power demand profile. A self-learning reinforcement learning algorithm was implemented in (Huotari;Ritari;Vepsäläinen;& Tammi, Q-Learning Based Autonomous Control of the Auxiliary Power Network of a Ship, 2019), where control responses were learned based on previously measured data. MPC was utilised in (Huotari;Ritari;Vepsäläinen;& Tammi, Hybrid ship unit commitment with demand prediction and model predictive control, 2020) where the future power demand profile was estimated based on the predicted future speed profile of the ship. To support the MPC model, a convex model for the optimization of a ship’s high-fidelity speed profile was the subject of most recent research. In addition to these models, an optimisation model concerning the use of a Flettner rotor for additional propulsion was developed in (Maruccia, 2019) and a convex optimisation model of a fuel cell

ferry for the purpose of unit commitment and speed profile optimisation was formulated in (Katzenburg, 2021).

5.3.1 Reinforcement learning

Reinforcement learning (Sutton & Barto, 1998) is a subgroup of machine learning, where an agent learns to adopt actions in an environment that maximize a numerical reward signal. The environment is formulated as a collection of possible states and actions in those states, formally called a Markov Decision Process (MDP). Numeric rewards are assigned to each state in the MDP, which simulates the benefit of reaching that state. The agent learns in this environment through trial and error, by trying out actions in different states and updating its knowledge about the environment using a value function:

$$v_\pi(s) = \sum_a \pi(a|s) \sum_{s',r} p(s', r|s, a)[r + \gamma v_\pi(s')],$$

Where $v_\pi(s)$ is the value of state *s* when following a sequence of actions given by policy $\pi(s)$, *a* is a possible action to take, *r* is the reward for reaching state *s* and *s'* is the next state reached by choosing action *a* in state *s*. $\pi(a|s)$ is the probability of choosing action *a* in state *s*, γ is a discount factor of future rewards and $v_\pi(s')$ is value, or expected cumulative sum of rewards, of the next state *s'*. Because the value function is iterative, through multiple iterations the agent learns the true value of each state, which depends on the immediate reward for reaching that state, and the expected cumulative rewards attainable from that state onwards. If the true value of each state is known, it is easy to derive an optimal control policy by selecting an action that leads to the state with the highest value. The benefit of reinforcement learning is that it is very flexible in terms of what can be modelled, and it has been previously used to control tasks that were previously impossible with other methods (Silver, ym., 2016). Furthermore, compared to dynamic programming, from which the methodology is originally derived from, reinforcement learning models do not have much computational overhead once the model has been trained. However, the models are notoriously difficult to train and sensitive to hyperparameter tuning.

For the purposes of ship energy system unit commitment, the energy system of a ship was modelled as an MDP in (Huotari;Ritari;Vepsäläinen;& Tammi, Q-Learning Based Autonomous Control of the Auxiliary Power Network of a Ship, 2019), where the states represented different legs on a journey, and the actions were chosen to be the on/off switching of generating sets. The rewards structure of states was based on fuel consumption at a certain state, with massive negative rewards assigned to undergoing a black-out. The model was trained based on data recorded from real journeys of the ferry Silja Serenade that operates in the Baltic Sea. The reinforcement learning model was successfully trained for the task of unit commitment of four generating sets, operating them close to optimal without undergoing black outs. The research demonstrated the applicability of the method

to the task, although more complex energy systems would require the use of methods that are still being researched.

5.3.2 Model predictive control

The unit commitment model developed in (Huotari;Ritari;Vepsäläinen;& Tammi, Hybrid ship unit commitment with demand prediction and model predictive control, 2020) combined the use of rule-based control, power demand prediction via machine learning and MPC. As a case study, the energy system was modelled to contain generator sets, a battery, and a fuel cell as power producers. Furthermore, the control system was given an additional goal of minimising the usage of fossil fuels near coasts. The resulting model performed unit commitment of the complex energy system near optimally.

The optimization model used in MPC was formalised by modifying the model developed in (Ritari;Huotari;Halme;& Tammi, 2020). The operating principle of the model was the following:

1. predict future power demand profile
2. optimise unit commitment for the rest of the journey
3. take the first action in the optimised unit commitment plan and
4. return to step 1.

The future power demand profile prediction was formulated as a novel combination of Gaussian process modelling (Rasmussen, 2006) and Bayesian ridge regression (Bishop, 2006). The prediction was formatted based on the future speed profile of the ship, which was assumed to be known throughout the journey. Since the optimization interval was set at 5 minutes, i.e. the frequency of going through the steps listed above, the model needed some simple control logic to follow between optimization steps. A rule-based control logic was developed for this task.

Since actual measured power demand profiles for the studied ship were available, the performance of the model could easily be tested against fully optimal control. The fully optimal control reference was attained by feeding the model the actual power demand profile, rather than the predicted one. It was demonstrated that the developed MPC model operated near optimally by saving 11.8 % in fuel consumption compared to 12.6 % savings with fully optimal control. These savings were calculated by comparing the control result to the actual measured ship operation data. Fossil fuel consumption near coasts was reduced by 68 % on average.

Since the developed MPC model relied on an estimate of the ship's future speed profile, current research was focused on ship speed profile optimization. For this purpose, a convex optimization model was developed as an extension to existing speed profile optimization methods. The results showed that the convex model reduced computational load of speed profile optimization significantly, and increased the fuel saving potential of the produced speed profile. Furthermore, the resulting optimised speed profile was continuous, while previous research on the

subject had mostly focused on methods that produce a discrete speed profile (Thalis;Harilaos;& Li, 2020). This is important especially in the context of using the speed profile for future power demand estimation.

5.3.3 Convex optimization

While solving general nonlinear programming (NLP) problems is very challenging, formulating an optimization model in a convex manner allows efficient and reliable solving of large scale and complex NLPs. During the last decade, algorithms and modelling tools for convex optimization have almost reached the level of linear programming. This modelling paradigm has gained popularity in many engineering optimization applications, in particular in optimal control problems (OCPs), although applications in the maritime field have been scarce.

In his MSc thesis, Katzenburg (Katzenburg, 2021) formulated an optimal control problem of fuel cell ferry. Convex models of vessel dynamics, fixed pitch propeller and fuel cell were demonstrated. This large-scale nonlinear programming problem, which incorporated over a hundred thousand variables and constraints, was solved under a few seconds with a standard desktop computer.

5.4 Discussion and conclusion

The optimization and machine learning based design and control methodologies discussed in this work enable the transition from conventional ship design based on heuristics, design rules and estimations, towards a systematic exploration of the design space. Formal optimization procedures have the promise of obtaining the best design instead of only a workable system that satisfies basic requirements. Given the increasingly strict environmental constraint facing the shipping industry, the adoption of advanced design methodologies is urgently called for. Optimized system attains the lowest cost, which is essential for scaling the low emission technologies and delivering the reality of a sustainable green shipping future.

Most optimization tasks in ship design are characterized by a combination of distinct decisions, represented by binary variables, and complex interactions described by nonlinear functions. These problems belong to the class of mixed-integer nonlinear programming (MINLP) problems, which are in general difficult to solve or even intractable. However, solution techniques for MINLP problems are constantly improving, and significant advances have been demonstrated in recent years. A particular subclass of MINLP, convex MINLP, shows great promise for many real-world optimization tasks in ship design. Convex MINLP is a versatile modelling paradigm with a number of advantageous properties, including availability of solver algorithms that guarantee convergence to the global optimum and the minimal tuning effort required.

Ship energy systems with multiple different types of power producers are expected to play a role in the ongoing maritime energy transition (DNV-GL, 2018). However, multiple power sources require significantly more advanced decision-

making systems in terms of unit commitment control. We presented three distinct and novel methodologies for this purpose: a machine learning model based on reinforcement learning, a predictive model where unit commitment was optimised utilizing mixed integer linear programming, and a convex optimisation model that included the longitudinal dynamics of the vessel. These models were developed based on measured operational data of actual ships. Furthermore, we introduced a novel convex optimisation model for the optimisation of a ship's speed profile under a fixed schedule. The developed models presented in this paper form a cohesive ensemble of methods for supporting the ongoing maritime energy transition.

References

[1] IMO. 2018. "Strategy on the reduction of GHG emissions from ships,". [Online]. Available: http://www.imo.org/en/MediaCentre/HotTopics/GHG/Pages/default.aspx. [Accessed 27 August 2020].

[2] IMO. 2020. "Index of MEPC resolutions and guidelines related to MARPOL Annex VI,". [Online]. Available: https://www.imo.org/en/OurWork/Environment/Pages/Index-of-MEPC-Resolutions-and-Guidelines-related-to-MARPOL-Annex-VI.aspx. [Accessed 7 December 2020].

[3] IMO. 2020. "Draft amendments to the marpol convention would require ships to combine a technical and an operational approach to reduce their carbon intensity,". [Online]. Available: https://www.imo.org/en/MediaCentre/PressBriefings/pages/42-MEPC-short-term-measure.aspx. [Accessed 7 August 2020].

[4] F. Baldi, S. Moret, K. Tammi and F. Maréchal. 2020. "The role of solid oxide fuel cells in future ship energy systems," Energy, vol. 194.

[5] A. Ritari, J. Huotari, K. Tammi and A. Narimanzadeh. 2020. "Optimization of heat integrated ship systems," Integrated Energy Solutions to Smart And Green Shipping: 2020 edition, vol. 380, pp. 80-88.

[6] A. Ritari, K. Spoof-Tuomi, J. Huotari, K. Tammi and S. Niemi. 2021. "Lifecycle optimization of ship energy system configurations under gradually tightening emission constraints," Manuscript in progress.

[7] F. Kanellos. 2013. "Optimal power management with GHG emissions limitation in all-electric ship power systems comprising energy storage systems," IEEE Transactions on power systems, vol. 29, pp. 330-339.

[8] A. Anvari-Moghaddam, T. Dragicevic, L. Meng, B. Sun and J. M. Guerrero. 2016. "Optimal planning and operation management of a ship electrical power system with energy storage system," Annual Conference of the IEEE Industrial Electronics Society, vol. 42, pp. 2095-2099.

[9] S. Paran, T. Vu, T. El Mezyani and C. Edrington. 2015. "MPC-based power management in the shipboard power system," IEEE Electric Ship Technologies Symposium (ESTS), pp. 14-18.

[10] T. Van Vu, D. Gonsoulin, F. Diaz, C. Edrington and T. El-Mezyani. 2017. "Predictive control for energy management in ship power systems under high-power ramp rate loads," IEEE Transactions on Energy Conversion, vol. 32, pp. 788-797.

[11] A. Haseltalab, R. Negenborn and G. Lodewijks. 2016. "Multi-level predictive control for energy management of hybrid ships in the presence of uncertainty and environmental disturbances," IFAC, vol. 49, pp. 90-95.

[12] D. Radan. 2008. Integrated control of marine electrical power systems, NTNU, Fakultet for ingeniørvitenskap og teknologi.

[13] J. Huotari, A. Ritari, J. Vepsäläinen and K. Tammi. 2019. "Q-Learning Based Autonomous Control of the Auxiliary Power Network of a Ship," IEEE Access, vol. 7, pp. 152879-152890.

[14] J. Huotari, A. Ritari, J. Vepsäläinen and K. Tammi. 2020. "Hybrid ship unit commitment with demand prediction and model predictive control," Energies, vol. 13, no. 18.

[15] A. Maruccia. 2019. Optimisation model for a ship's hybrid energy system with a Flettner rotor, MSc thesis. Aalto University, Espoo, Finland.

[16] N. Katzenburg. 2021. Convex programming for optimal control of a fuel cell hybrid ferry, MSc thesis. Aalto University, Espoo, Finland.

[17] R. Sutton and A. Barto. 1998. Introduction to reinforcement learning, Cambridge: MIT press.

[18] D. Silver, A. Huang, C. J. Maddison, A. Guez, L. Sifre, J. Van Den Driessche, I. Schrittwieser, V. Antonoglou and M. Panneershelvam et al. 2016. "Mastering the game of Go with deep neural networks and tree search," Nature, vol. 529, p. 484.

[19] A. Ritari, J. Huotari, J. Halme and K. Tammi. 2020. "Hybrid electric topology for short sea ships with high auxiliary power availability requirement," Energy, vol. 190.

[20] C. E. Rasmussen. 2006. Gaussian processes in machine learning, MIT Press.

[21] C. M. Bishop. 2006. "Pattern recognition and machine learning," Springer, pp. 152-158.

[22] Z. Thalis, P. Harilaos and D. Li. 2020. "Ship weather routing: A taxonomy and survey," Ocean Engineering, vol. 213.

[23] DNV-GL. 2018. "Assessment of selected alternative fuels and technologies," DNV-GL-Maritime.

6. Hybrid system modelling: Hardware-in-the-loop testing and visualization of virtual vessel operation

Ville Kumlander[1]
Wärtsilä Oyj Abp

6.1 Introduction

INTENS project offered a great platform to develop different concepts around hybrid vessels, which, in this case, referred to a battery assisted vessels. We will present the reader two different concepts in this topic: Hardware-In-the-Loop (HiL) testing and computer application development. HiL makes it possible to connect real components and machines with simulation models. With computer application development, results from virtual vessel simulation can be made more appealing. First part of this extended abstract will focus on HiL and the second part on the application development. Conclusions and list of references are given in the end.

6.2 Hardware-in-the-loop

Hardware-In-the-Loop, commonly known as HiL, offers an efficient way to test a component or a machine as part of a larger system. The idea of HiL is to connect real components with simulation models. In this paper, an internal combustion engine (ICE) is operating in a closed loop with a model of virtual vessel propulsion system. HiL concept introduces more realistic operation conditions to test engine's functionalities compared to a test where constant load is given to an engine.

HiL concept was developed together with VEBIC, which is a platform for research and innovation hosted by University of Vaasa. In parallel, there were Wärtsilä internal activities around this topic and the test results presented in this paper are from the test conducted in Wärtsilä laboratory.

[1] Contact: firstname.lastname@wartsila.com

The aim of the HiL testing is to make the engine to believe that it is operating in a real vessel. This can be done by simulating the vessel power train and connecting the simulation model to engine's loading system. As stated before, HiL concept consists of two main parts: the hardware under test and the virtual model of the rest of the system. Figure 1 illustrates the schematics of the HiL concept presented in this paper.

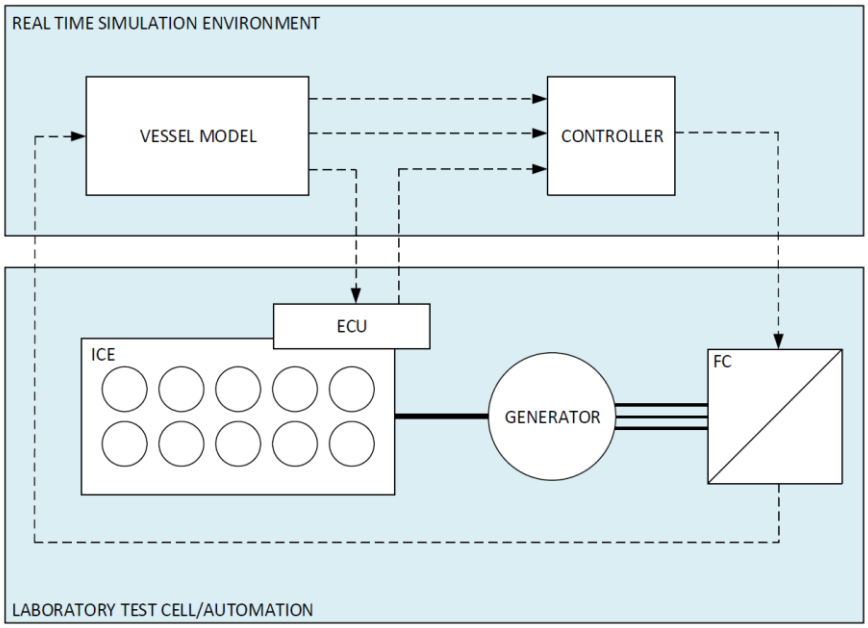

Figure 1. Schematics of HiL concept.

The simulation part of the HiL included virtual vessel model and a controller. Purpose of the controller is to request correct load from the frequency converter (FC) during the HiL test. Engine is acting as the hardware and the generator and the FC are needed to load the engine.

To conduct a successful HiL test, certain requirements need to be met. Firstly, the hardware, in this case an ICE, needs to have a proper testing environment. In this case, the engine was locating in a test cell in the engine laboratory of Wärtsilä.

Secondly, the HiL test needs a suitable simulation model of the rest of the system, meaning the system where the ICE is operating. Thus, a simulation model of virtual vessel power train was developed. The virtual vessel consisted of gearbox, controllable pitch propeller (CPP), hull, drive, electric generator/motor (G/M), battery and hotel grid model. Figure 2 below shows the single line diagram of the modelled virtual power train.

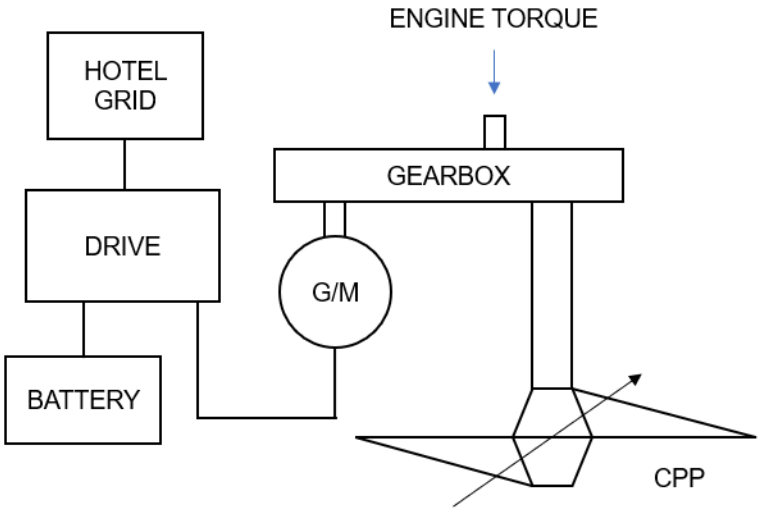

Figure 2. Single line diagram of modelled, virtual vessel power train.

The model itself was built by using one rotating mass modelling principle: all the inertia of the rotating parts is reflected to a single point in the shaft line where the system rotational speed is resolved. If, for example, a pitch value, meaning the angle of the propeller blades, is changed, there is an instant response on the system rotational speed.

Thirdly, the simulation model needs to run real-time. This gives requirement to the model itself but also to a platform where the simulation model is running. In this test, the vessel power train simulation model was created in Simulink and exported as a Functional Mock-up Unit (FMU). FMU is an executable unit which is in accordance with Functional Mock-up Interface (FMI) standard. The FMI standard defines a container and an interface to exchange dynamic models irrelevant from the source software [1]. The virtual power train FMU model was running on a computer, which had, beside Windows, a real-time executed platform.

As fourth requirement, the simulation model needs to communicate with the system where the component is tested, which can, for example, be a laboratory automation system. The communication should work with short enough latency: if the latency is too long, the closed loop interaction will not work as the model and real hardware would operate in different phases.

After all the requirements were fulfilled, a HiL test was conducted. In the test, a predefined virtual vessel operation profile was executed, and it lasted 500 s. Figure 3 illustrates the load and rotational speed of the engine during the HiL test.

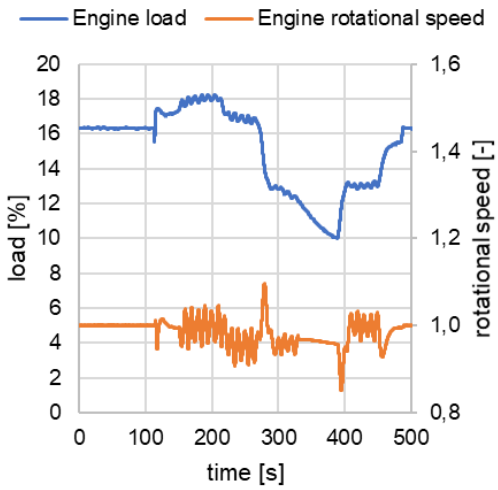

Figure 3. Engine load and rotational speed during the HiL test.

There is variance on both the load and rotational speed, due to weather conditions, or more precisely, wave conditions in the virtual model. Simulation model included wave model to represent the forces waves put on the propeller. There is a moment between 330 s and 400 s where the load is more balanced. During this time the electric motor and the battery is taking the load fluctuations and engine can operate on more stable load. The next figure, Figure 4, shows the virtual G/M power output during the test.

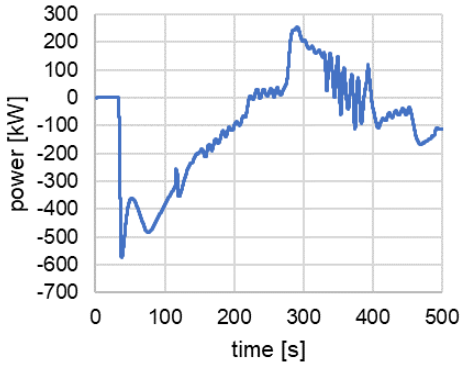

Figure 4. Electric generator/motor load in virtual vessel during the HiL test.

The G/M assists the ICE during the first 220 s of the test. After that the G/M delivers power towards drive as the propulsion power was decreasing. From 330 s onwards,

the G/M is smoothing the power and engine is operating on more stable load. Virtual vessel accelerated first half of the test before stabilizing to 8-9 kts. Figure 5 shows the virtual vessel speed during the test.

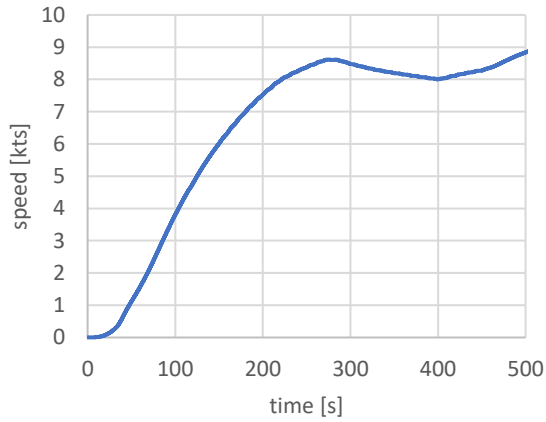

Figure 5. Virtual vessel speed during the HiL test.

To conclude the HiL part, it can be stated that this type of new testing is possible to do on large ICEs. HiL offers interesting use-cases, for example, to showcase engine functionalities to customers or to tune engine control parameters already before the engine is delivered to a vessel. It can also verify the fuel consumption in certain hybrid operation modes: multiple predefined operation profiles can be run in HiL to compare the actual fuel consumption of each profile.

6.3 Visualization of virtual vessel operation

The second part of the paper introduces the development done on visualizing the virtual vessel operation. As a starting point, there are great engineering tools to develop and simulate different systems. However, often these tools lack simplified view to visualize the modelled system and results so that colleagues outside the engineering department or customers could quickly get an understanding of what the results are telling. Within INTENS project, two standalone applications were developed to visualize more clearly the results from system simulation of vessel power trains.

Activities in this task were done together with 3D Studio Blomberg and Gambit. Aim was to create standalone applications which could bring results from simulation models into more appealing view. In both cases, the principle of how the application was developed, was the same: simulation model of the virtual vessel was exported as an FMU or multiple FMUs and then user interface and backend of the application were developed to run and obtain results from the set of FMUs.

The first part the text goes through the work done together with 3D Studio Blomberg and visualization of virtual fishing vessel operation. The second part explains the work done with Gambit and visualizing virtual ferry operation.

6.3.1 Visualization of virtual fishing vessel operation

To begin with, a simulation model of virtual fishing vessel was developed in MATLAB/Simulink. The virtual installation consisted of simulated engine, gearbox, controllable pitch propeller (CPP), electric generator/motor (G/M), drive system, battery and hotel grid. Configuration of the virtual fishing vessel is shown in Figure 6.

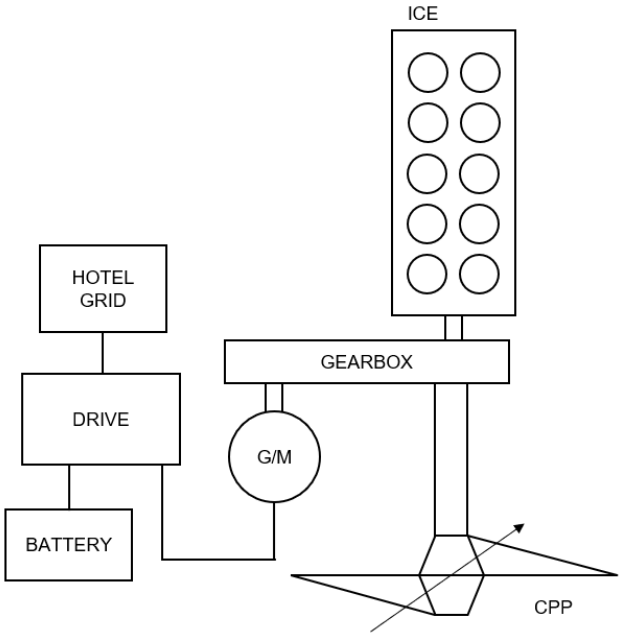

Figure 6. Configuration of virtual fishing vessel.

The complete system model was then exported from Simulink as a single FMU. 3D Studio Blomberg developed the application to send and receive data from the exported FMU. The application was developed with Unity [2] and there was a python package running the FMU. The user has the possibility to define the operation profile: operator can decide when main engine is started or stopped; when to operate purely with battery; when to accelerate the vessel or when to increase the hotel load request. Figure 7 illustrates how the user interface looks on the application.

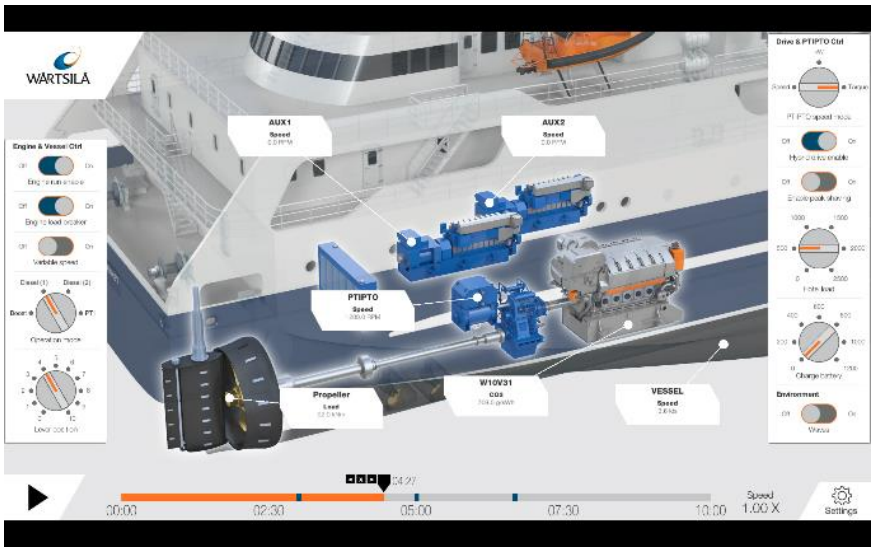

Figure 7. Virtual fishing vessel application.

6.3.2 Visualization of virtual ferry operation

Visualization of ferry operation was done together with Gambit. In this task, the simulation model was further developed to cover a larger system. This time the virtual vessel model included two mechanical propulsion lines, drive systems and three auxiliary generating sets. Figure 8 below presents the configuration of the virtual ferry.

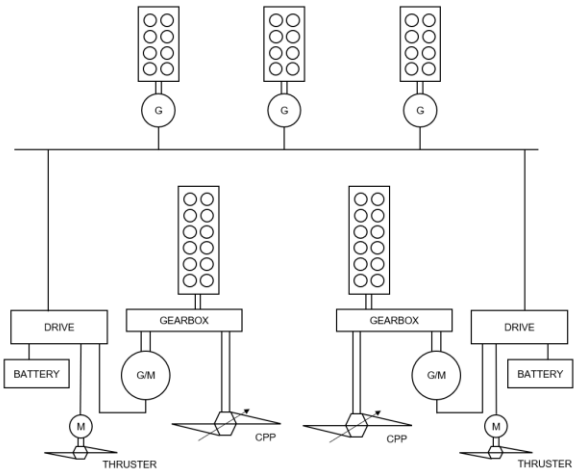

Figure 8. Configuration of virtual ferry.

In this task, the gearbox model was developed in AVL Cruise and rest of the simulation models in MATLAB/Simulink. All the individual simulation models were then exported as FMUs. The FMUs were connected in AVL Model.CONNECT. Model.CONNECT offers a platform to connect simulation models irrelevant from their origin software [2]. After the configuration was built in Model.CONNECT and tested that all functionalities work, it was exported as System Structure and Parameterization (SSP) package. SSP defines systems consisting of one of more FMUs. It includes the parametrization of all models and the parameterization file can be transferred to another simulation tool [3]. SSP package requires a tool to run it as SSP includes only the FMUs and an xml-file. To simulate the package, a python script was developed. Basic python packages were used to read the xml-files and to simulate the FMUs, *PyFMI* package was used. This package makes it possible to simulate and interact with FMUs [4]. At this stage, it was possible to run the whole virtual vessel model of a ferry with python script.

Once the python script was ready, Gambit developed browser-based application to run the virtual vessel model. Backend of the application was done with Flask [5] which interacted with the script created to simulate the FMUs. Frontend was created with React [6]. In this application, it was not possible to define new operation profile as the simulation was run with predefined operation profile. User interface of the virtual ferry application is shown in the Figure 9.

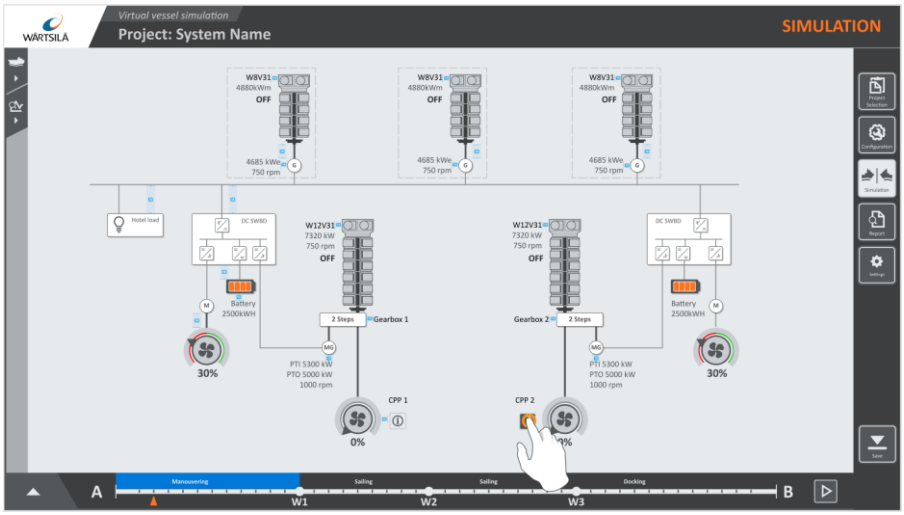

Figure 9. User interface of virtual ferry application.

To conclude the visualization part, FMU-based simulation models, together with experts from software development, introduce unlimited number of possibilities to develop applications to visualize virtual vessel operation. There are many technologies to choose from and we have presented a way to do this with FMUs and python combined with proper frameworks for user interface. New, simplified

user interfaces bring out more clearly the operation of hybrid vessels which is more appealing to show e.g. to customers.

6.4 Conclusions

We presented the reader two concepts around hybrid vessels: Hardware-In-the-Loop, better known as HiL, and application development to visualize virtual vessel operation. To conduct HiL tests, certain requirements need to be fulfilled: proper testing environment for the component; simulation model of the rest of the system; platform to run simulation real-time; and low latency communication between simulation and component testing environment. HiL brings value, for example, in showing how the engine works in hybrids setups, tuning the engine control parameters or comparing the actual fuel consumption in different hybrid operation modes.

The other part of the paper focused on application development to visualize virtual vessel operation. We illustrated a technological selection how to build such an application: simulation model is generated into a set of FMUs and user interface is built around it. Visualization of virtual vessel operation aims to show the operation of virtual vessels in more understandable way.

References

[1] Functional Mock-up Interface. Online, cited 19.4.2021. *https://fmi-standard.org/*

[2] AVL Model.CONNECT. Online, cited 23.4.2021. *https://www.avl.com/tr/-/model-connect-*

[3] SSP System Structure and Parameterization. Online, cited 28.4.2021. *https://ssp-standard.org/*

[4] PyFMI. Online, cited 23.4.2021. *https://jmodelica.org/pyfmi/index.html#*

[5] Flask. Online, cited 23.4.2021. *https://palletsprojects.com/p/flask/*

[6] React. Online, cited 23.4.2021. *https://reactjs.org/*

7. Real-time simulation of combined engine and electrical equipment model in Simulink RT

Saana Hautala[1], Emma Söderäng[1], Seppo Niemi[1]
University of Vaasa

7.1 Introduction

This chapter presents steps towards real-time simulation of a combined engine and electrical equipment model in Simulink Real-Time (RT). This is a continuation of earlier work of Digital-twinning the engine research platform in VEBIC [1]. In this research, the goal was to build a digital twin of the engine research platform in VEBIC. When moving towards a digital twin, one of the first essential steps was to have a real-time capable model of the research platform. Real-time simulation capability was necessary for running the model and its real-world counterpart in parallel. The parallel simulations are needed to establish the model ability to emulate the real operation in the engine laboratory.

7.2 Modelling the hybrid power generation system

Earlier modelling work covered the validation of a GT-Power model of a 4-cylinder common rail medium speed diesel engine (W4L20) and electrical equipment consisting of an induction machine, a frequency converter and a battery in Simulink. The real-time capability of the electrical component models has already been established [1]. In this section, the engine model's conversion to real-time and the coupling between the engine and electrical equipment models are covered.

7.2.1 Fast Running Model of the 4L20 engine

For real-time capable simulations, the execution time of the 4L20 GT-Power model was required to be decreased. The selected route to cover faster simulation time for the engine model was selected to be Fast Running Model (FRM). Reason for this decision was that the FRM conversion process was relatively simple and some

[1] Contact: firstname.lastname@uva.fi

details could be kept in the model. Furthermore, real-time capability could be yet achieved with this format [2]. In addition, the map-based approach in Mean Value (MV) modelling, which was earlier considered [1], would have required more measurement data that was available at this point. Basically, the reduction process from detailed engine model to FRM covers the first the steps of MV conversion. Thus, the simplifications of FRM process should be carried out first to see whether the model's simulation time is reduced to an acceptable level or additional simplifications are still needed. Throughout the process, the manuals provided in the GT-ISE software were followed and the conversion steps and their order were performed as recommended [3].

7.2.1.1 Conversion from detailed engine model to FRM

The FRM converter tool in the software was used and subsystems, which were pre-defined from the flow-components, were merged and simplified in terms of either speed or accuracy. All created subsystems, i.e., exhaust manifold, exhaust pipes, intake manifold, compressor outlet pipes (including CAC) and intake pipes, were simplified in terms of accuracy respectively. Afterwards, the exhaust manifold was simplified in terms of speed to further decrease the simulation time of the model. Since combustion profile was already used in the detailed model, simplifications for combustion or cylinders were not required during FRM conversion process. Calibration was embedded in the step-by-step reduction process and performed after merging the volumes when needed. Depending on whether the pressure lost or temperature wanted to be calibrated, the optimization parameter was selected to be either the subsystem's orifice diameter or heat transfer multiplier respectively. The calibration was performed for a single case which was the highest load point. The optimized value resulted in the calibration was used for all load points. In Figure 1, the FRM is presented after the conversion process has been carried out.

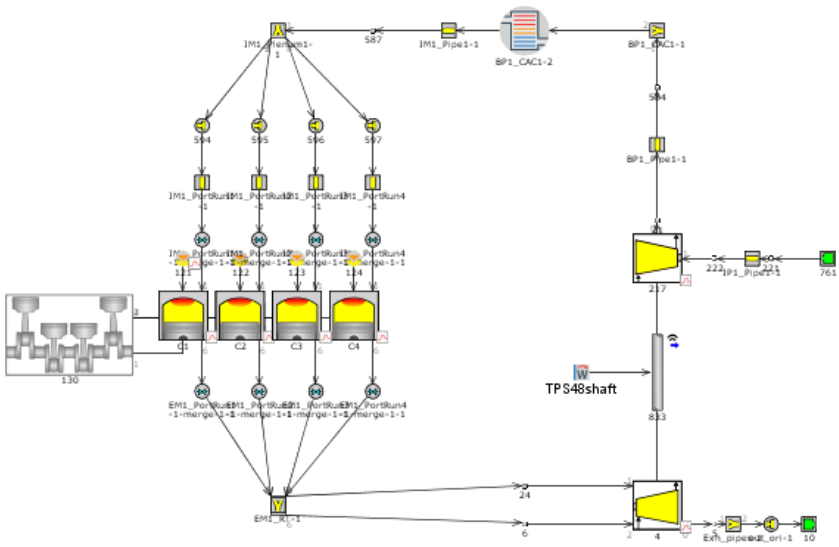

Figure 1. The FRM of the 4L20 engine.

7.2.1.2 Validation and real-time capability

After the model was converted into the FRM, the simulation results were compared to the results with the detailed engine model. The parameters observed were the parameters used previously in the detailed 4L20 model validation, i.e., BMEP, BTE, maximum cylinder pressure and exhaust temperature before turbine [1]. Simulation results of both models are presented in Figure 2.

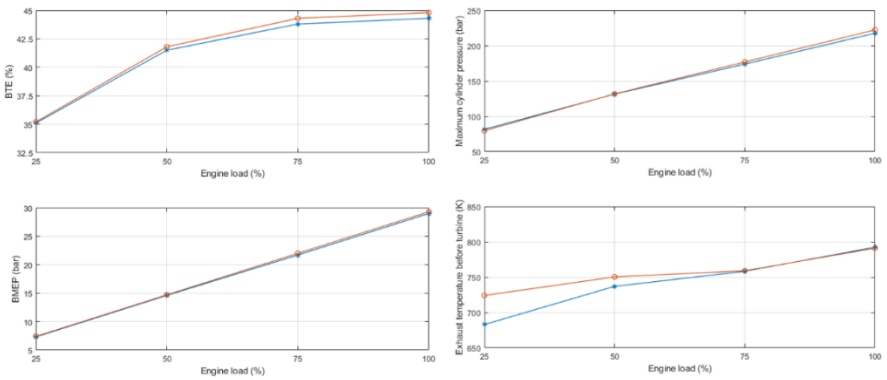

Figure 2. Simulation results of detailed 4L20 engine model (blue) and FRM (orange).

It was expected that, during the simplifications and reduction process, increasing the simulation speed would cause the accuracy of the results somewhat deteriorate. It was aimed that the errors between the simulation results of FRM and detailed model would remain inside ± 5 %. When the results presented in Figure 2 were observed more closely, it was noticed that the exhaust temperature before turbine at 25 % load point was outside of the desired error range. Since calibration was performed only for the highest load point, it can cause larger errors for the lower load. Thus, it should be noted that a closer, case dependent and multi-objective calibration could produce more accurate results. However, in this case, the case-dependent calibration method was not a suitable option, as case-dependent inputs had to be replaced before real-time simulations. The model was accepted with this limitation for the intended use.

After the FRM conversion, the real-time capability of the model was observed. The last step to implement the model to real-time simulations and to be connected in Simulink, was to change the license type into GT-SUITE-RT. Simultaneously, the FRM accelerator tool in the software was used to implement settings that would decrease the simulation time. Some small modifications were performed to enable the model work as before the change. In addition, some case-dependent values were replaced by functions or tables in order to smooth the coupling with Simulink. The real-time factor, which presents the model's real-time capability, was approximately 0.35. This was sufficient since the model should be able to performance in real time with planned implementation already with average factor of 0.5-0.6 [4].

7.2.2 Combining the engine and electrical equipment model in Simulink

After model's real-time readiness was confirmed, the links between the two software were created. Inputs for the FRM were decided based on the inputs used earlier in the engine model and the available signals from engine laboratory's data acquisition system that could be used in parallel simulations. These input parameters for the engine model were reference engine speed, ambient temperature and pressure. One limitation was injected fuel mass that was earlier used as input for the engine model. This parameter was not continuously measured from the engine and therefore could not be used as an input for the model. Nevertheless, since reference load was used as control signal in the engine laboratory it was decided to be used in the FRM as well. A brake power controller was added to the model and used as input instead of injected fuel mass. This did not have major effects on the simulation results. The biggest difference was in BMEP with 50-100% load points where the relative error was approximately -1.4 %. The main output from the engine model to the electric equipment models in Simulink was brake torque which was used as input to the electric machine. In addition, BMEP, cylinder pressure, burned mass fraction of fuel at CA50 (CA, crank angle) and exhaust temperature at turbine inlet were used to observe the engine model performance.

In Simulink, the engine model was imported using the GT-SUITE specific library and in particular the block GT-SUITE-RT. In that way, the engine model was represented as an s-function. The combined model in Simulink is presented in Figure 3.

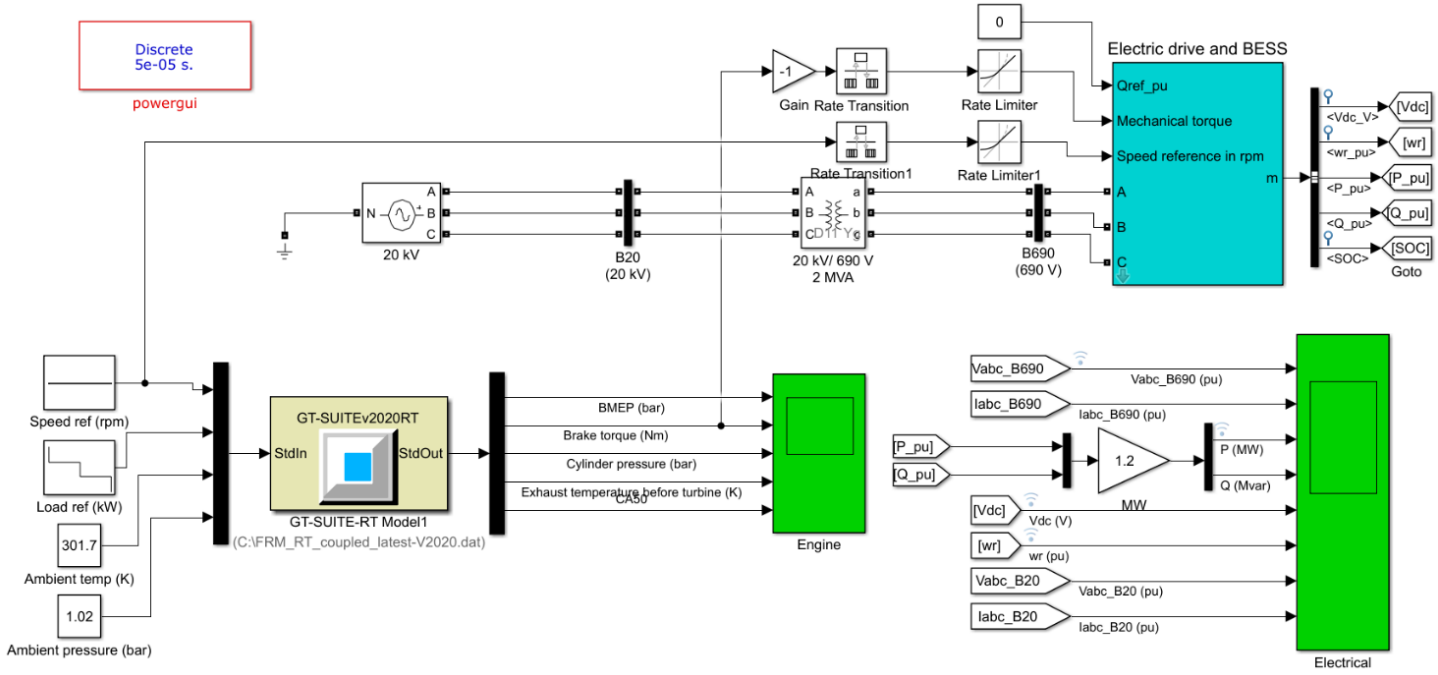

Figure 3. The combined engine and electrical equipment model in Simulink.

7.3 Simulation of the combined engine and electrical equipment model in Simulink

After the engine model was imported to Simulink, the whole model could be simulated. The model was simulated for 200 seconds in order to demonstrate its functionality. Four load points were included in the simulation by using load reference (kW) as input. The other constant inputs were the engine speed reference (rpm), ambient temperature (K) and ambient pressure (bar). As stated earlier, the outputs from the engine model included in Simulink were BMEP (bar), cylinder pressure (bar), brake torque (Nm) and exhaust temperature before turbine (K). The brake torque (Nm) was an input to the electric machine. The speed reference (rpm) was also an input to the speed controller. In addition, the reactive power reference was an input to the frequency converter. Table 1 presents the inputs to the engine model and how they vary with time for the simulation case presented here.

Table 1. Events during the simulation.

Time (s)	Speed reference (rpm)	Load reference (kW)	Ambient temperature (K)	Ambient pressure (bar)
0	1000	848.2	301.7	1.02
50	1000	637.7	301.7	1.02
100	1000	426.6	301.7	1.02
150	1000	213.9	301.7	1.02

The simulation results are presented in Figure 4 and Figure 5. Figure 4 shows the outputs from the engine and Figure 5 the outputs from the electrical equipment. The outputs from the electrical equipment were chosen from a point located after the frequency converter and before the 690 V / 20 kV transformer. For this case, four outputs were chosen: the active power output (kW), the power factor cos (φ), the 690 V bus RMS currents (A) and the grid frequency (Hz). The electrical outputs were validated against measurement data and the engine outputs were the same as the outputs for the FRM when simulated in GT-SUITE.

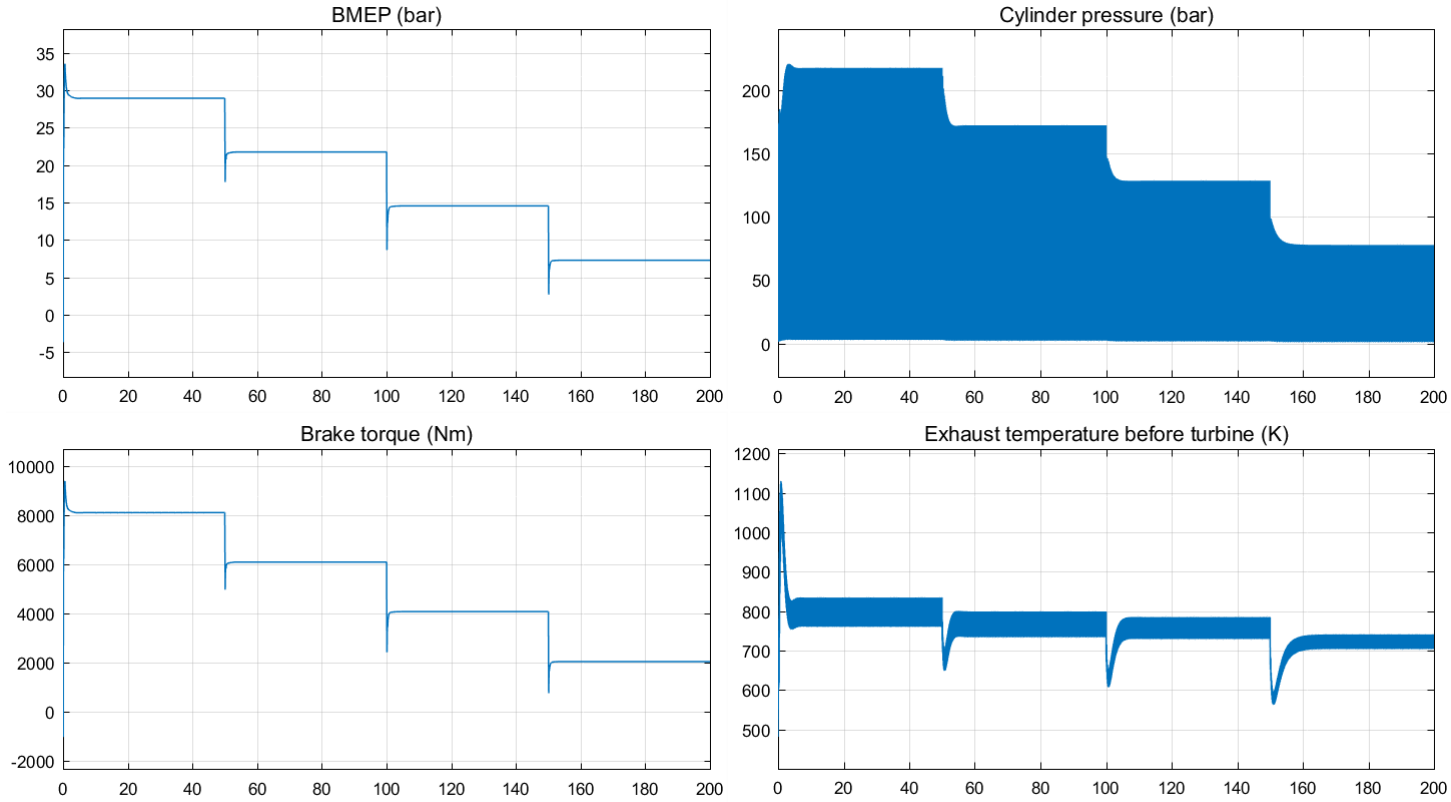

Figure 4. The engine measurement outputs in Simulink.

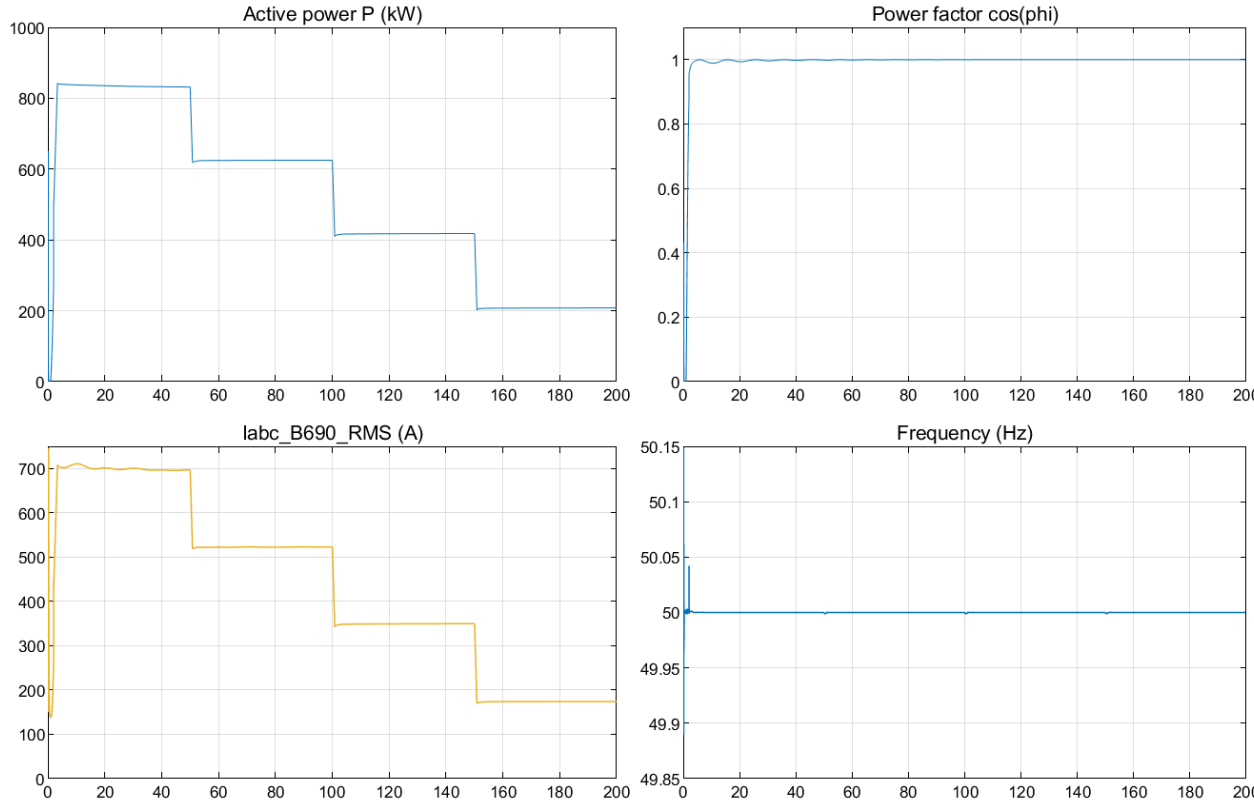

Figure 5. The electrical equipment measurement outputs in Simulink.

7.4 Real-time simulation and future work

Subsequently, when the combined model had been successfully simulated on the development computer, next step was to convert it into a real-time application and run it on the target PC using Simulink Real-Time. However, the GT-SUITE-RT block caused several problems in the compiling phase. After an extensive investigation, it was possible to compile the GT-SUITE-RT block and obtain a real-time application for the combined model. The electrical equipment model was already earlier proved to be real-time capable. The engine model was proved to be real-time capable, but it required a large sample time, which was not optimal for the output accuracy. Figure 6 shows the engine model outputs when running on the target PC as a real-time application, with a sample time of 1 s. As it can be seen, the average task execution time (TET) for this model on the specific computer used was 0.807 s, and the large sample time caused the cylinder pressure output to fail.

Figure 6. Engine model run on the target PC in Simulink Real-Time. Scope 1 is BMEP (bar), scope 2 is brake torque (Nm), scope 3 is cylinder pressure (bar) and scope 4 is exhaust temperature before turbine (K).

The whole combined model was not real-time simulation capable on the target PC. The target PC was however an old PC with lower computational power than the Speedgoat. Therefore, next step is to investigate how to get the combined real-time application running on the real Speedgoat Performance Real-Time Target Machine.

It was concluded that more computational power is needed in order to be able to use a smaller sample time for the engine model and to run the whole combined model as a real-time application.

References

[1] S. Hautala, E. Söderäng, S. Niemi, “Digital-twinning the engine research platform in VEBIC,” Integrated energy solutions to smart and green shipping - 2020 Edition, pp. 120-128, October 2020, VTT Technology, ISBN: 978-951-38-8740-7

[2] Gamma Technologies, “GT-SUITE Engine Performance Application Manual”, 2019.

[3] Gamma Technologies, “GT-SUITE Engine Performance Tutorials”, 2019.

[4] S. Hautala, E. Söderäng (University of Vaasa); P. Dimitrakopoulos (Gamma Technologies). Personal communication via email, 2021.

8. Robust vessel power system operation studies using ship emulator

Tuomo Lindh[1], Henri Montonen[1], Jani Alho[1]
LUT University

8.1 Introduction

It is not possible to have diesel engines or propeller drives with actual propeller and environment in the LUT laboratory. However, setups with different electrical networks, battery energy storage system (BESS) and frequency converter driven motors can be constructed. Therefore, it was constructed two distribution networks, one AC-network connected to BESS and another DC-network. The construction and testing of AC-network already started during the FESSMI[2] research project.

Hybrid vessel emulator system consists of real hardware and virtual simulators. The main hardware components are electric network, generators and battery energy storage and controllers. Diesel motors are emulated with electric motor drives where dynamics of diesels are simulated. Also propeller drives and loading are emulated with motor drives and with power electronics.

The purpose of the emulator setup is A) to verify simulation models, B) to test energy balancing and control of vessel hybrid power train when battery energy storage is used, C) to test different normal operation modes and fault cases and D) to demonstrate the combination of the vessel control and scheduling optimization in real time.

More general is the research of the HIL simulation itself, which concentrates on finding the benefits, limitations and dynamic performance of hardware-in-loop simulation (HIL) in a complex power train system.

The laboratory level demonstration systems offer tools to verify the simulation results and to understand model uncertainties and technical challenges existing in a real marine hybrid system.

---

[1] Contact: firstname.lastname@lut.fi

[2] FESSMI - FUTURE ENERGY STORAGE SOLUTIONS IN MARINE INSTALLATIONS - is a Business Finland co-funded research project.

8.2 Emulator setup

HIL systems have been used for years for a rapid prototyping in different applications [1,2,3,4,5]. The HIL system under investigation combines the Hardware-In-the-Loop simulations and Power-In-the-Loop simulations. Most of the studies present their setups and demonstrate the performance by giving experimental results. The properties of the electric drives as a load emulator have been discussed in a few studies [1,6,7]. In the HIL concept, an actual drive under test (DUT), or some components of it, are used as a part of simulation setup. The actual application motor drive can be tested on the real-time simulation of mechanics and of an electric motor drive that emulates this mechanics.

In this research, the emulators are used as part of robust vessel power system demonstration. The system consists of hybrid power system emulator itself, communication path, database for power system, a simulator and optimization. A simulator was designed to analyse problems in control. An optimization algorithm calculates the usage of generators, battery energy storage and propulsions.

The vessel operates according to the optimized route plan which changes due to different operation conditions. In the demonstration, the emulator reads the operational plan from the database (MySQL), sends the measurement data and status of devices to a database using OPC-UA communication protocol between emulator and python script which writes and reads the database data using a native MySQL connector. The communication with Matlab is implemented using Matlab engine by MathWorks Inc. The idea behind the setup is described in Figure 1.

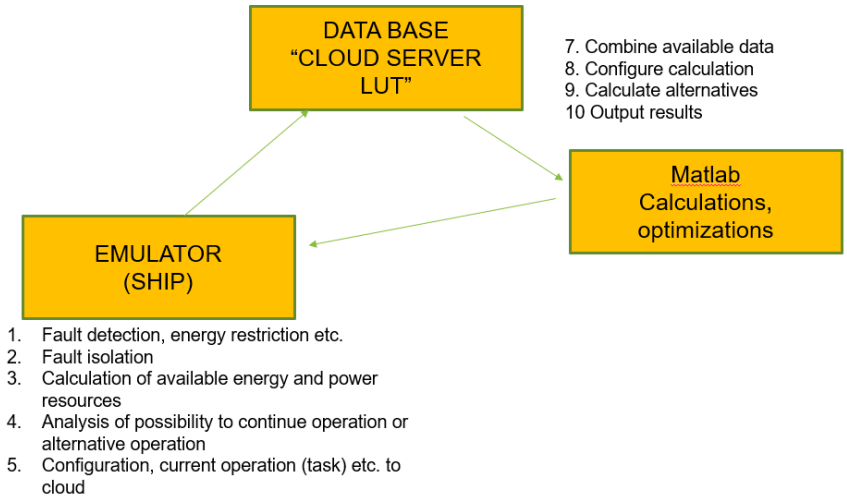

Figure 1. The emulator setup for the connection with optimization and simulation.

8.2.1 Hardware-in-the-loop emulation

Hardware-in-the-loop (HIL) emulator setup is divided into two parts: AC-network emulator and DC-network emulator. They are further described in the following sections.

8.2.1.1 AC- network emulator hardware

The AC- network and power train emulator was constructed originally for testing the dynamic performance and control of the hybrid power train in Wärtsilä LLC-type (Wärtsilä Low Loss Concept). In LLC concept, the network is divided into two parallel networks connected together with a transformer that provides 30 degrees phase shift between parallel networks. In this concept, 12 pulse diode rectification can be done directly from these two sections without two secondary windings fed to propeller drives. When diesel gensets are connected evenly to both sections, the transformer between sections can operate in no load conditions. The LLH-concept is a modification of LLC, in which the three winding transformer is for the connection of a battery energy storage system (BESS).

The emulator hardware, presented in schema of Figure 2, includes a LLH-concept network, battery energy storage, one propulsion emulator with actual motor drive and propulsion load emulator drive (110-kW induction motor and 315-kW induction generator). The diesel genset emulator in the first parallel network section consists of a 200-kW/800-kW induction motor that emulates diesel and an 800-kVA synchronous generator. Diesel dynamics is modelled in an industrial PC embedded with PLC controllers. In the second network section there exists a 4-quadrant network inverter, which can at the same time emulates both propeller loads and diesel gensets.

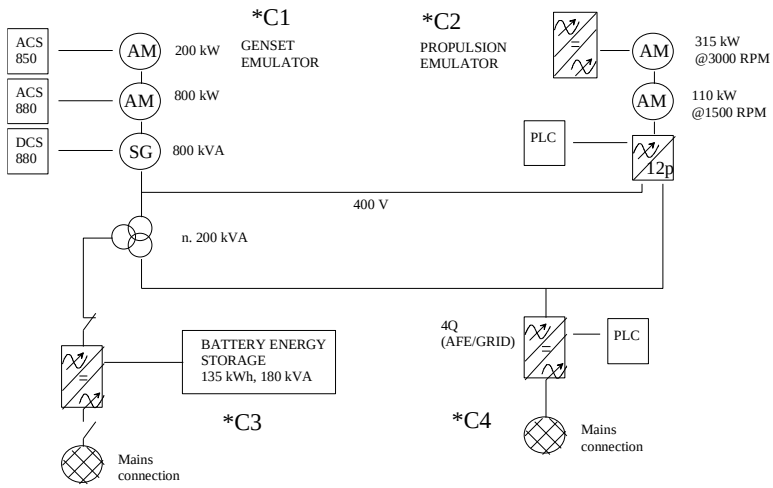

Figure 2. A laboratory setup for testing a power train of a future hybrid vessel. The main components in addition to network itself are a genset emulator unit *C1, a propulsion emulator *C2 , a battery energy storage C3 and a multi-purpose emulator *C4.

8.2.1.2 DC- network emulator hardware

The DC network emulator of Figure 3 is a smaller scale emulator than the AC network emulator, but more complex. The DC network emulator consists of two diesel genset emulators. In the first emulator a 55-kW induction motor is used as a diesel genset emulator. This motor is connected to synchronous generator (110 kVA) feeding the DC network via diode rectifier. Another multi-purpose emulator can be used as a combined diesel genset and propulsion emulator. It consists of two back-to-back connected 5.5-kW induction machines. One machine is connected to mains via 4Q-inverter setup so that it can be used as a load (generator) as well as a motor. Similarly, the 4-kW setup is as a main propeller load emulator. The setup does not include actual battery energy storage but, instead, uses a grid inverter to emulate battery. Battery characteristics can be programmed as emulator code in the main controller or battery energy storage of AC-setup can be used in parallel with the emulator when the battery energy storage is connected with mains instead of vessel network. In this case, emulator code calculates scaling between voltages and currents of actual BESS and emulated one. This way, the battery emulator can emulate both controlled BESS and BESS that is directly connected to DC vessel net-work. It is worth mentioning that emulation is not restricted to battery storage and other storages such as super capacitor or flywheel storages can be emulated as well. The DC- and AC-network emulators share same main controller, DAQ and supervisory control.

The main controller of the emulator setup is an industrial PC. The propulsion emulator and the battery energy storage have their own programmable controllers so that they can execute, if set so, their own emulator algorithms in a distributed manner but all the emulations can be calculated in the main controller as well. The distributed emulations are required only if very fast dynamics is emulated. At the moment, all emulations are executed in main controller which limits the control cycle of load emulator to 1-2 milliseconds and of battery energy storage control to 300 milliseconds. The emulations can be implemented by programs written using C- or IEC61131-3 languages. In addition, Simulink models can be translated to IEC 61131-3 function blocks using PLC Coder from Mathworks Inc. or compiled using Beckhoff TE1400 TwinCAT 3 target for Matlab/Simulink. The latter option enables one to visualize simulations in real-time. The emulation results can be graphically displayed in real time and recorded with 1 millisecond time resolution.

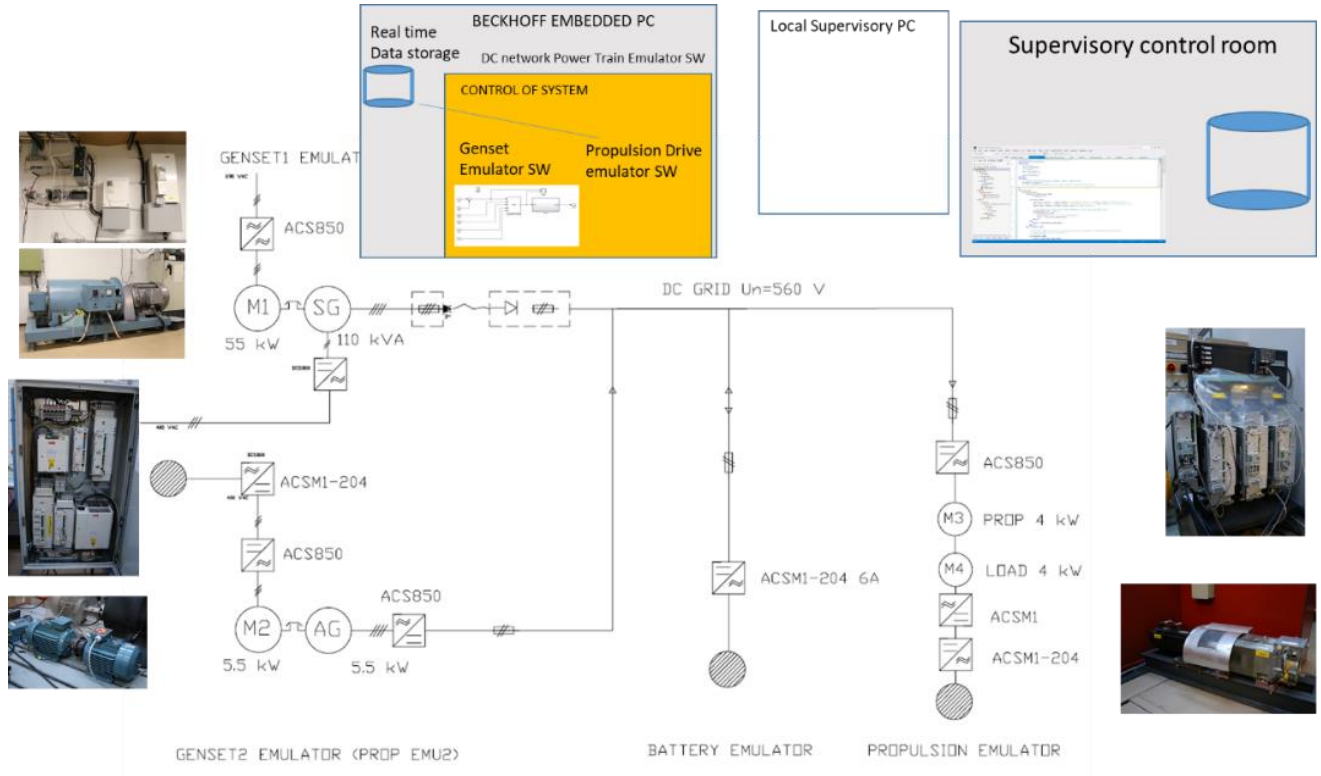

Figure 3. Hardware and software components of the DC-network hybrid power drive emulator.

8.3 Use cases

The first use case combines two objectives: A) Emulator is used to verify the simulation model behaviour, specifically if control works similarly in real network and in Simulink, and B) to demonstrate the possibility to analyse control problems as a digital twin of real vessel power system. Another use case is presented for demonstration purposes: a connection between emulator and database and Matlab/Simulink was created. When some rare event, such as generator fault, occurs at vessel (emulator), the vessel status information is relayed to Matlab/Simulink environment where fault and restoration can be simulated and new operation plan for hybrid power train can be optimized and sent back to vessel. Figure 4 presents a Simulink simulation model for vessel power distribution network (PDS). The model can be used for simulating vessel power balance e.g. in different fault scenarios. Parts of the simulation model can also be used in the emulator, such as the power balance controllers and diesel engine models.

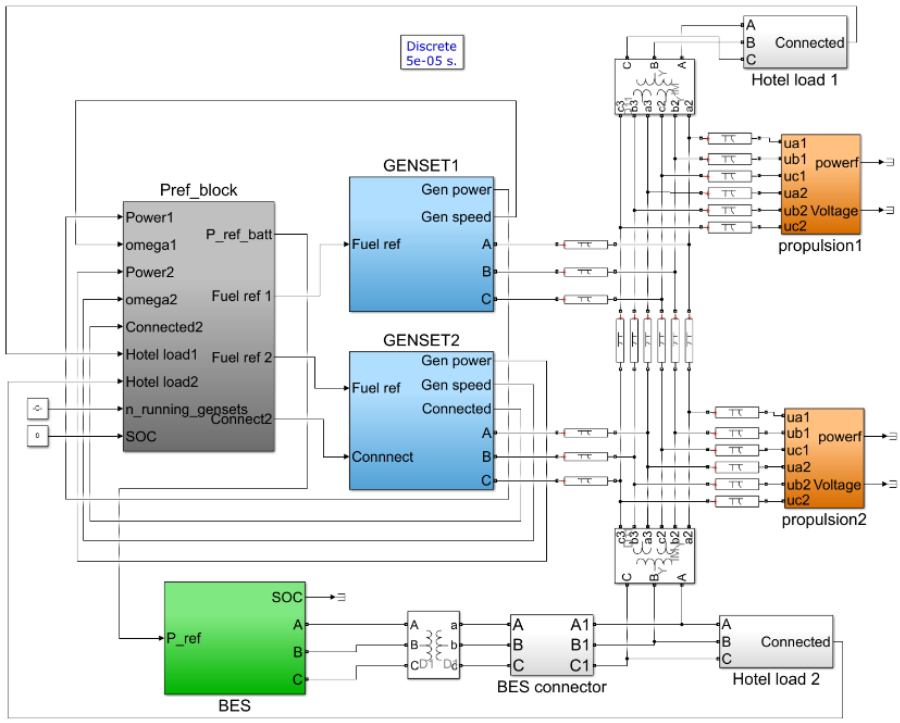

Figure 4. Simulation model for vessel power distribution network containing models for diesel gensets, propulsion load, hotel load, battery energy storage system and LLH transformers.

Example use case with setup of Figure4 using AC-emulator. The main controller calculates the control block (Pref_block) which sends references to the genset blocks for calculating diesel dynamics (for both Gensets of Figure 4.) The calculated torque of the diesel engine of GENSET1 is given as reference to AM1 of Figure 2 and generator SG creates the power network. After that, the calculated torque of diesel of GENSET2 is set as reference to the C4 emulator which starts feeding the lower branch of network of Figure 2. Recorded propulsion load data from an actual vessel is given as a reference to back-to-back propulsion emulator C2 (Figure 2) in case of propulsion1 block of Figure 4. The propulsion2 block is executed as simulation in main controller and the calculated power taken by propulsion motor is added as a reference to multi-purpose emulator C4. The results of hardware emulator and simulator are compared in order to verify the dynamic properties introduced by the BESS.

Example use case with setup for route planning. This use case is still under development (the optimization part has not been actually tested in a system described in section 2, Figure 1). In this case example, a route plan and ship equipment are imaginary. The case specifications cover the required parameters and setting up of the optimization problem. The route plan is calculated in optimization computer (cloud server LUT). The route plan is divided into distance steps and an optimization algorithm is used to determine the optimal way of producing power, deploying energy storage systems and controlling propulsion. The data is sent via database connection back to the main controller of the emulator and driving of emulator is executed similarly to what is explained in the first use case description. An example of re-optimized route plan after a generator failure is shown in Figure 5.

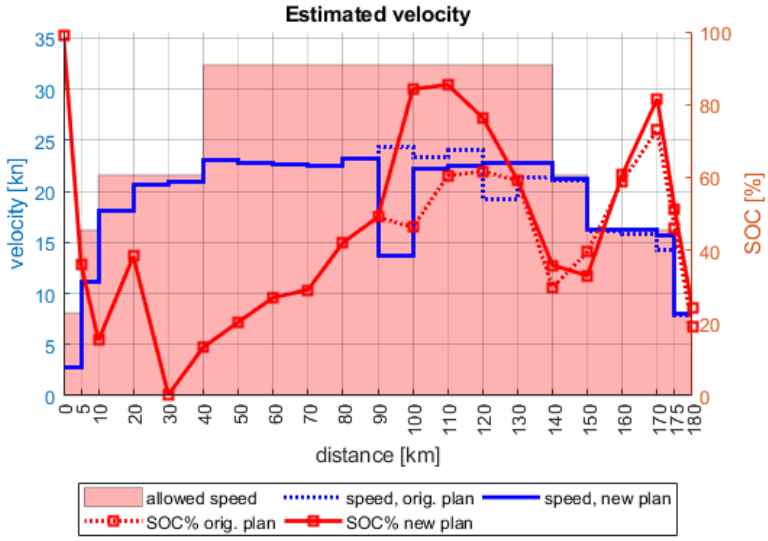

Figure 5. An example of re-optimized route plan after failure of one generator half-way on the trip.

References

[1] Youngsong L. and Woon-Sung L.," Hardware-in-the-loop Simulation for Electro-mechanical Brake" SICE-ICASE International Joint Conference 2006, October 2006, Bexco, Busan, Korea

[2] Zhang Q., Reid J. F., Wu D., "Hardware-in-the-loop simulator of an off-road vehicle electrohydraulic steering system", Trans. on ASAE, September 2001, pp. 1323-1330

[3] W. Lhomme, R. Trigui, P. Delarue, A. Bouscayrol, B. Jeanneret, F. Badin, "Validation of clutch modeling for hybrid electric vehicle using Hardware-In-the-Loop simulation", IEEE-VPPC'07, Arlington (USA), September 2007R. Nicole, "Title of paper with only first word capitalized," J. Name Stand. Abbrev., in press.

[4] Jeeho L., Namju J., Hyeongcheol L., "HIL Simulation Approach for Feasibility Study of a Tram with Onboard Hybrid Energy Storage System", in Proc. ICCAS-SICE, 2009, pp. 5305-5312

[5] Hanselmann, H., "Hardware-in-the-Loop Simulation Testing and its Integration into a CACSD Toolset," in Proceedings of the 1996 IEEE International Symposium on Computer-Aided Control System Design.

[6] Lentijo S., D'Arco S., Monti A., "Comparing the Dynamic Performances of Power Hardware-in-the-Loop Interfaces", IEEE Trans. Ind. Electron., Vol. 57, no. 4, pp.1195-1207, April 2010

[7] Lindh T., Montonen H., Niemelä M., Nokka J., Laurila L., Pyrhönen J. "Dynamic Performance of Mechanical-level Hardware-In-the- Loop Simulation", EPE-ECCE 2014.

9. Models and benefits of digital twin for power cycle based waste heat recovery system

Radheesh Dhanasegaran[1], Antti Uusitalo[1] Teemu Turunen-Saaresti[1]
LUT University

9.1 Introduction to Digital Twin

In the recent years, the term 'Digital Twin (DT)' has attained increasing attention and has become one of the cutting-edge research topics in both academia and industry. In principle, a Digital Twin is a digital or a virtual rendition/ counterpart of a physical system or process. Adding to this definition, Grieves and Vickers [1], the people who first use this term, describe the three major inherent characteristics for a Digital Twin that it must consist of a physical product, a virtual representation of that product and a bi-directional data transfer between them. This bi-directional data connection enables a mutual or two-way communication between the physical system and its virtual counterpart. It was Grieves [2], who described this two-way communication as 'mirroring' or 'twinning' hence leading to the epithet 'Digital Twin.' In addition to these features, Jones et al. [3] have summarized the additional characteristics of a Digital Twin, such as Physical and Virtual environments, State, Realization, Metrology and Twinning rate.

The prime motive of building a Digital Twin is to monitor the system/process' performance and present control methodologies for its operation through the two-way communication between the physical system and its virtual counterpart. The application of Digital Twins is now being widespread, such as in aerospace, automotive, buildings, healthcare, marine, powerplants and other process industries. GE is using them to monitor wind turbines [4], Fingrid for power grid monitoring [5] and Akselos for the hydropower plant at the Turlough Hill, Ireland [6]. The digital twins can be done for single component or large systems. There are no standards or norms for digital twins [7] and all twins are made from scratch to certain purpose. Therefore, it is extremely hard to get detailed view what is meant by digital twins used in industry. Especially, the quality and amount of data collected from the

[1] Contact: firstname.lastname@lut.fi

physical product and the details of models used in digital twin are very hard to find. Clearly, close cooperation between industry and academia would be needed.

9.2 Digital Twin for Marine Industry

9.2.1 Principles of Digital Twin

With the ongoing Industry 4.0, energy savings and thereby achieving improved energy efficiency have been one of its substantial goals in which data-driven methods seems to play a significant role. Teng et al. [11] classifies the data-driven energy savings method into four steps: (i) data acquisition, (ii) data pre-processing, (iii) data modelling and analysis and (iv) industrial implementation. Out of these steps, real-time data acquisition remains to be a challenging one with respect to Digital Twin construction according to Uhlemann et al. [8]. An online adaptation of Digital Twins for a driveline in a marine thruster without any sensor at the point of interest has been studied and the challenges with respect to such adaptation has been discussed by Nikula et al [9]. Similarly, the use of Digital Twin to do online error and correction of data from a heat exchanger for a marine energy vessel subsystem has been proposed by Manngård et al [10].

9.2.2 Digital twin for Waste Heat Recovery Power Cycle

The power cycle-based waste heat recovery system could be one of the potential areas where the Digital Twin could be utilized especially in a marine industry where Organic Rankine Cycles (ORC) could be a potential technology enhance energy efficiency in the future. In such environments, the data-driven energy savings method could offer significant increase in its cycle efficiency by continuously assessing its system performance through building a physics-based dynamic model.

For generating digital twin for waste heat recovery system used in marine sector, the starting point has been Organic Rankine Cycle power system in the laboratory of fluid dynamics, LUT. The physical system uses exhaust gases of diesel engine to generate electricity. This entire WHR can be termed as a small scale and high-temperature ORC system where the power range of the WHR from the exhaust gases is between 100-200 kW and that of the ORC is 5-10 kW. The general layout of the digital twin and connections are shown in Figure 1.

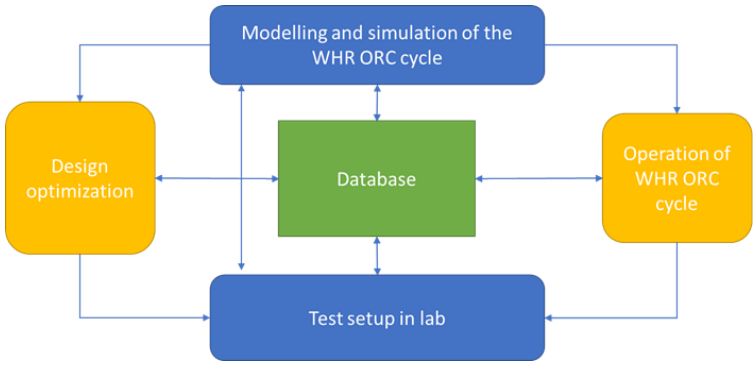

Figure 1. Layout and connections of digital twin for WHR ORC.

The digital twin is build based on dynamic model of the cycle consisting of major components, (i) the high-speed turbogenerator consisting of a supersonic radial turbine, a Barske type main feed pump and a generator all being connected to the same shaft, (ii) the heat exchanger components such as the condenser, evaporator, and recuperator, and (iii) a pre-feed pump. All the heat exchanger components are of the plate & shell type. Matlab-Simulink environment has been chosen to create the dynamic model where the components are modelled using first principles that enables the data transfer between the physical system to the virtual counterpart and the reverse data transfer could provide information about operating the cycle with the optimal inputs to achieve a higher cycle efficiency.

Models describing the behaviour of system are particularly important to have well working digital twin. CoolProp has been utilized for calculating fluid thermodynamic and transport properties. In creating the virtual entities/counterparts, all the components are modelled using a block modelling approach in Simulink by categorizing them as the turbogenerator, heat exchanger components and pre-feed pump separately. The components have been modelled mathematically using a reduced order modelling approach. The models used in the digital twin are based on thermodynamic behaviour of the components and the mechanical behaviour of the components are not considered at this stage. Only exception is the inertia of the moving parts i.e., the turbine shaft.

9.3 Dynamic Model as an Avenue towards Digital Twin

Incorporating Digital Twin for power plant environments demands monitoring, fault diagnosis and predictive maintenance of power generation equipment and power control centers, and real-time operational control of the power grid. Through the integration of transient data from the dynamic model of a power plant, Digital Twin will have the potential to respond to changes in control environment during its start-up, peak performance, shut-down and other off-design conditions. As per General Electric (GE), the Digital Twin provides insights into speed, stability, emissions, and

stresses as well as predicting the limitations of the plant with configuration and operational changes. Moreover, accurate data collection from the physical model will help in realizing a high-fidelity mapping of the virtual interface or entity.

9.3.1 Purpose of digital twin

The digital twin developed is based on thermodynamic models of the ORC. This means that the digital twin can be used for estimating performance of the waste heat recovery system at the different operation conditions and help design a system for marine environment. The choice was natural although the technology is still under development. The life cycle of the parts cannot be estimated or evaluated using the designed digital twin. However, the mechanical digital twin of the turbogenerator can be added later since 3D models of the turbine is available. Using accurate models for components and for thermodynamical properties is important for digital twin used for performance estimation and system design. However, this inherently leads to time consuming simulations and the capability to used digital twin real time is not feasible. If the digital twin will be used for real-time control or life cycle and maintenance evaluation the models used should be simpler and computationally more efficient.

9.3.2 Twinning & Communication

A physical-to-virtual twinning methodology has been followed here, where the state of the physical product has been transferred to and realized in the virtual environment. Figure 2 shows its corresponding process. As mentioned earlier, the real-time data acquisition is challenging. However, in our present study, the turbogenerator's efficiency and the inlet pressure, as a function of the rotational speed, have been fed as an input to the virtual counterpart which helps calculate the cycle's performance parameters.

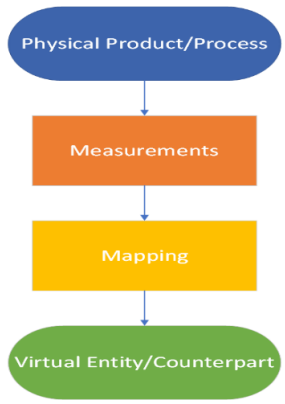

Figure 2. Physical-to-Virtual Twinning Process.

9.4 Summary & Scope for Future Works

In a digital twin, the data must be constantly exchanged and updated between systems. With the chosen approach of one-way (physical-to-virtual) connection currently being in the developmental phase, live and continuous transfer of the states from the physical-to-virtual environment is not yet accomplished. Therefore, both the physical and virtual environment are working as a stand-alone entity. The communication or data transfer from the physical system and its virtual counterpart includes sensor data and status data. This data collection from the physical system or twin facilitates the accomplishment of the digital twin. Once that live data transfer is established, then the realization phase will become complete in this one-way connection. On the other hand, the virtual-to-physical communication through the flow of information or processes from the digital twin to the physical system requires the measurement of the state or the parameters in the virtual twin also called as the metrology phase [3] to be established. Apart from the conventional control routine feature of a Digital Twin where the change in the state of a system (physical or virtual) is transmitted through one of the above-mentioned communication processes and utilized to synchronize the corresponding state/parameter in its counterpart as stated from the literature, the existing control routine of a power cycle can be made to operate in an optimal mode by utilizing the information transfer from the virtual twin model through the metrology phase. This can be only achieved once the virtual twin-to-physical system communication is established, which is yet to be modelled and demands a great effort. But a digital twin could also work with a one-way physical-to-virtual connection as per the definition of Grieves.

In this work, a framework on Digital Twins and how it can be utilized for power-cycle based waste heat recovery energy systems have been presented. Although there lies a diversification in the interpretation of the definition for Digital Twin, especially pertaining to the energy industry, an attempt has been made to incorporate Digital Twins for an ORC based WHR power cycle by integrating the transient data from the dynamic model built from the physical-to-virtual twinning process. In the upcoming work, we aim for a two-way communication between the physical and the virtual counterpart to make the Digital Twin model complete for our ORC power cycle that could be applied for a marine based WHR system in the future.

References

[1] M. Grieves, J. Vickers Digital twin: mitigating unpredictable, undesirable emergent behavior in complex systems,Transdisciplinary perspectives on complex systems (2017), pp. 85-113

[2] M. Grieves, Digital twin: manufacturing excellence through virtual factory replication (2014)

[3] D. Jones, C. Snider, A. Nassehi, J. Yon, B. Hicks, Characterising the Digital Twin: A systematic literature review, CIRP Journal of Manufacturing Science

and Technology, Volume 29, Part A, 2020, Pages 36-52, ISSN 1755-5817, https://doi.org/10.1016/j.cirpj.2020.02.002.

[4] D. Pomerantz, The French Connection: Digital Twins From Paris Will Protect Wind Turbines Against Battering North Atlantic Gales, 2018. https://www.ge.com/news/reports/french-connection-digital-twins-paris-will-protect-wind-turbines-battering-north-atlantic-gales. Accessed 5.5.2021.

[5] Fingrid, ELVIS project. https://www.fingrid.fi/en/pages/news/news/2016/fingrids-elvis-project-completed/ Accessed 5.5.2021

[6] H. Vella, Inside the world's first digital twin of a hydroelectric power station, 20 Apr 2020, https://www.power-technology.com/features/inside-the-worlds-first-digital-twin-of-a-hydroelectric-power-station/ Accessed 5.5.2021

[7] F. Tao and Q. Qinglin, Make more digital twins, Nature 573, 490-491 (2019) doi: https://doi.org/10.1038/d41586-019-02849-1

[8] THJ. Uhlemann, C. Lehmann, R. Steinhilper. The digital twin: realizing the cyberphysical production system for industry 4.0. Procedia CIRP; 2017. https://doi.org/10.1016/j.procir.2016.11.152.

[9] R . Nikula, M. Paavola, M. Ruusunen, J. Keski-Rahkonen. Towards online adaptation of digital twins. Open Engineering. 2020;10(1): 776-783. https://doi.org/10.1515/eng-2020-0088

[10] M. Manngård, & W. Lund, J. Björkqvist, (2020). Using Digital Twin Technology to Ensure Data Quality in Transport Systems, TRA2020 Rethinking transport Conference.

[11] S.Y. Teng, M. Touš, W.D. Leong, B.S. How, H.L. Lam, V. Máša, Recent advances on industrial data-driven energy savings: Digital twins and infrastructures, Renewable and Sustainable Energy Reviews, Volume 135, 2021, 110208, ISSN 1364-0321, https://doi.org/10.1016/j.rser.2020.110208.

[12] A. Fuller, Z. Fan, C. Day and C. Barlow, "Digital Twin: Enabling Technologies, Challenges and Open Research," in IEEE Access, vol. 8, pp. 108952-108971, 2020, doi: 10.1109/ACCESS.2020.2998358.

10. Catalytic aftertreatment methods for marine applications

Teuvo Maunula[1], Kauko Kallinen
Dinex Finland Oy

10.1 Introduction

The need to improve energy efficiency and reduce emissions has been a driving force in the marine industries during the last years. Aftertreatment systems (ATS) are depending on the fuel (diesel oil, natural gas) and its quality (Sulfur content) (Figure 1). The main focus has been on the emission reduction of SO_x and NO_x in marine applications but oxidation catalysts for CO and hydrocarbons (HCs) are applied also for low-sulfur fuels. NO_x emissions have been reduced with ammonia (urea) on sulfur-tolerant Selective Catalytic Reduction (SCR) and Ammonia Slip Catalysts (ASC).

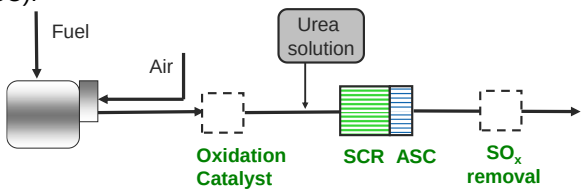

Figure 1. ATS in marine applications.

Natural gas with very low sulfur content (thus, low SO_x) is a good alternative to conventional heavy-oil liquid fuels. Methane produces less carbon dioxide (CO_2) emissions compared to diesel HCs and the particulate matter emissions are very low with natural gas, but it is a strong greenhouse gas (GHG effect 25xCO_2) and its emissions have been limited. Methane oxidation in lean exhaust gas requires the use of expensive Platinum Group Metal (PGM) catalysts. High-loaded, palladium-

[1] Contact: tma@dinex.fi

rich methane oxidation catalysts (MOC) are the best, but they are often sensitive particularly for the sulfur deactivation [1, 2].

Sulfur can be regenerated from the catalyst surface at elevated temperatures. Marine engines are operating in lean conditions and very high temperature is then required to decompose sulfates. However, sulfates can be decomposed at lower temperatures in stoichiometric or rich conditions. The catalyst performance has been restored by the regenerations in enriched gas mixtures in earlier studies [3,4]. The SO_x traps were demonstrated in INTENS project, which had a task to protect MOC against sulfur poisoning.

10.2 Experimental

Sulfur poisoning of Pd-rich MOCs was simulated in synthetic gas bench (SGB) using lean exhaust gas conditions (λ=1.8, 100 ppm SO_2). Sulfur was adsorbed by catalysts at 400°C and 550°C, simulating a higher adsorption of SO_2 and the use conditions at pre-turbo position. Desulfation regeneration was examined at 550°C by a regeneration feed mixture, where λ was rich (0.99). Sulfur is accumulated on the surface as sulfates either on the active sites or porous support. Sulfate adsorption is depending on SO_2 oxidation rate to SO_3 (thus, SO_4) and the bond strength between SO_4 and metal cations on catalysts. When MOCs are usually alumina-based catalysts, the strength of Al-SO_4 (aluminium sulfate) is a base line for SO_x adsorbent comparisons. SO_2 oxidation on noble metals is much faster than on base metal catalysts. Therefore, adsorbent catalysts or materials were examined with and without noble metals.

The SCR and ammonia slip catalyst functionality was investigated by SGB and engine experiments. Due to medium temperature operation window, high sulfur in fuels and catalyst costs, the SCR has been based on vanadium/TiO_2-WO_x catalysts. The SCR functionality was investigated in steady-state condition with fixed or varying NH_3/NO_x ratio. Catalysts were investigated as fresh or hydrothermally aged. The feed gases in SGB simulations are summarized in Table 1.

Table 1. Feed gases in experimental simulations.

Compound	Lean NG MOC test	MOC Sulfation	MOC Regeneration	SCR
NO, ppm	500	500	500	1000
NO_2, ppm	-	-	-	-
Methane, ppm	1500	1500	3000	-
Ethane, ppm	300	300	500	-
Propane, ppm	100	100	100	-
Acetaldehyde ppm	150	150	150	-
CO, ppm	1200	1200	4000	-
Oxygen, %	10	10	0.91	10
CO_2, %	7.5	7.5	7.5	-
Water, %	8	8	8	10
NH_3, ppm	-	-	-	1000
SO_2, ppm	-	100	-	-
Nitrogen	Bal.	Bal.	Bal.	Bal.
λ	1.78	1.78	0.99	lean
Space velocity, h^{-1}	50.000 varying	50.000 varying	50.000	50.000

10.3 Results

10.3.1 Development of MOC

Sulfur durability is a key development target for MOC. Even if desulfation is possible at elevated temperatures, the base sulfur tolerance of MOC in use is essential to extend time periods for regenerations. Development had resulted in improved concepts, which are similar as fresh state but stand better sulfur in use. The new concepts showed a particular stability in sulfur containing NG exhaust gas conditions: T_{50} of 470°C with MOC1 dev, when 530°C with REF (Figure 2). MOC development and durability studies will be continued based on the new concepts.

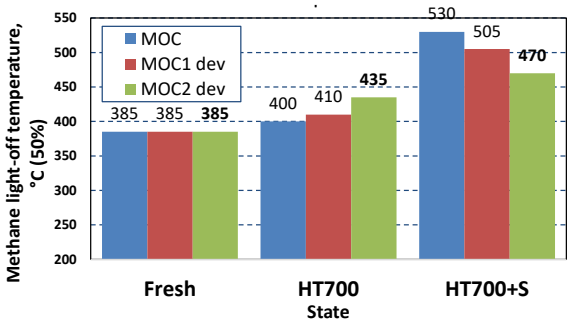

Figure 2. Methane light-off temperatures as fresh, hydrothermally aged (HT700/20H) and sulfated (HT700/20h + sulfation with 100 ppm SO_2 for 1h at 400°C) with new developmental MOCs in comparison to the reference MOC (SGB experiments. Lean MOC feed, 50.000 h^{-1}).

10.3.2 Sulfur durability and regeneration of methane oxidation catalysts

When MOC is sulphated in exhaust gas, lean SO_x trap (LST) was applied to protect MOC and collect SO_x during lean periods. During regeneration periods SO_x is removed from LST and should pass MOC downstream. The effect of LST should be compared as an additional unit or it replaces MOC volume. Even if LST increases the volume and causes pressure drop, it is cheaper than the PGM-rich MOC with the same total volume. The cost equivalency (investment, use) for volumetric ratio of MOC/LST is a base for design (Figure 3).

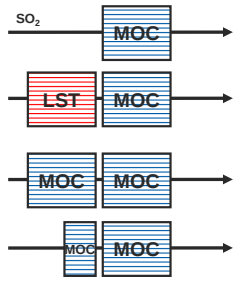

Figure 3. Lean SO_x trap and MOC in lean natural gas exhaust purification.

The screening results at 400°C and 550°C showed that SO_x was adsorbed well on LSTs. There were also differences by LSTs in the regeneration at 550°C with λ=1. SO_2 adsorption increased in the presence of a low amount of platinum in all the examined compositions. However, it existed wide differences by LST types which conditions were requires for SO_2 release. Methane conversion remained on a higher level with the combinations of LST and MOC in the presence of SO_2 containing feed gas (Figure 4). A saturation was detected by longer experiments (4 hours, corresponding about 400 h in use conditions) and then SO_2 started to come through. SO_x deactivates methane oxidation due to sulfate accumulation and the presence in gas phase.

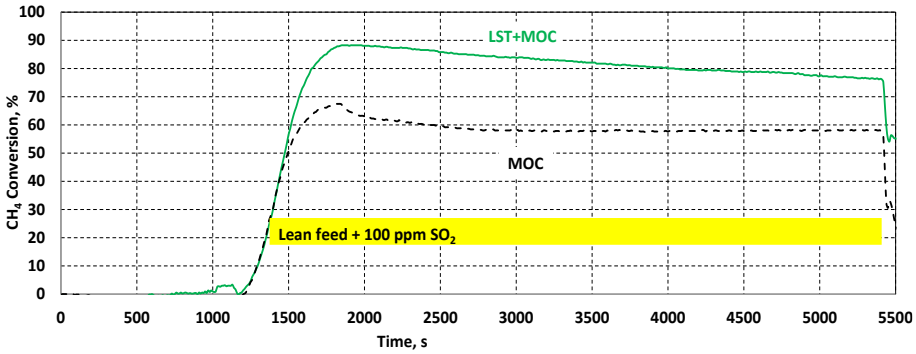

Figure 4. Methane conversion during sulfation on LST + MOC.

These results confirmed the potential utilization of SO_x traps to improve MOC efficiency. However, further development, regarding the composition and sizing, is needed to optimize LST+MOC systems for real applications.

10.3.3 NO_x removal with vanadium SCR catalysts

Vanadium-SCR catalysts (V_2O_5/TiO_2-WO_3) are the mainstream for marine applications, where temperatures are mainly 300-400°C, high-sulfur fuels are used and the catalyst cost is critical. Originally Dinex has prepared metal substrated V-SCR catalysts even if the same catalyst compositions can be added on ceramic substrates too. The activity and hydrothermal (HT) durability are dependent on vanadium concentration (range of 1 - 4 wt-%) in TiO_2-WO_3 based supports [5]. Higher V_2O_5 loadings (>3 wt-%) result in improved low temperature activity but lower HT durability. SCR catalysts with low V_2O_5 loading (<2 wt-%) are developed for high temperature applications. New types of metal vanadates have been also investigated for marine applications. Metal vanadates are less harmful for human health than conventional vanadium salts in manufacturing process.

Mechanically durable metal subtracted SCR catalysts are a good alternative to ceramic or extruded catalysts also in pre-turbo location, where the vibration, temperatures and pressure are high. Pre-turbo installation enhances the catalyst light-off and is a way to reduce the volume. Properties and preparation process of metal substrates were also developed in the project. When emission catalyst coatings are usually porous base metal oxides, the adhesion is more challenging on flat metal alloy (Al-Cr) surfaces than on porous ceramic substrates. Therefore, an oxide layer has been created on thin metal foils to improve adhesion of coatings and oxidation resistance. Heat treatments at 700-950°C with varying times have a direct effect on oxidation layer formation rate, composition and thickness, as well as on tensile strength and adhesion. It was possible to form fast at high temperatures porous, protecting Al_2O_3 layers but too high diffusion amount of metal atoms up to top foil surface decreased also the foil strength and did not improve more the adhesion. Based on the SEM, XRF, adhesion and mechanical strength analysis (at University of Jyväskylä and University of Oulu), the pre-treatment conditions were optimized, which resulted in changes and cost savings in manufacturing conditions. In addition, the corrosion resistance of metallic foils was confirmed to be good in the presence of ammonia, NO_x and SO_x by laboratory studies at VTT Tampere.

V-SCR catalyst was, without Pt, very poor both for NH_3 and CO oxidation in NH_3 only feed even at high temperatures (Figure 5). A small amount of Pt, 2, 5 or 15 g/cft, mixed into V-SCR coating, increased the oxidation activity of aged catalysts significantly up to over 95% with 15 g/cft Pt. However, that loading was too high, resulting in high NO_x and N_2O formation.

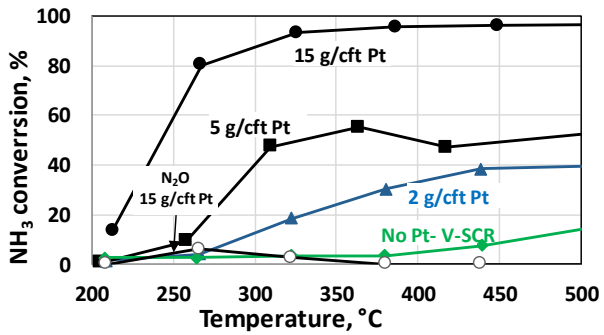

Figure 5. NH_3 conversions on aged (HT600/20h) V-SCR catalyst and PtV-ASC with 2, 5 and 15 g/cft Pt in laboratory simulations in NH_3 only feed gas (100.000 h^{-1}). N_2O (open circle) showed for 15 g/cft Pt.

References

[1] Reza Abbasi, Guangyu Huang, Georgeta M. Istratescu, Long Wu and Robert E. Hayes, Methane Oxidation Over Pt, Pt:Pd and Pd based Catalysts: Effects of pre-treatment. *The Canadian Journal of Chemical Engineering, 9999 (2015) 1-9.*

[2] T. Maunula, K. Kallinen, N. Kinnunen, M. Keenan and T. Wolff, Methane abatement and catalyst durability in heterogeneous lean-rich and dual-fuel conditions*. Topics in Catalysis 62 (2019) 315-323.*

[3] Mari Honkanen, Jianguang Wang, Marja Kärkkäinen, Mika Huuhtanen, Hua Jiang, Kauko Kallinen, Riitta L. Keiski, Jaakko Akola and Minnamari Vippola, Regeneration of sulfur-poisoned Pd-catalyst for natural gas oxidation. *Journal of Catalysis 358 (2018) 253-265.*

[4] N.M. Kinnunen, J.T. Hirvi, K. Kallinen, T. Maunula, M. Keenan, and M. Suvanto, Case study of a modern lean-burn methane combustion catalyst for automotive applications: what are the deactivation and regeneration mechanisms? *Appl. Catal. B Environ. 207 (2017) 114-119.*

[5] Maunula, T., Savimäki, A., Viitanen, A., Kinnunen, T., and Kanniainen, K., Thermally durable vanadium-SCR catalysts for diesel applications, SAE Paper 2013-01-0796.

11. Performance of methane oxidation catalyst

Kati Lehtoranta[1a], Hannu Vesala[1a], Päivi Koponen[1a], Kauko Kallinen[b], Teuvo Maunula[2b], Heikki Korpi[3c], Juha Kortelainen[3c]

[a]VTT Technical Research Centre of Finland Ltd,
[b]Dinex Finland Oy,
[c]Wärtsilä Oyj Abp

11.1 Introduction

The emissions from ships can be a significant source of air pollution in coastal areas and port cities and can have negative impact on human health and climate. Therefore, the International Maritime Organization (IMO) has implemented regulations to reduce emissions from ships. To answer these requirements emission reduction technologies are needed, namely fuel technologies, combustion technologies and/or exhaust gas aftertreatment technologies [1]. One solution is to use natural gas (NG) as a fuel. With liquefied natural gas (LNG) utilization, both SO_x and NO_x regulations of IMO can be achieved without any need for aftertreatment. In addition, particle emissions from natural gas combustion are low and, in practice, no black carbon is formed from NG combustion [2]. Moreover, CO_2 emission is lower with the NG use compared to diesel fuels, because NG is mainly composed of methane with a higher H/C ratio compared to diesel. The hydrocarbon emissions, on the other hand, are higher with NG compared to diesel fuels [3–6]. Because natural gas is mainly methane, most of the hydrocarbon emissions is also methane.

Three different gas engine groups are used for marine applications, namely lean burn spark ignited engines, low pressure dual fuel engines and high-pressure dual fuel engines [7]. For dual fuel engines, the natural gas and air mix is ignited with a small diesel pilot injection. In addition, the diesel can be utilized as the main fuel (back-up fuel) if LNG is not available, making this dual fuel concept the most popular one in marine applications. According to Sharafian et al., [8] LNG utilization in high-

[1] Contact: firstname.lastname@vtt.fi
[2] Contact: tma@dinex.fi
[3] Contact: firstname.lastname@wartsila.com

pressure dual-fuel (HPDF) engines, which are used only for large low-speed oceangoing vessels, can reduce greenhouse gas (GHG) emissions by 10% compared to their HFO-fuelled counterparts. While, the current deployment of medium speed low-pressure-dual-fuel (LPDF) cannot reliably reduce GHG emissions. This is primarily due to the high levels of methane slip from these engines.

One option to reduce methane emissions is the use of oxidation catalyst. In order to oxidize methane, a highly efficient catalyst is needed. The challenge in the development of methane oxidation catalyst is the catalyst deactivation since as little as 1 ppm SO_2 present in the exhaust has already been found to inhibit the oxidation of methane [9,10].

In this study the emissions from one medium speed LPDF are investigated and utilized as a starting point to study the performance of one methane oxidation catalyst (MOC). In addition to MOC only, in this study, we combine a sulphur trap or SOx trap, utilizing it at the upstream of the MOC, to see its capability to protect the MOC against sulphur poisoning.

11.2 Experiment

Experiments were conducted, prior to current work, in a marine engine laboratory. The engine was a Wärtsilä Vasa 4R32, a four-cylinder medium-speed 4-stroke marine engine that was retrofitted to enable operation with natural gas in dual fuel (DF) mode. Taking the emission results as a reference, the present study was conducted with a smaller engine, namely a passenger car gasoline engine that was modified to run with natural gas. The engine and test facility operation targeted in producing similar exhaust gas matrix with the marine engine (Figure 1 A). The test engine with the test facility was presented in detail by Murtonen et al.[11].

The NG was from Nord Stream and was high in CH_4 content (>95%). The sulphur content of the gas was below 1.5 ppm. The lubricating oil utilized for medium speed LNG engines was selected and used in this smaller test engine as well. Methane oxidation catalyst (MOC) utilized platinum-palladium as active metals. The SO_x trap utilized platinum as the catalyst.

Additional SO_2 was fed into the exhaust (see Figure 1B) in part of the ageing tests contributing to a 1 ppm increase in the exhaust gas while any sulphur from the natural gas and lubricating oil led to a SO_2 level of approximately 0.5 ppm in the exhaust gas. Altogether, three similar experimental campaigns were conducted. Two tests were done with the MOC only, one with additional SO_2 and the other without SO_2 addition. The third test was conducted with SO_x trap installed in front of the MOC (including the additional SO_2 in the exhaust gas).

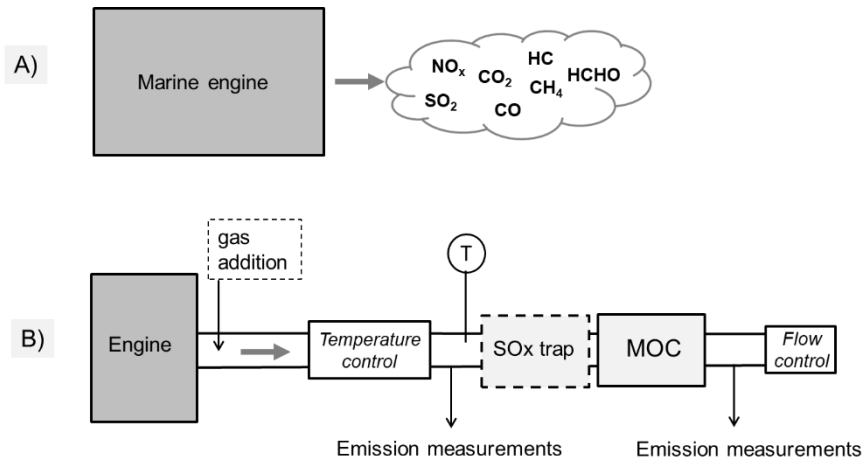

Figure 1. The experiment setup.

The experiments were conducted over a 180-hour ageing at the selected driving mode with exhaust temperature adjusted to 550º C and exhaust flow to 60 kg/h. The engine was running without stops and once a day regeneration was done by turning the engine to stoichiometric condition for 5 minutes' time.

Emission measurements were done at both the upstream and downstream of the catalyst system (see Figure 1). This included a Horiba PG-250 analyser used to measure NO_x, CO, CO_2, and O_2. Online SO_2 emissions were determined by a Rowaco 2030 1 Hz FTIR Spectrometer. A MicroGC was used to measure the hydrocarbons and hydrogen (H_2). In addition, multiple gaseous components were measured continuously by two Gasmet FTIR spectrometers simultaneously at the upstream and downstream of the catalyst system.

11.3 Results and discussion

The earlier measured exhaust gas matrix from one medium speed dual fuel marine engine run with NG in two different engine loads is presented in Table 1. Comparing these values to the values of present study's selected driving mode (Table 1), we see that these are in the same order of magnitude.

Table 1. Engine out exhaust gas composition from one medium speed dual fuel marine engine run with natural gas as the main fuel and with the test engine of MOC studies.

Engine out	CO	CO_2	NO_x	O_2	CH_4	C_2H_6	C_2H_4	HCHO
	ppm	vol%	ppm	vol%	ppm	ppm	ppm	ppm
Marine engine 85% load	342	5,5	337	10,9	1823	41,8	7,2	44,7
Marine engine 40% load	650	5,3	380	11,1	3750	89,0	23,1	76,0
Test engine for MOC studies	549	8,0	226	6,5	970	14,6	30,3	55,7

The MOC was found to achieve methane conversion near 70-80% in the beginning. The conversion was, however, found to decrease over time rather quickly, but the regeneration, done once a day, was found to recover the catalyst efficiency. This can be seen from Figure 2, where the methane conversion calculated from the simultaneously measuring FTIR devices' methane results are presented roughly for a two-day period. After the second regeneration, i.e. at the 44-hour point, all the catalysts resulted in similar methane conversions. The conversion after the regeneration decreases more quickly in the case of 'MOC+SO_2' than for the two other cases ('MOC only' and 'trap+MOC') that seem to behave very similarly. After the regeneration the conversion is recovered, in all cases, and similarly to earlier day, the conversion after the regeneration (68 hours) decreases more quickly in the case of 'MOC+SO_2' than for the two other cases. The methane conversion is approx. 10-15 percent higher when the trap is placed at the upstream of the MOC, meaning there are more active sites for methane to convert in the MOC downstream the trap. This indicates the SO_2 level inside the MOC is lower when trap is involved compared to the MOC-only case.

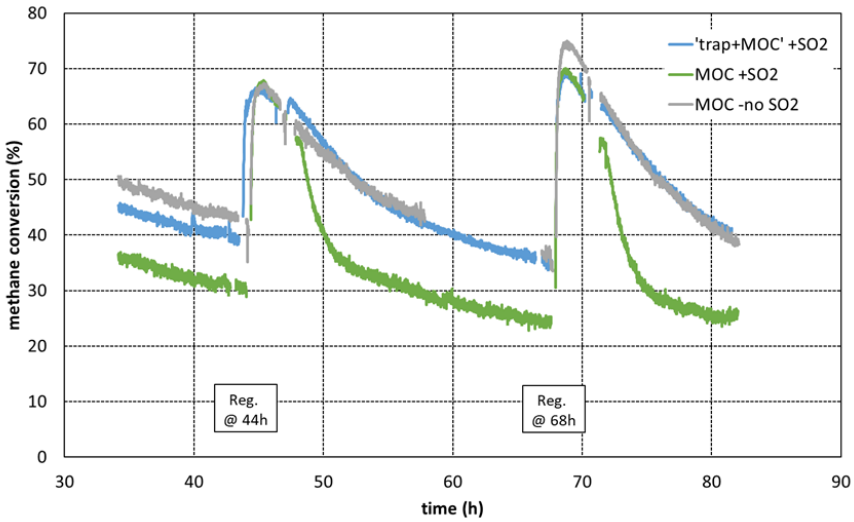

Figure 2. Methane conversion based on two simultaneously measuring FTIRs.

The regeneration, recovering the catalyst efficiency for methane oxidation, already indicates SO_2 is most probably released from the catalyst during the regeneration and the SO_2 measurement confirms this. In each case, during the 5-minute regeneration a release of SO_2 was detected with the FTIR at the downstream of the catalyst. The total SO_2 amounts released over the 5-minute regeneration periods are collected to Table 2. If we look at for example the third regenerations (Table 2), we see that in the case of "MOC-no SO_2", 0.33 g SO_2 was released while in the case of "MOC + SO_2" 0.54 g SO_2 was released. In the case of "trap + MOC" the SO_2

released during the regeneration was 1.52 g (see Table 2), indicating roughly that the “trap” is contributing to the release with SO_2 amount of 0.98 g. This means that the trap is collecting at least the same amount of SO_2. In addition, this SO_2 release indicates that the trap itself is regenerating at the same time as the MOC. These results are discussed in more detailed in Lehtoranta et al. [12].

Table 2. The SO2 amounts (g) released during regenerations. *Note. 4.reg was done after weekend. In case of Italic labelled values, engine driving mode was not exactly as intended.

hours		MOC only, w/o SO_2 add	MOC only, with SO_2 add	trap+MOC, with SO_2 add
20	1.reg	0.35	0.51	1.29
44	2.reg	0.18	0.54	1.51
68	3.reg	0.33	0.54	1.52
140	4.reg*	0.35	0.58	*2.26*
164	5.reg	*0.09*	0.52	*2.00*
188	6.reg	*0.21*	0.51	

Currently, LNG is a viable marine fuel deployed to substantially reduce pollutant emissions (NOx, SOx and particles) from ships. The use of LNG has therefore a notable effect on air quality and human health. In addition, LNG can provide reduction in GHG emissions if methane slip is controlled. This methane slip challenge needs to be solved to maximize LNG’s potential to contribute to climate neutrality. The present study shows that the MOC can play a role here. As it is an after-treatment system, it has potential for both new vessels and retrofits of existing vessels. However, further studies are needed to find the optimized solution for MOC and performance on different engine loadings as well as in transient loading relevant in vessel operation.

References

[1] Ni, P.; Wang, X.; Li, H. A Review on Regulations, Current Status, Effects and Reduction Strategies of Emissions for Marine Diesel Engines. *Fuel*. Elsevier Ltd November 1, 2020, p 118477. https://doi.org/10.1016/j.fuel.2020.118477.

[2] Lehtoranta, K.; Aakko-Saksa, P.; Murtonen, T.; Vesala, H.; Ntziachristos, L.; Rönkkö, T.; Karjalainen, P.; Kuittinen, N.; Timonen, H. Particulate Mass and Nonvolatile Particle Number Emissions from Marine Engines Using Low-Sulfur Fuels, Natural Gas, or Scrubbers. *Environ. Sci. Technol.* **2019**, *53* (6), 3315–3322. https://doi.org/10.1021/acs.est.8b05555.

[3] Anderson, M.; Salo, K.; Fridell, E. Particle- and Gaseous Emissions from an LNG Powered Ship. *Environ. Sci. Technol.* **2015**, *49* (20), 12568–12575. https://doi.org/10.1021/acs.est.5b02678.

[4] Lehtoranta, K.; Murtonen, T.; Vesala, H.; Koponen, P.; Alanen, J.; Simonen, P.; Rönkkö, T.; Timonen, H.; Saarikoski, S.; Maunula, T.; Kallinen, K.; Korhonen, S. Natural Gas Engine Emission Reduction by Catalysts. *Emiss. Control Sci. Technol.* **2017**, *3* (2), 142–152. https://doi.org/10.1007/s40825-016-0057-8.

[5] Hesterberg, T. W.; Lapin, C. A.; Bunn, W. B. A Comparison of Emissions from Vehicles Fueled with Diesel or Compressed Natural Gas. *Environ. Sci. Technol.* **2008**, *42* (17), 6437–6445. https://doi.org/10.1021/es071718i.

[6] Liu, J.; Yang, F.; Wang, H.; Ouyang, M.; Hao, S. Effects of Pilot Fuel Quantity on the Emissions Characteristics of a CNG/Diesel Dual Fuel Engine with Optimized Pilot Injection Timing. *Appl. Energy* **2013**, *110*, 201–206. https://doi.org/10.1016/j.apenergy.2013.03.024.

[7] Ushakov, S.; Stenersen, D.; Einang, P. M. Methane Slip from Gas Fuelled Ships: A Comprehensive Summary Based on Measurement Data. *Journal of Marine Science and Technology (Japan)*. Springer December 1, 2019, pp 1308–1325. https://doi.org/10.1007/s00773-018-00622-z.

[8] Sharafian, A.; Blomerus, P.; Mérida, W. Natural Gas as a Ship Fuel: Assessment of Greenhouse Gas and Air Pollutant Reduction Potential. *Energy Policy* **2019**. https://doi.org/10.1016/j.enpol.2019.05.015.

[9] Ottinger, N.; Veele, R.; Xi, Y.; Liu, Z. G. Desulfation of Pd-Based Oxidation Catalysts for Lean-Burn Natural Gas and Dual-Fuel Applications. *SAE Int. J. Engines* **2015**, *8* (4), 1472–1477. https://doi.org/10.4271/20l5-0l-0991.

[10] Lampert, J. K.; Kazi, M. S.; Farrauto, R. J. Palladium Catalyst Performance for Methane Emissions Abatement from Lean Burn Natural Gas Vehicles. *Appl. Catal. B Environ.* **1997**, *14* (3–4), 211–223. https://doi.org/10.1016/S0926-3373(97)00024-6.

[11] Murtonen, T.; Lehtoranta, K.; Korhonen, S.; Vesala, H.; Koponen, P. Imitating Emission Matrix of Large Natural Gas Engine Opens New Possibilities for Catalyst Studies in Engine Laboratory. In *28th CIMAC World Congress*; 2016; Vol. Paper #107.

[12] Lehtoranta, K.; Koponen, P.; Vesala, H.; Kallinen, K.; Maunula, T. Performance and Regeneration of Methane Oxidation Catalyst for LNG Ships. *J. Mar. Sci. Eng* **2021**, *2021*, 111. https://doi.org/10.3390/jmse9020111.

12. Effect of different injection strategies on combustion characteristics in RCCI conditions

Bulut Tekgül[1a], Shervin Karimkashi[1a], Heikki Kahila[2b], Ossi Kaario[1a], Jari Hyvönen[2b], Eric Lendormy[2b], Ville Vuorinen[1a]
[a] Department of Mechanical Engineering, Aalto University School of Engineering, Espoo, Finland
[b] Wärtsilä Finland Oy, Vaasa, Finland

12.1 Introduction

Low temperature combustion (LTC) at leaner mixture conditions is a promising technique for reducing harmful emissions [1,2]. This study presents our recent analysis investigating the effect of different injection strategies on ignition delay time (IDT) and heat release rate (HRR) behavior for Reactivity Controlled Compression Ignition (RCCI) engine conditions. This is a continuation of our previous work, where we investigate the effect of a single injection strategy on ignition and HRR characteristics under the same conditions [3]. We use large-eddy simulation (LES) with detailed chemistry modeling in order to investigate the mixing and ignition characteristics of high-low reactivity mixture blends obtained with different injection strategies at RCCI conditions. A compression heating model is utilized to account for the ambient temperature and pressure increase due to compression effects. A diesel surrogate (*n*-dodecane) is injected into a homogeneous air-methane mixture with various different double-injection strategies. In total, we investigate 3 different injection strategies by adjusting the first and second injection timings (SOI_1,SOI_2): 1) adjusting the SOI_1 with keeping SOI_2 constant, 2) adjusting the SOI_2 while keeping SOI_1 constant, and 3) adjusting the injected mass split between two injections.

[1] Contact: firstname.lastname@aalto.fi
[2] Contact: firstname.lastname@wartsila.com

12.2 Methodology

12.2.1 Numerical Methods

The gas-phase flow is governed by the compressible Navier-Stokes equations with Favre filtering, using OpenFOAM-8 CFD solver [4]. The pressure implicit splitting of operators (PISO) method is used for pressure-velocity coupling. An implicit turbulence modeling approach is used by using a dissipative discretization scheme for the convection terms.

The injected high-reactivity liquid diesel spray is modeled using Lagrangian Particle Tracking (LPT) method. A no-breakup model is used with a constant droplet diameter, with the assumption that the injected particles have already undergone the droplet breakup process. A validation analysis for this assumption is provided in Figure 1 by comparing our numerical results against the experimental Engine Combustion Network (ECN) Spray A data available in literature.

For combustion modeling, we use our in-house model called DLBFoam [5] in order to speed up the chemistry reaction rate calculation. DLBFoam utilizes a dynamic load balancing model and an analytical Jacobian formulation with improved ordinary differential equation (ODE) solution routines. A skeletal *n*-dodecane oxidation chemical mechanism developed by Yao et al. [6] (54 species, 269 reactions) is used.

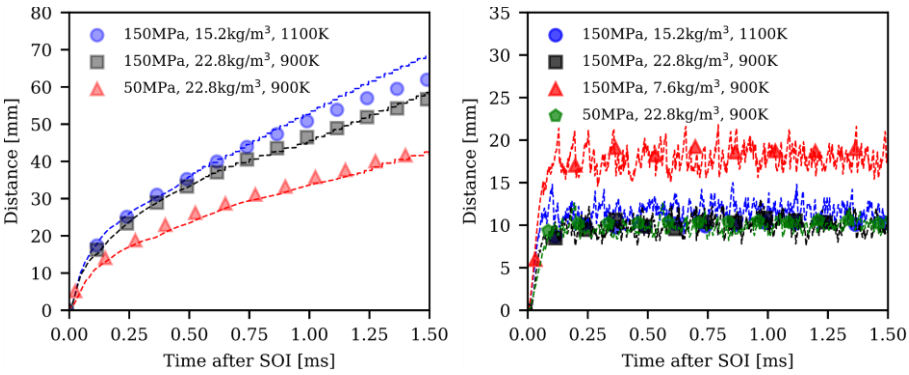

Figure 1. The vapor liquid penetration profiles obtained from simulations (line) and compared against the available experimental ECN spray data (symbol) for different operating conditions.

12.2.2 Compression Effects

In order to take the compression effects into account during compression stroke at RCCI conditions, we utilize a compression heating source term approach in the governing flow equations following the works [7] and [8]. The derivation of the source term is described in Equations 1 and 2. A schematic describing our numerical domain along with the validation of the compression heating model is presented in Figure 2.

$$P_m(t) = P_{0,m}[1 + g^2\pi^2 \frac{t - {t_0}^2}{{t_c}^2}]^{-n} \quad (1)$$

$$\dot{m} = \frac{\rho}{P}\frac{dP_m}{dt} \quad (2)$$

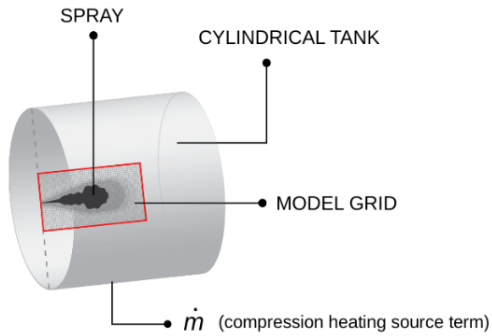

(a)

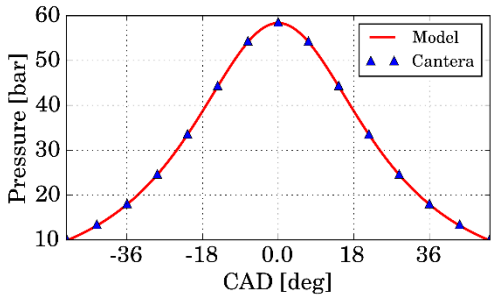

(b)

Figure 2. (a) A schematic of the numerical setup used in the simulations (b) Motored pressure with compression heating model (red) and a 0D homogeneous reactor (blue) under same compression conditions.

12.2.3 Investigated Conditions

A double injection *n*-dodecane configuration is adopted with an injection pressure of 50 MPa, and with keeping the injected mass constant (~1.1 mg). As mentioned previously, 3 different double-injection strategies are adopted, the details of which are given in Figure 3.

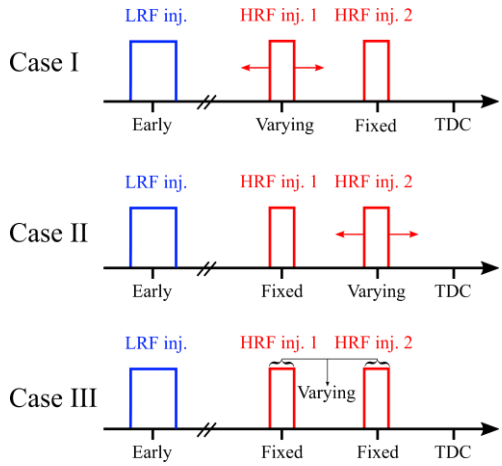

	First Injection (CAD BTDC)	Second Injection (CAD)	Split fraction (mass %)
Case 1.1	21.8	14.4	60-40
Case 1.2	28.8	14.4	60-40
Case 1.3	36	14.4	60-40
Case 2.1	28.8	21.6	60-40
Case 2.2	28.8	14.4	60-40
Case 2.3	28.8	7.2	60-40
Case 3.1	36	14.4	60-40
Case 3.2	36	14.4	70-30
Case 3.3	36	14.4	80-20

Figure 3. The 3 different injection strategies utilized in the study.

12.3 Results and Discussion

The temporal evolution of the HRR in CAD space along with a 3D visualization of each case is given in Figure 4. From the results, the following observations can be made: 1) for Case 1, the increase in dwell time between two injections leads to increased reactivity stratification, reducing the peak HRR value and increasing combustion duration; 2) for Case 2, while spatial stratification is observed for different injection strategies, the peak HRR value appears unaffected by adjusting the SOI_2; 3) for Case 3, while increasing the mass split ratio of SOI_1 leads to higher level of reactivity stratification, it reduces the temporal stratification and leads to higher peak HRR values.

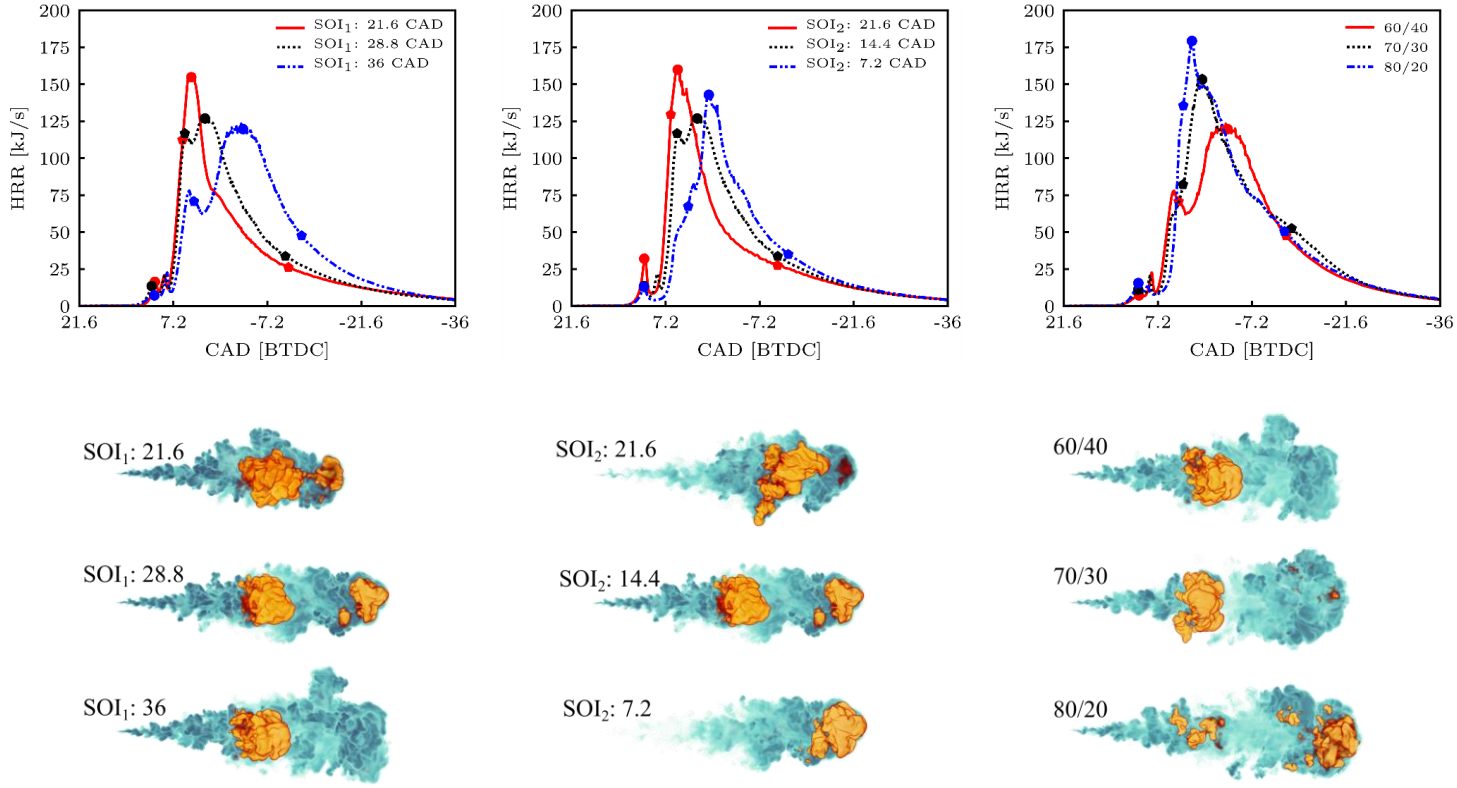

Figure 4. Top: the temporal evolution of HRR as a function of CAD for Cases 1 (left), 2 (middle) and 3 (right). Bottom: A 3D visualization of the same cases at their corresponding IDT+0.2 ms time instances.

Acknowledgements

The authors acknowledge Wärtsilä Co. for financial and academic support. The computational resources for this study were provided by CSC - Finnish IT Center for Science.

References

[1] Reitz, R. D. (2013). Directions in internal combustion engine research. Combustion and Flame, Vol. 160, pp. 1–8. https://doi.org/10.1016/j.combustflame.2012.11.002 .

[2] Reitz, R. D., & Duraisamy, G. (2015). Review of high efficiency and clean reactivity controlled compression ignition (RCCI) combustion in internal combustion engines. Progress in Energy and Combustion Science, 46, 12–71. https://doi.org/10.1016/j.pecs.2014.05.003 .

[3] B. Tekgül, H. Kahila, S. Karimkashi, O. Kaario, Z. Ahmad, É. Lendormy, J. Hyvönen, V. Vuorinen, Large-eddy simulation of spray assisted dual-fuel ignition under reactivity-controlled dynamic conditions, Fuel, Volume 293, 2021, 120295, https://doi.org/10.1016/j.fuel.2021.120295 .

[4] H. G. Weller, G. Tabor, H. Jasak, C. Fureby, A tensorial approach to computational continuum mechanics using object-oriented techniques, Computers in Physics 12 (6) (1998) 620. https://doi.org/10.1063/1.168744

[5] B. Tekgül, P. Peltonen, H. Kahila, O. Kaario, V. Vuorinen,DLBFoam: An open-source dynamic load balancing model for fast reacting flow simulations in OpenFOAM, arXiv preprints, https://arxiv.org/abs/2011.07978

[6] Yao, T., Pei, Y., Zhong, B. J., Som, S., Lu, T., & Luo, K. H. (2017). A compact skeletal mechanism for n-dodecane with optimized semi-global low-temperature chemistry for diesel engine simulations. Fuel, 191, 339–349. https://doi.org/10.1016/j.fuel.2016.11.083

[7] A. Bhagatwala, R. Sankaran, S. Kokjohn, J. H. Chen, Numerical investigation of spontaneous flame propagation under RCCI conditions. Combustion and Flame, 162(9), 2015 3412–3426. https://doi.org/10.1016/j.combustflame.2015.06.005

[8] Luong, M. B., Sankaran, R., Yu, G. H., Chung, S. H., & Yoo, C. S. (2017). On the effect of injection timing on the ignition of lean PRF/air/EGR mixtures under direct dual fuel stratification conditions. Combustion and Flame, 183, 309–321. https://doi.org/10.1016/j.combustflame.2017.05.023

Series title and number

VTT Technology 394

Title	**Integrated Energy Solutions to Smart and Green Shipping** 2021 Edition
Author(s)	Zou Guangrong | Saara Hänninen (Editors)
Abstract	Finland has a long tradition of pioneering maritime technological innovation. The INTENS project is one of the recent examples and major showcases for that, with special focus on maritime digitalization and decarbonization towards smart and green shipping. From its inception, INTENS has been a blessing to the consortium partners and wider Finnish maritime cluster. It has given the INTENS partners a unique opportunity to dedicate enormous efforts to jointly research and develop industry-leading novel solutions and innovations to address the major challenges faced by the global shipping industry. During the last three and a half years, the INTENS group have committed themselves to the project and achieved a long list of tangible R&D results, making the INTENS project a notable success. Interactive research-industry co-innovation has been the other crucial factor in and showcase for the INTENS' success. The collaboration within and outside of the consortium has made the INTENS project a recognized and rewarding platform, not only for the technological innovation and development, but also for the knowledge sharing and technology transfer. This book acts as part of the final report of the INTENS project and partly as the proceedings of the 2021 INTENS AFTERNOON public webinar series, featured with a collection of extended abstracts of the most recent project results. Hope this 2021 edition, together with earlier 2019 and 2020 editions, could showcase what have been achieved in the INTENS project and give a sneak peek at how digitalization and decarbonization could transform the shipping cluster. INTENS intensifies smart and green shipping by maritime digitalization and collaboration.
ISBN, ISSN, URN	ISBN 978-951-38-8755-1 ISSN-L 2242-1211 ISSN 2242-122X (Online) DOI: 10.32040/2242-122X.2021.T394
Date	June 2021
Language	English
Pages	113 p.
Name of the project	INTENS -Integrated Energy Solutions to Smart and Green Shipping
Commissioned by	Business Finland, Aalto University, Deltamarin Ltd, Dinex Finland Oy, LUT University, Meyer Turku Oy, NAPA Oy, Parker Hannifin Manufacturing Finland Oy, Pinja Oy (Protacon technologies Oy), Vahterus Oy, University of Vaasa, Wärtsilä Oyj Abp, Åbo Akademi University, and VTT Technical Research Centre of Finland Ltd
Keywords	Smart and green shipping, ship energy systems, energy efficiency, emissions reduction, digitalization, decarbonization, collaboration
Publisher	VTT Technical Research Centre of Finland Ltd P.O. Box 1000, FI-02044 VTT, Finland, Tel. 020 722 111, https://www.vttresearch.com

Integrated Energy Solutions to Smart and Green Shipping

2021 Edition

ISBN 978-951-38-8755-1
ISSN-L 2242-1211
ISSN 2242-122X (Online)
DOI: 10.32040/2242-122X.2021.T394

VTT beyond the obvious